

DTIC FILE COPY

WRDC-TR-90-3057

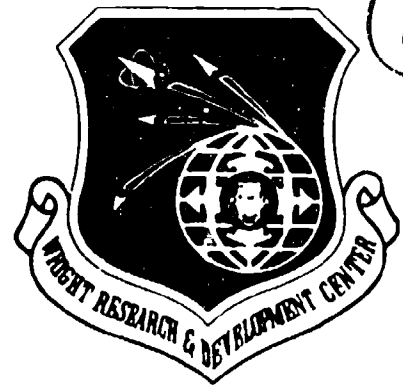
COMMENTS ON HYPERSONIC BOUNDARY-LAYER TRANSITION

Kenneth F. Stetson
High Speed Aero Performance Branch
Aeromechanics Division

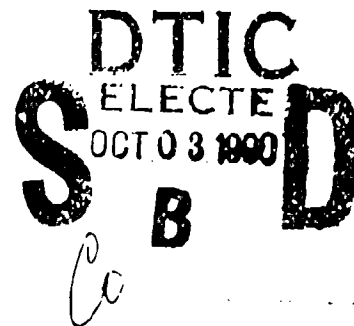
September 1990

Final Report for Period October 1984 - July 1990

Approved for Public Release; Distribution Unlimited



AD-A227 242



FLIGHT DYNAMICS LABORATORY
WRIGHT RESEARCH AND DEVELOPMENT CENTER
AIR FORCE SYSTEMS COMMAND
WRIGHT-PATTERSON AIR FORCE BASE, OHIO 45433-6553

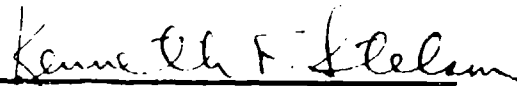
96


NOTICE

WHEN GOVERNMENT DRAWINGS, SPECIFICATIONS, OR OTHER DATA ARE USED FOR ANY PURPOSE OTHER THAN IN CONNECTION WITH A DEFINITELY GOVERNMENT-RELATED PROCUREMENT, THE UNITED STATES GOVERNMENT INCURS NO RESPONSIBILITY OR ANY OBLIGATION WHATSOEVER. THE FACT THAT THE GOVERNMENT MAY HAVE FORMULATED OR IN ANY WAY SUPPLIED THE SAID DRAWINGS, SPECIFICATIONS, OR OTHER DATA IS NOT TO BE REGARDED BY IMPLICATION, OR OTHERWISE IN ANY MANNER CONSTRUED, AS LICENSING THE HOLDER, OR ANY OTHER PERSON OR CORPORATION; OR AS CONVEYING ANY RIGHTS OR PERMISSION TO MANUFACTURE, USE, OR SELL ANY PATENTED INVENTION THAT MAY IN ANY WAY BE RELATED THERETO.


THIS REPORT HAS BEEN REVIEWED BY THE OFFICE OF PUBLIC AFFAIRS (ASD/PA) AND IS RELEASABLE TO THE NATIONAL TECHNICAL INFORMATION SERVICE (NTIS). AT NTIS IT WILL BE AVAILABLE TO THE GENERAL PUBLIC INCLUDING FOREIGN NATIONS.

THIS TECHNICAL REPORT HAS BEEN REVIEWED AND IS APPROVED FOR PUBLICATION.


KENNETH F. STETSON
Project Engineer
High Speed Aero Performance Branch


VALENTINE DAHLEM, Chief
High Speed Aero Performance Branch
Aeromechanics Division

FOR THE COMMANDER


ALFRED C. DRAPER
Chief
Aeromechanics Division

IF YOUR ADDRESS HAS CHANGED, IF YOU WISH TO BE REMOVED FROM OUR MAILING LIST, OR IF THE ADDRESSEE IS NO LONGER EMPLOYED BY YOUR ORGANIZATION PLEASE NOTIFY WRDC/PLMG, WRIGHT-PATTERSON AFB, OH 45433-6553 TO HELP MAINTAIN A CURRENT MAILING LIST.

COPIES OF THIS REPORT SHOULD NOT BE RETURNED UNLESS RETURN IS REQUIRED BY SECURITY CONSIDERATIONS, CONTRACTUAL OBLIGATIONS, OR NOTICE ON A SPECIFIC DOCUMENT.

| REPORT DOCUMENTATION PAGE | | | | Form Approved OMB No. 0704-0188 | |
|--|-------|--|--|--|--------------------------------|
| 1a REPORT SECURITY CLASSIFICATION UNCLASSIFIED | | | 1b RESTRICTIVE MARKINGS | | |
| 2a SECURITY CLASSIFICATION AUTHORITY | | | 3 DISTRIBUTION / AVAILABILITY OF REPORT Approved for Public Release, Distribution unlimited. | | |
| 2b DECLASSIFICATION / DOWNGRADING SCHEDULE | | | 5 MONITORING ORGANIZATION REPORT NUMBER(S) | | |
| 4 PERFORMING ORGANIZATION REPORT NUMBER(S) WRDC-TR-90-3057 | | | 7a. NAME OF MONITORING ORGANIZATION | | |
| 6a NAME OF PERFORMING ORGANIZATION Flight Dynamics Laboratory | | 6b OFFICE SYMBOL (If applicable) WRDC/FIMG | | 7b ADDRESS (City, State, and ZIP Code) | |
| 6c ADDRESS (City, State, and ZIP Code) Wright Research and Development Center WRDC/FIMG Wright-Patterson AFB OH 45433-6553 | | | 9 PROCUREMENT INSTRUMENT IDENTIFICATION NUMBER | | |
| 8a NAME OF FUNDING / SPONSORING ORGANIZATION | | 8b OFFICE SYMBOL (If applicable) | | 10 SOURCE OF FUNDING NUMBERS | |
| 8c ADDRESS (City, State, and ZIP Code) | | PROGRAM ELEMENT NO 61102F | | PROJECT NO 2307 | TASK NO N4 |
| | | | | WORK UNIT 59 | ACCESSION NO. |
| 11 TITLE (Include Security Classification) Comments on Hypersonic Boundary-Layer Transition | | | | | |
| 12 PERSONAL AUTHOR(S) STETSON, KENNETH F. | | | | | |
| 13a TYPE OF REPORT Final | | 13b TIME COVERED FROM 841001 TO 900731 | | 14 DATE OF REPORT (Year, Month, Day) 1990 September | |
| 15 PAGE COUNT 114 | | | | | |
| 16 SUPPLEMENTARY NOTATION | | | | | |
| 17 COSATI CODES | | | 18 SUBJECT TERMS (Continue on reverse if necessary and identify by block number) | | |
| FIELD | GROUP | SUB-GROUP | Boundary-Layer Transition. | | |
| 20 | 04 | | Boundary-Layer Stability | | |
| | | | Hypersonic Boundary-Layer Transition | | |
| 19 ABSTRACT (Continue on reverse if necessary and identify by block number) This is a survey paper on the subject of hypersonic boundary-layer transition. Part 1 discusses boundary-layer stability theory, hypersonic boundary-layer stability experiments, and a comparison between theory and experiment. Part 2 contains comments on how many configuration and flow parameters influence transition. Part 3 discusses some additional general aspects of transition. Part 4 discusses problems of predicting transition and comments on three prediction methods. Part 5 contains some general guidelines for prediction methodology. | | | | | |
| 20 DISTRIBUTION / AVAILABILITY OF ABSTRACT <input checked="" type="checkbox"/> UNCLASSIFIED/UNLIMITED <input type="checkbox"/> SAME AS RPT <input type="checkbox"/> DTIC USERS | | | 21 ABSTRACT SECURITY CLASSIFICATION UNCLASSIFIED | | |
| 22a NAME OF RESPONSIBLE INDIVIDUAL KENNETH F. STETSON | | | 22b TELEPHONE (Include Area Code) (513)255-5419 | | 22c OFFICE SYMBOL WRDC/FIMG |

PREFACE

This document will be a portion of the material presented at the Third Joint Europe/US Short Course in Hypersonics, held at the University of Aachen, Aachen, FRG in October 1990. This study was conducted by the High Speed Aero Performance Branch (WRDC/FIMG), Aeromechanics Division, Flight Dynamics Laboratory, Wright Research and Development Center, Wright-Patterson Air Force Base, Ohio. The work was performed under Work Unit 2307N459, Experimental Boundary Layer Stability Investigation.



| | |
|--------------------|-------------------------------------|
| Accession For | |
| NTIS GRA&I | <input checked="" type="checkbox"/> |
| DTIC TAB | <input type="checkbox"/> |
| Unannounced | <input type="checkbox"/> |
| Justification | |
| By _____ | |
| Distribution/ | |
| Availability Codes | |
| Dist | Avail and/or Special |
| A-1 | |

TABLE OF CONTENTS

| | <u>PAGE</u> |
|---|-------------|
| PART 1: COMMENTS ON HYPERSONIC BOUNDARY-LAYER INSTABILITY PHENOMENA | |
| a) INTRODUCTION..... | 3 |
| b) THEORY..... | 3 |
| c) STABILITY EXPERIMENTS..... | 8 |
| d) COMPARISON OF THEORY AND EXPERIMENT..... | 15 |
| PART 2: COMMENTS ON PARAMETRIC TRENDS | |
| a) INTRODUCTION..... | 17 |
| b) EFFECT OF MACH NUMBER..... | 17 |
| c) EFFECT OF NOSETIP BLUNTNESS..... | 18 |
| d) EFFECT OF CROSSFLOW..... | 21 |
| e) EFFECT OF UNIT REYNOLDS NUMBER..... | 22 |
| f) EFFECT OF THE ENVIRONMENT..... | 24 |
| g) EFFECT OF WALL TEMPERATURE..... | 27 |
| h) EFFECT OF SURFACE ROUGHNESS..... | 29 |
| i) EFFECT OF PRESSURE GRADIENT..... | 30 |
| j) EFFECT OF MASS TRANSFER..... | 31 |
| k) EFFECT OF HIGH TEMPERATURES/NON-EQUILIBRIUM..... | 32 |
| l) EFFECT OF VIBRATION..... | 32 |
| PART 3: SOME ADDITIONAL GENERAL COMMENTS | |
| a) MECHANISMS DESCRIBED BY A LINEAR THEORY..... | 33 |
| b) MECHANISMS NOT DESCRIBED BY A LINEAR THEORY..... | 34 |
| c) CONFIGURATION DIFFERENCES..... | 35 |
| d) SOME PROBLEMS OF WIND TUNNEL TRANSITION DATA..... | 37 |
| e) LENGTH OF THE TRANSITION REGION..... | 39 |
| f) SOME PROBLEMS WITH FLOW FIELD CALCULATIONS..... | 40 |
| PART 4: COMMENTS ON SOME PREDICTION METHODS | |
| a) INTRODUCTION..... | 43 |
| b) $Re_{\theta_T}/M_e = \text{CONSTANT}$ | 44 |
| c) $Re_{N^{\frac{2}{3}}_T}$ VS X/R_N | 45 |
| d) e^N METHOD..... | 47 |

PART 5: COMMENTS ON PREDICTION METHODOLOGY

| | |
|--|----|
| a) NOSETIP..... | 49 |
| b) EARLY FRUSTUM..... | 50 |
| c) CROSSFLOWS..... | 50 |
| d) LEADING EDGE CONTAMINATION..... | 51 |
| e) ADVERSE PRESSURE GRADIENTS/GÖRTLER INSTABILITIES..... | 53 |
| f) SECOND MODE..... | 53 |
| g) DOMINANT MECHANISMS..... | 55 |
| h) ESTIMATE UPPER AND LOWER BOUNDS..... | 55 |

| | |
|----------------------------|----|
| PART 6: CONCLUDING REMARKS | 56 |
|----------------------------|----|

| | |
|-----------------|----|
| REFERENCES..... | 57 |
|-----------------|----|

| | |
|--------------|----|
| FIGURES..... | 63 |
|--------------|----|

LIST OF ILLUSTRATIONS

| FIGURE | | PAGE |
|--------|--|------|
| 1 | A Schematic of a Stability Diagram | 63 |
| 2 | Maximum First and Second Mode Spatial Amplification Rates at $R = 1500$ | 64 |
| 3 | Boundary-Layer Fluctuation Spectra..... | 65 |
| 4 | Fluctuation Spectra Overlayed..... | 66 |
| 5a | Fluctuation Spectra, Normal to the Surface. Outside the Boundary Layer, Looking in..... | 67 |
| 5b | Fluctuation Spectra, Normal to the Surface. From the Surface Looking out..... | 68 |
| 6 | Wavelengths of the Most Unstable Second Mode Disturbances... | 69 |
| 7 | Experimentally Derived Stability Diagram..... | 70 |
| 8 | Fluctuation Spectra..... | 71 |
| 9 | Maximum Amplification Rates Associated with the Second Mode..... | 72 |
| 10 | Second Mode Maximum Amplification Rates..... | 73 |
| 11 | Second Mode Disturbance Growth..... | 74 |
| 12 | Maximum Growth Rates for Second Mode Disturbances..... | 75 |
| 13 | Spatial Amplification Rate vs Frequency at $R = 1731$. Points are from Experimental Data..... | 76 |
| 14 | Second Mode Maximum Amplification Rates..... | 77 |
| 15 | Effect of Mach Number on Transition..... | 78 |
| 16 | Wind Tunnel and Flight Transition Results..... | 79 |
| 17 | Cone Transition Reynolds Number Data for Wind Tunnels and Flight..... | 80 |
| 18 | A Schematic of Flow Over a Slender Blunt Cone..... | 81 |
| 19 | Calculations of Local Flow Properties on an 8-Deg. Half Angle Cone with 2% Bluntness at $M_\infty = 5.9$ | 82 |
| 20 | Entropy-Layer-Swallowing Distance Parameter..... | 83 |
| 21 | Effect of Nosedip Bluntness on Cone Frustum Transition at $M_\infty = 5.9$ | 84 |

LIST OF ILLUSTRATIONS

| FIGURE | | PAGE |
|--------|---|------|
| 22 | Nosetip Instability Effects on Cone Frustum Transition..... | 85 |
| 23 | Transition Movement With Angle of Attack..... | 86 |
| 24 | Transition Pattern on a Sharp Cone at $\alpha = 2$ Deg..... | 87 |
| 25 | Transition Asymmetry With Angle of Attack for a Sharp Cone.. | 88 |
| 26 | Transition Pattern on a Blunt Cone at $\alpha = 2$ Deg..... | 89 |
| 27 | Transition Asymmetry With Angle of Attack for 10% Nosetip Bluntness..... | 90 |
| 28 | Unit Reynolds Number Effect in a Ballistic Range..... | 91 |
| 29 | Effect of Freestream Disturbances on Transition Reynolds Number..... | 92 |
| 30 | Effect of Boundary-Layer Cooling on Transition..... | 93 |
| 31 | Effect of Wall Cooling on Transition Reynolds Number..... | 94 |
| 32 | A Schematic Illustration of Gortler Vortices..... | 95 |
| 33 | Correlation of Axisymmetric and Planar Transition Reynolds Numbers..... | 96 |
| 34 | Boundary-Layer Profiles..... | 97 |
| 35 | Transition Reynolds Number as a Function of Local Mach Number..... | 98 |
| 36 | An Illustration of Re_0/M_0 Variations..... | 99 |
| 37 | Re_x Variations as a Function of $Re_0/M_0 = \text{Constant}$ | 100 |
| 38 | Re_{0T} vs X/R_n Correlation for Mach 20 Reentry Vehicles..... | 101 |
| 39 | Transition Onset at the Attachment Line of a Swept Cylinder. | 102 |
| 40 | Transition Reynolds Number Variations Within the Entropy Layer..... | 103 |
| 41 | Entropy Layer Effects on a Slender Cone..... | 104 |

NOMENCLATURE

| | |
|----------------------------|---|
| A | Disturbance amplitude (arbitrary units) |
| F | Dimensionless frequency ($2\pi f/u_e Re_e/FT$) |
| G | Görtler number, $G = Re_\theta (\theta/R_c)^{1/2}$ |
| h | Enthalpy |
| k | Roughness height |
| kHz | Kilohertz |
| K | Entropy layer swallowing constant |
| M | Mach number |
| N | $\ln(A/A_o)$ |
| p | Pressure (psia) |
| R | Radius (inches), also $(Re_x)^{1/2}$ |
| Re | Reynolds number |
| R_c | Radius of curvature |
| Re_{XT}, Re_{ϵ_T} | Transition Reynolds number based upon conditions at the edge of the boundary layer and surface distance from the sharp tip or stagnation point to the location of transition. |
| Re_θ | Reynolds number based upon conditions at the edge of the boundary layer and the laminar boundary layer momentum thickness |
| T | Temperature (R) |
| U | Velocity |
| u | Tangential velocity component |
| u' | Velocity fluctuations |
| w | Crossflow velocity component |
| X, S | Surface distances (inches or feet) |
| X_{sw} | Entropy layer swallowing distance (see Fig. 15) (inches or feet) |
| X_T | Surface distance from the sharp tip or stagnation point to the onset of transition (inches or feet) |
| α | Angle of attack (deg.) |

| | |
|------------|--|
| $-a_1$ | Amplification rate, $(1/2A) \partial A/\partial R$ |
| δ | Boundary layer thickness (inches) |
| θ | Laminar boundary layer momentum thickness (inches) |
| θ_c | Cone half angle (deg) |
| λ | Wavelength of disturbance |
| μ | Viscosity |
| ρ | Density |
| ψ | Wave obliqueness angle (deg) |
| ϕ | Cone meridian angle (deg) |

Subscripts

| | |
|-------------|------------------------|
| AD | Adiabatic |
| B | Beginning or blunt |
| D | Diameter |
| e, δ | Edge of boundary layer |
| E | End |
| N | Nose |
| O | Reservoir or initial |
| S | Sharp |
| ST | Model stagnation point |
| T | Transition, total |
| W | Wall |
| ∞ | Freestream |

FOREWORD

Boundary-layer transition is a problem which has plagued several generations of aerodynamicists. There are very few things about transition that are known with certainty, other than the fact that it happens if the Reynolds number is large enough. Researchers have been frustrated by the many unsolved transition phenomena, by the fact that transition sometimes by-passes the known linear processes, and by the difficulties of sorting out the many interrelated and complicated effects for investigation. Transition predictors are confronted with many transition prediction methods, all with serious limitations, and insufficient information as to the best method to accomplish their task. Transition history has many examples of conflicting ideas and interpretations, and sudden changes in perspective are not uncommon. Research studies have emphasized the great complexity of the transition process and how little is known about the problem. A good prediction of transition is sometimes perceived as an impossible task. In spite of this negative situation, transition predictions must be made and people are tasked with the job of making transition predictions. How then does the transition predictor prepare himself for this task? As very general guidelines, it is thought that he should make maximum use of available research information, be knowledgeable of the available data base, try to understand the various prediction methods and their limitations, evaluate the risks involved, and, finally, try to keep an open mind when dealing with the problems (clearly, a formidable task).

Current emphasis on powered hypersonic vehicles has increased the frustrations of predicting hypersonic boundary-layer transition. In the past, most hypersonic problems have been associated with reentry vehicles. During reentry, transition moved forward on the vehicle in only a few seconds and was followed by a longer period of time of essentially all-turbulent boundary-layer flow. Knowledge of the exact altitude at which transition occurred was not critical to the design of the thermal protection system and the risks involved in the transition prediction were not large. For powered hypersonic vehicles we have a new class of configuration and new flight paths which may include long periods of time within the upper atmosphere (e.g., the National Aero-Space Plane). Boundary-layer transition now becomes a much stronger driver of the vehicle configuration, the thermal protection system, and the engine requirements. Hypersonic boundary-layer transition predictions now

take on a significance never before experienced and a relevant data base does not exist. This current situation has surfaced after a number of years of little activity in the area of hypersonics. Most of the new understanding of boundary-layer transition has been in the area of incompressible boundary layers, with little new knowledge of hypersonic boundary-layer instabilities. Thus, much hypersonic transition guidance must be speculated from subsonic and supersonic results and old hypersonic data must be retrieved and re-evaluated.

Not that it helps with the boundary-layer transition prediction problems, but there is some small gratification in knowing that design uncertainties are not unique to transition. Whenever a design involves a new configuration flying new flight paths, there are many uncertainties associated with the design. For new hypersonic designs, ground tests provide only partial simulation of the flight conditions and do not include important high temperature-related phenomena, flow field computations are made with unverified codes and incomplete modeling of the flow phenomena, and unproven propulsion systems are under consideration. The uncertainty in the location of boundary-layer transition is just one of many uncertainties which must be dealt with.

This report includes data, comments, and opinions on selected topics, primarily in those areas where the author is most familiar. The discussion has been kept brief and it is realized that many important points and details have been omitted. The listed references are only a sampling of the transition literature. The reader is referred to other documents for additional details and a more extensive list of references. A report by Morkovin,¹ although written over 20 years ago, provides much valuable information which remains relevant to current hypersonic transition problems. Surveys by Reshotko,^{2,3} Arnal,⁴ and Morkovin and Reshotko⁵ are also recommended reading.

PART 1: COMMENTS ON HYPERSONIC BOUNDARY-LAYER INSTABILITY PHENOMENA

(1.a) INTRODUCTION

Most of our knowledge of hypersonic boundary-layer instability phenomena has come from the theoretical work of Mack,^{6,7} supported by the stability experiments of Kendall,⁸ Demetriades,⁹ and Stetson, et al.¹⁰⁻¹⁴ There have been a considerable number of hypersonic transition experiments; however, these data generally provide only parametric trends (e.g., the effects of nosetip bluntness on transition location). When the only information obtained is the location of transition it is impossible to determine details of the boundary-layer disturbance mechanisms which caused the transition. In order to obtain fundamental information about hypersonic boundary-layer instability phenomena it is necessary to perform stability experiments which describe the disturbances in the laminar boundary layer prior to transition. It is unfortunate that such an important topic as hypersonic stability has received so little attention. An understanding of hypersonic instability phenomena is important for obtaining a better understanding of hypersonic transition and is essential for analytical prediction methods. The following discussion will briefly discuss our current understanding of hypersonic boundary-layer instabilities.

(1.b) STABILITY THEORY

It is now generally believed that the onset of boundary-layer turbulence is the result of instability waves in the laminar boundary layer; however, the direct relationship between instability and transition is unknown. Stability theory provides a means of understanding the characteristics of instability waves and, consequently, a better understanding of transition. Numerical solutions of the stability equations can provide important details of boundary-layer instability; such as, the identity of those disturbance frequencies which are stable and those which are unstable, the minimum critical Reynolds number at which disturbances start to grow, their growth rates, their return to a stable condition, the particular disturbance frequency which will obtain the maximum disturbance amplitude, and the effect of various parameters (e.g., Mach number, pressure gradient, wall temperature, etc.) Stability theory can provide much valuable information about boundary-layer disturbances, but it cannot predict transition. This is an important point. There is no transition

theory. All transition prediction methods are empirical. Transition prediction methods based upon stability theory (e.g., the e^N method) must relate transition to some empirically determined condition.

The introduction of linear boundary-layer stability theory by Tollmien and Schlichting met with strong opposition. This was primarily because the wind tunnel experiments of that time could find no evidence of the instability waves predicted by the theory, and there seemed to be no connection between linear stability theory and transition.¹⁵ The classic experiments of Schubauer and Skramstad¹⁶ completely changed the opinions. Wind tunnels in use at that time had high freestream turbulence levels which completely obscured the existence of small boundary-layer disturbances. The low-turbulence wind tunnel of Schubauer and Skramstad provided the first demonstration of the existence of instability waves in a laminar boundary layer, their connection with transition, and the quantitative description of their behavior by the theory of Tollmien and Schlichting. These experiments, as well as subsequent experiments, provided verification that when the freestream disturbance amplitudes are small, linear stability theory adequately described the onset of small disturbance growth in a subsonic boundary layer and the growth characteristics of the disturbances through their major growth history, up close to the transition location. Subsequently, linear stability theory found wide applications in the description of instability parameters and in the prediction of transition for subsonic flows.

If boundary-layer transition results from instabilities as described by linear stability theory, then the disturbance growth histories follow a prescribed pattern and are dependent upon disturbance frequency. Disturbances of a particular frequency will have the largest growth and become the first disturbances which obtain the critical amplitude required for breakdown to turbulence. Other disturbances may be unstable and experience growth, but they do not grow enough to cause transition. These events can be conveniently illustrated by means of a stability diagram such as schematically shown in Fig. 1 (from Ref. 17). The bottom of this figure illustrates a standard "thumb curve" stability diagram which graphically shows the boundary between stable and unstable regions in terms of disturbance frequency and Reynolds number. The solid lines (I and II) are the neutral boundaries which separate the stable and unstable regions. If one follows a specific frequency with increasing distance (increasing Reynolds number), disturbances at that fre-

quency are initially stable and experience no growth. As they reach the Reynolds number which corresponds to the crossing of neutral branch I they become unstable and start to grow. The initial disturbance amplitude at the crossing of neutral branch I (A_0) is an important parameter since it directly influences the amount of growth required to obtain the critical breakdown amplitude (A_c). The initial disturbance amplitude depends upon the characteristics of the disturbances to which the boundary layer is exposed, the receptivity of the boundary to these disturbances, and the extent of the initial stable region. As the disturbance waves proceed downstream they become better "tuned" to the boundary-layer thickness and they amplify at increasing rates. They reach a point of optimal tuning (the maximum amplification rate) and then gradually detune as they approach neutral branch II. The amplification rate decreases to zero at the Reynolds number which corresponds to the crossing of neutral branch II and the disturbances have obtained their maximum amplitude. Plots of amplitude vs Reynolds number (such as shown in the top portion of Fig. 1) are inflected curves with a zero slope at branches I and II. In the example illustrated in Fig. 1, disturbances of frequency F_1 and F_2 obtain their maximum growth and then attenuate before boundary-layer transition occurs. These disturbances are presumed to have no influence on transition. Note that the onset of disturbance growth for the F_2 disturb. (the crossing of neutral branch I) occurs at a larger Reynolds number than the F_1 disturbances; however, the F_2 disturbances have a longer period of growth and obtain a larger amplitude. If boundary-layer transition occurs at R_T , then the F_3 disturbances are the dominant disturbances since they are the first disturbances to grow to the amplitude required for breakdown. These disturbances presumably cause transition. F_4 disturbances have the potential of obtaining even larger amplitudes, but they do not get the opportunity since the boundary layer becomes transitional first. It is generally assumed that the growth rate of the disturbances is not influenced by changes in the freestream turbulence levels (as long as the turbulence levels are not large enough to force boundary-layer disturbance growth by some mechanism other than boundary-layer instability). Therefore, the effect of the freestream turbulence levels is felt through its influence of A_0 . Increasing A_0 for a 1 frequencies would shift all of the growth curves upward, such that some higher frequency, such as F_2 , would first obtain the critical amplitude. Reducing A_0 (as a quiet tunnel) would lower the curves and some

lower frequency, such as F_4 , would then be the first disturbance to obtain the critical amplitude.

Major developments in the application of linear stability theory to hypersonic boundary layers were made by Mack.^{6,7} Mack's stability equations were derived from the linearized Navier-Stokes equations for a compressible, viscous, heat-conducting perfect gas and most of his numerical results have been for sharp flat-plate boundary layers. His results disclosed a number of unique features of a hypersonic boundary layer.

As the Mach number increases, the distribution of angular momentum through the boundary layer changes in a manner such that the generalized inflection point (the location in the boundary layer where the gradient of the product of density and vorticity is zero) moves out toward the outer edge of the boundary layer. Since the major boundary-layer disturbances in a hypersonic boundary layer are in the neighborhood of the generalized inflection point, the largest disturbances in a hypersonic boundary layer can be expected to be near the outer edge of the boundary layer. There is another very important consequence of the generalized inflection point moving farther away from the wall. If there is a region in the boundary layer (e.g., near the wall) where the flow is supersonic relative to the mean velocity at the generalized inflection point, the mathematical nature of the stability equations changes. Mack^{6,7} demonstrated that, for this condition, there were multiple solutions of the stability equations. These additional solutions were called the higher modes. The higher instability modes are a unique feature of high Mach number boundary layers and, physically, they represent new instabilities that can influence hypersonic transition. Of the many contributions that Mack has made toward the understanding of hypersonic boundary-layer stability, the discovery of the higher modes is probably the most significant (the higher modes are sometimes called "Mack modes" to honor the importance of Mack's contribution). Thus, subsonic and low supersonic boundary layers contain relatively low frequency, vorticity disturbances called first mode disturbances (Tollmien-Schlichting waves) and hypersonic boundary layers contain both first mode and Mack mode disturbances.

First mode disturbances in an incompressible flow are most unstable as two-dimensional waves. For supersonic and hypersonic boundary layers, the most unstable first mode disturbances are always oblique waves. The wave angle of the most unstable first mode disturbance increases rapidly with Mach

number and is in the range from $55^\circ - 60^\circ$ above $M = 1.6$. The amplification rates of first mode disturbances decrease with increasing Mach number. Even the most unstable oblique inviscid disturbance was found to have a lower amplification rate than the maximum incompressible viscous amplification rate.

The first of the higher modes is called the second mode and is the most unstable of all the modes. The second mode disturbances are expected to be the dominant instability in most hypersonic boundary layers. Mack's calculations showed that the effect of viscosity on the higher modes was always stabilizing, so that the maximum amplification rate occurs as the Reynolds number approaches infinity. For the second and higher modes, two-dimensional disturbances are the most unstable. Second mode disturbances are high frequency, acoustical-type disturbances whose most unstable frequency will be an order of magnitude larger than the most unstable subsonic/supersonic frequencies.

Fig. 2 is an example of Mack's calculations for a flat-plate boundary layer with an adiabatic wall. The maximum amplification rates of the most unstable first and second mode waves at $R = 1500$ ($R = \sqrt{Re_x}$) are given as a function of freestream Mach number. These results illustrate the characteristics previously described.

Another significant finding from Mack's numerical results was the effect of wall cooling on boundary-layer stability. The results of early linear stability theory (Lees¹⁸) was that the boundary layer could be made completely stable by wall cooling, thus implying that the boundary layer could be kept laminar at any Reynolds number with sufficient wall cooling. The criterion for complete stabilization was based upon an asymptotic theory for two-dimensional disturbances and did not consider oblique first mode waves or the higher instability modes. Mack's calculations indicated that the first mode was strongly stabilized by cooling; however, complete stabilization was not possible since more cooling was required to stabilize oblique disturbances than two-dimensional disturbances and the higher modes were destabilized by surface cooling. Thus, if second mode disturbances are the major instabilities, then a cold surface would be expected to produce a smaller transition Reynolds number than a hot surface. Mack has warned that parameters such as pressure gradients and mass addition or removal may also affect second mode disturbances in a different manner than first mode disturbances.

As mentioned previously, most of the hypersonic stability results are applicable to the simple boundary layer on a flat plate in a perfect gas flow

field. Recently, Mack,^{19,20} Gasperas,²¹ and Malik²²⁻²⁴ have obtained solutions which pertain to the perfect gas flow over cones at zero angle-of-attack. Clearly, much work remains to be accomplished before useful solutions of three-dimensional flow fields with high temperature boundary layers can be obtained.

The quality of the numerical solutions of the stability equations is clearly dependent upon the validity of the assumptions used and the quality of the mean flow boundary-layer profiles utilized. A basic assumption utilized by all current hypersonic numerical solutions is the assumption that the boundary-layer disturbances are small and the stability equations can be linearized. As with most linear theories, it is difficult to pre-judge the range of conditions over which the results can be meaningfully applied. The mean boundary-layer profiles are an essential ingredient of the stability calculations. Therefore, it is not just a matter of having a valid theory, but also one of having valid mean boundary-layer profiles to provide data to input to the stability equations. The success of linear stability theory for subsonic and low supersonic boundary layers does not guarantee its success with a hypersonic boundary layer. There are so many different features of hypersonic boundary-layer stability that an independent verification is required. Section 1.d will discuss the first attempt at verification of hypersonic linear stability theory.

(1.c) STABILITY EXPERIMENTS

There are only three sets of hypersonic stability experiments; those of Kendall,⁸ Demetriades,⁹ and Stetson, et al.¹⁰⁻¹⁴ Kendall's pioneering stability experiments⁸ provided the first confirmation of the existence of second mode disturbances in a hypersonic boundary layer and that they were the dominant instability. Subsequently, stability experiments⁹⁻¹⁴ at $M_\infty = 8$ in a different wind tunnel provided additional confirmation of second mode disturbances and further details of their characteristics. Several examples of the experimental data will be given to illustrate some of the characteristics of hypersonic boundary-layer disturbances. These data were obtained with a constant current hot-wire anemometer. Details of the hot-wire anemometer instrumentation and the data reduction procedures of Stetson, et al., are given in Ref. 10.

Figures 3-5 are from Ref. 10 and include data obtained on a sharp, 7-deg. half angle cone at a Mach number of 8 (equilibrium wall temperature). Fig. 3

shows the fluctuation spectra at the location of peak energy in the boundary layer (at approximately 0.98) in a pictorial format to illustrate the growth of disturbances in a hypersonic laminar boundary layer. Large disturbances were found to grow in the frequency range from about 70 to 150 kHz. These fluctuations have been identified (primarily on the basis of a comparison with Mack's theoretical results) as second mode disturbances. Second mode disturbances are highly "tuned" to the boundary-layer thickness, resulting in considerable selectivity in the disturbance frequencies which are most amplified. The most amplified second mode disturbances have a wavelength of approximately twice the boundary-layer thickness. Second mode disturbances are not related to a specific frequency range, but can occur anywhere from relatively low frequencies (for "thick" boundary layers) to very high frequencies (for "thin" boundary layers). Situations which correspond to a change in boundary-layer thickness change the frequency of the second mode disturbances. For example, going to higher altitudes thickens the boundary layer and lowers the second mode disturbance frequencies. The normal growth of the boundary layer along a vehicle surface results in a steady lowering of the most amplified disturbance frequencies. Second mode disturbances grow much faster than first mode disturbances and rapidly become the dominant disturbances. It can also be observed in Fig. 3 that disturbance growth is occurring at frequencies higher than the ridge of second mode disturbances. These disturbances are believed to be a first harmonic (nonlinear disturbances) of the second mode. All of the previously mentioned hypersonic stability experiments have observed the high frequency nonlinear disturbances. Even though the boundary-layer disturbances had grown to a relatively large amplitude by the end of the model, the boundary layer still had the mean flow characteristics of a laminar boundary layer.

Fig. 4 contains the same data as shown in Fig. 3, with spectral data from several stations overlayed to better illustrate the disturbance frequencies. The first and second mode fluctuation frequencies are merged. The lower frequency fluctuations, which show an increase in amplitude without any special selectivity in frequency of the disturbances which are amplified, are predominantly first mode disturbances. These disturbances are similar to the Tollmien-Schlichting instability of incompressible flow. The large increase in fluctuation amplitude in the frequency range of about 70 to 150 kHz are second mode disturbances. As the boundary layer grows, the second mode

disturbance peaks shift to lower frequencies, illustrating the tuning effect of the boundary layer.

Fig. 5 is a pictorial view of the fluctuation spectra normal to the surface. Fig. 5a is a view from outside the boundary layer, looking in and Fig. 5b is a view from the surface, looking out. It can be seen that the disturbances did not grow in the inner half of the boundary layer, the maximum disturbance growth occurred high in the boundary layer (at 88% of the boundary-layer thickness), and disturbances extended well beyond the defined boundary-layer edge.

Since the second mode disturbances were highly tuned to the boundary-layer thickness, it was of interest to compare the disturbance wavelength with the boundary-layer thickness. The wavelength can only be estimated since the wave velocity is not known. Since the major disturbances were located near the edge of the boundary layer, the wave velocity was estimated by assuming it to be the same as the boundary-layer edge velocity. Fig. 6 illustrates the relationship between the wavelength of the largest disturbances and the boundary-layer thickness. The major second mode disturbances were found to have a wavelength approximately twice the boundary-layer thickness. The disturbances which were believed to be a first harmonic (data not shown) had a wavelength approximately equal to the boundary-layer thickness. As a means of comparison, the major first mode disturbances in lower speed flows have a much longer wavelength, typically being several times the boundary-layer thickness. The relationship of the wavelength of the major second mode disturbances to the boundary-layer thickness provides a simple method for estimating second mode frequencies, requiring only an estimate of the boundary-layer thickness and the velocity at the edge of the boundary layer ($f \approx u_e / 2\delta$). (Note that for a given Mach number, the boundary-layer edge velocity is much larger in flight than in a wind tunnel. Therefore, corresponding second mode frequencies in flight are larger than in a wind tunnel. Note, also, that the boundary-layer thickness is inversely proportional to the square root of the unit Reynolds number. In flight, the unit Reynolds number changes approximately an order of magnitude for a change in altitude of 50,000 feet. Therefore, for a given station on the vehicle, a change in altitude of 50,000 feet will change the major second mode disturbance frequencies about a factor of three.) Knowledge of the frequencies of the major second mode disturbances can be a consideration when making a judgement of the uncertainty of a transition prediction. For

example, if the major second mode disturbances have frequencies of several hundred kilohertz, there is a good possibility that they may not exist in flight, due to a lack of stimulus from the environment to excite them. This point will be discussed under section 2.f. Such a situation would be expected to produce a larger transition Reynolds number than if the second mode disturbances were present.

Fig. 7 is a stability diagram derived entirely from the experimental data of References 10 and 13. F is the non-dimensional frequency and R is the square root of the length Reynolds number. The two neutral branches (I and II) enclose the combined first and second mode unstable regions. The lower frequency portion of this region is predominantly a first mode unstable region and the lower neutral branch (I) corresponds to first mode instability. That is, this neutral branch relates to the experimentally detectable critical Reynolds number and the initial disturbance amplitude of first mode disturbances. Second mode instabilities are the major boundary-layer instabilities and occupy the upper portion of the unstable region. The maximum disturbance amplitudes (A_{\max}), the maximum amplification rates ($-\alpha_1$)_{max}, and the upper neutral branch (II) are all associated with second mode instabilities. Note that if one follows the history of disturbances at a particular frequency, their initial growth occurs as first mode disturbances. As the Reynolds number increases, that frequency may be unstable to second mode instabilities and disturbance growth may continue as second mode disturbances. Very little is known about the coupling of first and second mode disturbances in this situation. Above the second mode upper neutral branch is a stable region. The neutral branch lines at higher frequencies enclose the unstable region which is believed to contain nonlinear disturbances. The nonlinear disturbances were observed at a relatively low Reynolds number of 1.9×10^6 ($R = 1400$) and their growth rates were nearly as large as the second mode growth rates. Transition was estimated to occur at a Reynolds number of about 4.8×10^6 ($R = 2200$) based upon the observation (data not shown) that the second mode disturbances had obtained their peak amplitude and started to decay and disturbances at second mode neighboring frequencies started to grow (spectral dispersion).

Small nosetip bluntness was found to greatly stabilize the laminar boundary layer on the frustum of a cone. Fig. 8 (from Ref. 11) shows in pictorial format the fluctuation spectra at the location of peak energy in the

boundary layer for a 7-deg. half angle cone with a 0.15 inch nosetip radius (approximately 3% of the base radius). Initially, disturbances of all frequencies were damped and remained stable until a local length Reynolds number of 5.1×10^6 was reached. It can be observed in the figure that the disturbance amplitudes are getting smaller in this region of the cone frustum. This stable region extended to an S/R_N of approximately 121. This corresponded to a location on the cone frustum where most of the entropy layer generated by the nosetip had been swallowed by the boundary layer. Thus, for this case, the region of the cone frustum where the entropy layer was being swallowed by the boundary layer was a stable region. The sharp cone, at corresponding local Reynolds numbers, showed a steady growth of disturbances. In fact, at a local length Reynolds number of 5.1×10^6 , the boundary-layer disturbances on the sharp cone had grown to sufficient amplitudes to initiate second mode wave breakdown (presumably, an early stage of transition).

Fig. 9 compares maximum amplification rates associated with second mode disturbances for the cone with sharp and $R_N = 0.15$ inch nosetips. As mentioned previously, this 3% blunt nosetip completely stabilized the laminar boundary layer to local Reynolds numbers corresponding approximately to transition on a sharp cone at a unit Reynolds number of one million. Once the disturbances started to amplify in the boundary layer of the cone with 3% nosetip bluntness, the amplification rates steadily increased and surpassed the maximum rates obtained for the sharp cone.

Hot-wire stability data were also obtained with a nosetip radius of 0.25 inches (approximately 5% of the base radius). For this configuration, the boundary layer remained stable to the last measuring station on the model, which corresponded to a local length Reynolds number of 10.2×10^6 . The larger nosetip radius increased the extent of the entropy layer swallowing region. For a nosetip radius of 0.25 inches, the entropy layer was estimated to be mostly swallowed at an S/R_N of 152, or near the end of the model. Therefore, for both of these nosetips, the region of the cone frustum where the entropy layer was being swallowed by the boundary layer was a stable region. Although details of how nosetip bluntness influences boundary-layer stability are not yet available, it is evident that small nosetip bluntness makes significant changes in the history of the disturbance growth in a laminar boundary layer. With a sharp nosetip the first onset of disturbance growth (the minimum critical Reynolds number - this corresponds to the first

crossing of the lower neutral branch in Fig. 7) occurred at a low Reynolds number and was unknown for the present experiments. The disturbances amplified at a nearly constant rate and transition occurred at Reynolds numbers several times the value of the expected critical Reynolds number. With small nosetip bluntness the critical Reynolds numbers were extremely large and the disturbances amplified rapidly once the critical Reynolds number was exceeded. Transition information was not obtained; however, it would be expected that transition Reynolds numbers would not be a great deal larger than the critical Reynolds numbers.

Transition experiments have shown that there is a definite cut-off in the increased stability benefits to be derived from nosetip bluntness.²⁵ (These transition data will be discussed in Part 2.c). While small nosetip bluntness was found to increase the transition Reynolds number, additional increases in nosetip bluntness resulted in a drastic reduction in transition Reynolds number. It can be observed in Fig. 8 that significant disturbances were present at the first measuring station ($Re_x = 2.1 \times 10^6$), yet the boundary layer was stable and they were damped. It is speculated that, as the nosetip radius is increased, these nosetip region disturbances have a greater distance to grow in the vicinity of the nosetip and exceed some threshold amplitude which forces continued growth further downstream. Some exploratory hot-wire measurements were made with 0.5 inch and 0.7 inch nosetip radius. These experiments found disturbances in the entropy layer outside of the boundary layer. It is well known from inviscid stability theory that a local maximum in the vorticity distribution corresponds to a region of instability. In order to determine if the inviscid flow above the boundary layer of a blunt cone should be expected to be unstable on the basis of the distribution of angular momentum, a number of inviscid profiles of $\rho \partial u / \partial y$ were calculated using two different techniques (Helliwell and Lubard²⁶ and Kaul and Chaussee²⁷). It was not possible to identify a local maximum (a generalized inflection point) in any of the $\rho \partial u / \partial y$ distributions. In the boundary layer there are large variations in vorticity and the location of maximum vorticity is clearly evident. Outside the boundary layer the rate of change of vorticity is small and the vorticity may not have a clearly discernable local maximum. The hot-wire experiments clearly observed significant disturbances in the entropy layer outside of the boundary layer and, as the entropy layer was swallowed, these disturbances entered the boundary layer and experienced rapid growth.

The source of the inviscid disturbances and why they were unstable within the boundary layer at Reynolds numbers which were stable for small bluntness, is unknown. A possible explanation for the boundary-layer disturbance growth is that the situation is analogous to the forcing concept described by Kendall⁸ and Mack.⁶ Kendall found that when the boundary layer was subjected to a strong external disturbance environment, disturbances were found to grow before the predicted location of instability. It may be that, as the nosetip radius is increased, the entropy layer disturbances experience more growth, until they become large enough to drive the boundary-layer disturbances. Additional details of these stability experiments can be found in Ref. 11.

Hot-wire boundary-layer stability data were also obtained on the sharp cone at angle-of-attack. Data were obtained on the windward meridian at 2 and 4 degrees angle-of-attack and on the leeward meridian at 2 degrees angle-of-attack. Fig. 10 compares these data with the zero angle-of-attack of Ref. 10. It was found that the growth rates of the boundary-layer disturbances were not greatly affected by angle-of-attack; however, the onset of disturbance growth was significantly affected. The onset of disturbance growth was delayed on the windward meridian and occurred earlier on the leeward meridian, as compared with the zero angle-of-attack data. These stability trends are compatible with the observed movement of transition location with angle-of-attack. Details of these stability results can be found in Ref. 12.

The theory of Mack^{6,7} indicated that second mode disturbances would be destabilized by lowering the surface temperature. The hypersonic boundary-layer stability experiments of Demetriades⁹ confirmed that cooling the surface increased the growth rates of second mode disturbances and that the transition Reynolds number was reduced by a corresponding amount.

Fig. 11 compares second mode disturbance growth for a cooled and uncooled cone (from Ref. 14). The two frequencies selected correspond to the frequency of the maximum amplitude disturbances, just prior to transition. These disturbances are presumably representative of the disturbances which cause transition. Amplitude ratios vs. Reynolds number are shown. A_1 is the disturbance amplitude at the first measuring station. It can be seen that disturbances in the boundary layer on the cold wall grew much faster than those in the boundary layer of the hot wall. The initial amplitudes (A_1) are most likely different for the two cases shown, therefore, the significance of the difference between amplitude ratios at transition is not known.

Fig. 12 compares maximum growth rates for second mode disturbances for a cooled and uncooled cone (from Ref. 14). As observed in the previous figure, the second mode disturbances grew much faster in a cold wall boundary layer. Thus, these stability experiments confirm the prediction of stability theory that cooling the wall is destabilizing for second mode disturbances. The increased growth rates of the second mode disturbances for the cooler wall condition would be expected to result in a reduction in the transition Reynolds number. Boundary-layer transition data obtained by Demetriades⁹ and Stetson, et al^{10,13} indicated that transition Reynolds numbers were changing in a corresponding manner.

(1.d) COMPARISON OF THEORY AND EXPERIMENT

The early experiments of Kendall⁸ verified the existence and dominance of second mode disturbances in a hypersonic boundary layer. A more extensive comparison between theory and experiment was not made until Mack^{19,20} obtained numerical solutions for the conditions of the experiments of Ref. 10. The comparison was for a sharp cone at zero angle-of-attack in a perfect gas, Mach 8 flow (cone half angle = 7 deg., $Re_{\infty}/FT = 1 \times 10^6$, $M_e = 6.8$, $T_o = 1310^\circ R$, $T_w = 1100^\circ R$). The results of this comparison pointed out some discrepancies which presently cannot be explained and need to be resolved.

Fig. 13 compares maximum amplification rates at a local Reynolds number of 3×10^6 ($R = 1731$). The numerical results are shown with a line and the points are from the experimental data. The nondimensional frequencies below 0.8×10^{-4} are first mode instabilities and the angles shown are the most unstable oblique waves. The numerical results indicated that, for the second mode, two-dimensional disturbances were the most unstable and the numerical results for $F > 0.8 \times 10^{-4}$ are for two-dimensional, second mode disturbances. Since the second mode disturbances are the major disturbances which presumably initiate transition, they become the most important comparison. The most unstable frequency (the peak) is in close agreement; however, the maximum growth rate and the location of the upper neutral branch (where the amplification rates goes to zero) are significantly different.

Fig. 14 looks further into differences in disturbance growth rates by comparing the maximum amplification rate as a function of the square root of the length Reynolds number. Mack^{19,20} commented that all linear stability calculations for self-similar boundary layers give the trend of $(-\alpha_1)_{\max}$

increasing with increasing Reynolds number. The experimental data initially follow this trend, but at $R = 1400$, where the nonlinear disturbances became evident, the trend changed. There are significant differences between the calculated and experimental growth rates. Additional discussion of these comparisons can be found in Ref. 28.

This discussion does not mean to imply that linear theory is not valid for hypersonic boundary layers. All that can be said at present is there is a lack of agreement and the reasons are unknown. For the linearized stability calculations, there is concern as to the effects of the relatively large second mode disturbances and the presence of nonlinear disturbances. For the experimental data there is concern about the effects of the uncontrolled freestream environment and the hot-wire data reduction techniques. The experimental data are presently being re-assessed to address several of the hot-wire data reduction procedures. The comparison between theory and experiment is always a basic technology issue and this is an area of hypersonic transition which requires future emphasis. For subsonic and supersonic flows, linear stability theory has played a very important role in the understanding and in the prediction of transition. Linear stability theory is expected to play the same important role for hypersonic transition, but requires additional verification checks to determine the extent to which this will be possible.

PART 2: COMMENTS ON PARAMETRIC TRENDS

(2.a) INTRODUCTION

The transition of a laminar boundary layer to turbulence is a complex phenomena which is influenced by many contributing factors. Even though some parameters may play only a minor role in the transition process, the effects of the major parameters are usually interrelated and usually difficult to interpret. Numerous transition experiments have been performed over the years. Usually the location of transition is monitored as a parameter is varied. Such experiments have provided valuable information about the trends of the various parametric effects, but little information regarding the details of the transition process. Most of these transition experiments were performed in wind tunnels which had freestream environments much noisier than expected in flight; therefore, the transition Reynolds numbers obtained cannot be directly related to flight situations. The limited transition experiments performed in low disturbance (quiet) wind tunnels provide transition Reynolds numbers which are more comparable to flight, but still do not provide an understanding of the transition process. The most valuable information that can be obtained from the great mass of available transition data is the trends of the data, not the absolute magnitude of transition Reynolds number.

Following are brief comments regarding how the various parameters influence transition. The cited references should be consulted for additional details.

(2.b) EFFECT OF MACH NUMBER

For many years wind tunnel transition data had been put in the format of transition Reynolds number vs Mach number. There were significant variations in the magnitude of transition Reynolds, yet the trends were generally the same. Between $M \approx 1$ and 2.5-3, transition Reynolds number decreased with increasing Mach number and a minimum occurred at $M \approx 3-4$. Further increases in Mach number consistently increased the transition Reynolds number. Fig. 15 (from Ref. 29) illustrates this trend. The disturbances in the freestream of a wind tunnel, generated by the turbulent boundary layer on the nozzle wall, clearly have a large effect on transition on models in wind tunnels. The decrease in transition Reynolds number with Mach number in the supersonic range is most likely the result of the disturbances in the freestream of the

wind tunnels. Flight experiments on a 5-deg. half angle cone supported this contention by demonstrating that transition Reynolds number increased with Mach numbers up to $M = 2$ (the maximum Mach number of the experiment). Fig. 16 shows some of the flight data and compares flight transition data with wind tunnel transition data. All data were obtained with the same model and same instrumentation (Fig. 16 is from Ref. 30). Wind tunnel results at hypersonic Mach numbers have consistently shown a large increase in transition Reynolds number with increasing Mach number. Unfortunately it has not been possible to separate out the wind tunnel effects and the Mach number effects. Most experimenters have speculated that the Mach number effect in the hypersonic regime is one of increasing transition Reynolds number with increasing Mach number. This conclusion is further supported by theory. The stability theory of Mack^{6,7} has shown that, at hypersonic Mach numbers, the maximum amplification rates decrease as the Mach number increases. A decrease in the maximum amplification rate would be expected to result in larger transition Reynolds numbers. The Mach number effect may not be as pronounced in flight transition data as in wind tunnel transition data since in a wind tunnel the environment effect varies with the Mach number. Fig. 17 (from Ref. 31) includes additional data to illustrate Mach number effects on transition and includes both wind tunnel and flight results. The flight data has variations due to nosetip bluntness, angle-of-attack, wall temperature differences; and, at the higher Mach numbers, ablation and high temperature flow field effects. So many effects are simultaneously influencing flight transition data that comparisons with wind tunnel data can be misleading.

Available data suggests that high transition Reynolds numbers are to be expected on cones with small nosetip bluntness and small angles-of-attack when the local Mach number is like 10 or above. There is uncertainty as to the magnitude or the functional relationship between transition Reynolds number and Mach number. The correlation, $Re_\theta/M_\infty = \text{constant}$, requires a judgement as to this functional relationship. This topic will be discussed in more detail under Part 4.

(2.c) EFFECT OF NOSETIP BLUNTNESS

Wind tunnel experiments^{25,32} at $M = 6$ and $M = 9$, along with shock tunnel experiments,³³ have demonstrated that nosetip bluntness has a large effect on transition on the frustum of a slender cone. Small nosetip bluntness increases

the transition Reynolds number and large nosetip bluntness decreases the transition Reynolds number relative to the sharp cone. Also, the local Reynolds number is reduced as a result of nosetip bluntness and this can have a large effect on the location of transition. The nosetip of a sphere-cone configuration in hypersonic flow generates high entropy fluid (usually referred to as the entropy layer) which is subsequently entrained in the boundary layer as the boundary layer grows on the frustum. This is illustrated in Fig. 18 (from Ref. 25). The extent of the frustum boundary layer influenced by the high entropy fluid and the boundary layer edge conditions at a given frustum station depend upon both geometric and flow parameters. For a slender cone in hypersonic flow, and particularly with the thinner boundary layers associated with a cold wall condition, the entropy layer extends for many nose radii downstream (e.g., several hundred). In Fig. 19, boundary-layer calculations illustrate the large effect of a 0.04 in. nosetip radius (from Ref. 25).

In order to account for nosetip bluntness effects upon transition, the entropy layer effect should be considered. A simple and easy method for estimating the extent of the entropy layer and variations of boundary layer edge conditions can be made by assuming sphere-cone configurations and similarity of flows. For example, the method of Rotta,³⁴ permits such estimates without the use of local flow field calculations. Note that Rotta's method only applies to the case of highly cooled walls. Fig. 20 (from Ref. 25) provides a method to estimate entropy layer swallowing distances for highly cooled sphere-cones. Of course, if one has boundary-layer calculations available for a case in question, the entropy layer effects are included in those results. A number of comparisons of entropy layer swallowing distances estimated by the method of Rotta were found to correspond to locations where boundary layer code results indicated the local Mach number was 96 to 98 percent of the sharp cone value. This is considered to be excellent agreement. The two major effects associated with the entropy layer are changes in the transition Reynolds number and reductions in the local Reynolds number. The reduction of the local Reynolds number is an extremely important piece of information in the interpretation of nosetip bluntness effects on frustum transition; however, this is not the major issue since this information is readily obtainable, with uncertainties being related only to the accuracy and limitations of the flow field program being utilized. The major problem area is associated with understanding how nosetip bluntness affects the transition

Reynolds number. Limitations in the Reynolds number capability of wind tunnels have limited wind tunnel results to Mach numbers less than 10. These results are useful to illustrate trends; however, the effects of higher Mach numbers and the magnitude of transition Reynolds numbers expected in free flight are not well known. Fig. 21 (from Ref. 25) contains the results from a large amount of nosetip bluntness data obtained in a Mach 6 wind tunnel. The movement of transition location is shown, along with changes in transition Reynolds number and the Reynolds number reduction which contributed to the changes in transition location. Note that when the entropy layer was nearly swallowed at the transition location (X_T/X_{sw} close to 1), the transition Reynolds numbers were significantly larger than sharp cone transition Reynolds numbers and the Reynolds number reduction was small. The change in transition location in this region was primarily a function of the change in transition Reynolds number. The maximum change in transition location occurred in regions of the entropy layer where the transition Reynolds numbers were less than the sharp cone values and the Reynolds number reduction was the major effect. For maximum transition displacement, the local Reynolds number was reduced by a factor of 7.3 and the transition Reynolds number was 58% of the sharp cone value, with the displacement being represented by the product of the two effects, or 4.2 times the sharp cone transition location.

The Reentry F flight experiment^{35,36} is probably the best source of data for the effect of nosetip bluntness on slender cone transition in hypersonic free flight. The lack of information regarding the nosetip changes during reentry as a result of ablation, along with small angles of attack, produce some uncertainties in the interpretation of the results.

There is another nosetip consideration that should be included - the very low transition Reynolds numbers associated with transition on the nosetip and the region of the frustum just downstream of the nosetip. Nosetip transition Reynolds numbers can be as much as two orders of magnitude less than cone frustum transition Reynolds numbers. This situation requires that a separate transition criteria be applied to this portion of a configuration. The potential of transition first occurring in this region, and producing a turbulent boundary layer over the entire portion of the configuration influenced by the tip, must be considered. It is well documented that blunt nosetips have low transition Reynolds numbers, even at hypersonic freestream Mach numbers (e.g., Refs. 37-39). Boundary-layer transition has been related

to the local boundary properties at the sonic point and the surface roughness. The low transition Reynolds numbers associated with the region of the frustum just downstream of the nosetip has only recently been identified²⁵ and the transition criteria for this region is not as well understood as that of the nosetip. It appears that transition in this region is dominated by the nosetip and may be related to nosetip conditions, analogous to nosetip transition criteria. Fig. 22 (from Ref. 25) provides an example of transition criteria for transition on the nosetip and also those conditions which produced early frustum transition for Mach 5.9 wind tunnel experiments.

(2.d) EFFECT OF CROSSFLOW

Crossflows associated with three-dimensional flow fields such as axisymmetric configurations at angle-of-attack, non-circular cross-sections at zero and nonzero angle-of-attack, spinning vehicles, and swept wings can be very unstable. Most of our knowledge of crossflow effects comes from low speed studies (e.g., Poll,⁴⁰ Arnal,⁴¹ and Saric and Reed⁴²). The flow field is broken down into a two-dimensional, streamwise profile and a crossflow profile. Transition is estimated by calculating a two-dimensional Reynolds number and a crossflow Reynolds number. It was found that when the crossflow Reynolds number exceeded a threshold value, the crossflow instability usually dominated. That is, if the crossflow Reynolds number was below the threshold value, transition could be estimated from the Reynolds number based upon the two-dimensional component of the flow. When the crossflow Reynolds number exceeded the threshold value, transition occurred regardless of the two-dimensional Reynolds number. For example, Owen and Randall's⁴³ subsonic experiments with a swept wing observed an instantaneous jump of transition from the trailing edge to near the leading edge when a critical crossflow Reynolds number was exceeded. This critical crossflow Reynolds number was approximately 175, based upon the maximum crossflow velocity, a thickness defined as nine-tenths of the boundary-layer thickness, and the density and viscosity at the edge of the boundary layer $(Re_{CF} = \frac{\rho_e w_{max}}{\mu_e} .9\delta)$.

Pate's⁴⁴ results indicated that this criterion could be extended to supersonic Mach numbers. However, higher values of critical crossflow Reynolds number have been obtained for incompressible flows and there is uncertainty as to the generality of this criterion. The appropriate value for hypersonic flows is unknown and must be estimated on the basis of lower speed transition experime

Most of the hypersonic data base associated with crossflow effects is for cones at angle-of-attack and the remaining discussion will be on this aspect of the problem. Intuition derived from boundary-layer transition results at zero angle-of-attack is not very helpful in predicting the transition trends on a sharp cone at angle-of-attack. The effect of angle-of-attack is to increase the local Reynolds number and decrease the local Mach number on the windward ray. One might logically assume that transition would then move forward on the windward ray with increases in angle-of-attack. On the leeward ray the local Reynolds number decreases and the local Mach number increases. Based upon results obtained at zero angle-of-attack, it might be expected that transition would move rearward on the leeward ray with increases in angle-of-attack. In reality, just the opposite of these trends occurs. Transition experiments with a sharp cone have consistently found a rearward movement of transition on the windward ray and a forward movement on the leeward ray (see, for example, Ref. 45). Transition location was found to be sensitive to small changes in angle-of-attack for both sharp and blunt-tipped configurations. For configurations with nosetip bluntness one has to consider the combined effects of nosetip bluntness and angle-of-attack. The angle-of-attack trends appear to be predictable; however, the magnitude of the resulting transition Reynolds numbers are not. Fig. 23 (from Ref. 45) illustrates the transition movement on the windward and leeward rays of sharp and blunt 8-deg. half angle cones at $M_\infty = 5.9$. The transition distance (X_T) is normalized by the transition distance on the sharp cone at $\alpha = 0$ deg. [$(X_{TS})_{\alpha=0}$ varies with unit Reynolds number]. Fig. 24 (from Ref. 45) is a sample of the transition patterns obtained for a sharp cone. $\phi = 0$ deg. is the windward meridian and $\phi = 180$ deg. is the leeward meridian. The shaded area represents the transition region, with curve B indicating the beginning of transition and curve E the end of transition. The beginning and end of transition at $\alpha = 0$ deg. is shown for reference. Fig. 25 (from Ref. 45) presents a summary of the sharp cone angle-of-attack results, in a nondimensionalized format. Figures 26 and 27 (from Ref. 45) present similar results for a cone with 10% nosetip bluntness ($R_n = 0.2$ in).

(2.e) EFFECT OF UNIT REYNOLDS NUMBER

For some time there has been evidence that transition Reynolds number was influenced by the unit Reynolds number. Numerous wind tunnel experiments have

documented the results that increasing unit Reynolds number increases the transition Reynolds number. A suitable explanation and an accounting of the phenomena involved is still not complete. Because the examples of this effect were almost exclusively from wind tunnel experiments and because of the possibility that wind tunnel freestream disturbances were responsible, there has been uncertainty as to whether the so-called unit Reynolds number effect exists in flight. Potter^{46,47} performed extensive ballistic range experiments to investigate unit Reynolds number effects in ballistic ranges. Potter's conclusions were that a unit Reynolds number effect existed in the free flight range environment. In fact, the increases of transition Reynolds number with increases in unit Reynolds number were even larger in the ballistic range than in wind tunnels. He found that none of the range-peculiar conditions could offer an explanation for this effect. Fig. 28 (from Refs. 46 and 47) is a sample of Potter's results. Additional discussions of unit Reynolds number effects on transition have been made by Reshotko⁴⁸ and Stetson, et al.^{12,13} Unit Reynolds number effects have a very important coupling with environmental effects. For a low disturbance environment, the environmental disturbances provide the stimulus for exciting boundary-layer disturbance growth and are responsible for the initial boundary-layer disturbance amplitudes. If, by some mechanism, the initial amplitude of the most unstable boundary-layer disturbances could be increased or decreased, the transition Reynolds number would correspondingly be increased or decreased (this will be discussed under the next topic, environmental effects). The unit Reynolds number, in effect, provides a possible mechanism. The frequencies of the most unstable boundary-layer disturbances are directly related to the unit Reynolds number (by the effect of unit Reynolds number on boundary-layer thickness, as discussed in Part 1). Thus, increasing unit Reynolds number increases the frequency of the most unstable boundary-layer disturbances, which means that the most important environmental disturbances are of higher frequency. The higher frequency environmental disturbances will, very likely, have a smaller amplitude and, in some situations, a suitable environmental stimulus may be lacking for some frequencies. Intuitively, it would be expected that unit Reynolds number, through its control of the frequency of the most unstable boundary-layer disturbances, would influence transition. Morkovin has commented many times that unit Reynolds number probably influences transition in several ways, thus other unit Reynolds number effects should be considered likely.

The conclusion is that until additional flight transition data is obtained, we should assume that unit Reynolds number will influence transition in flight. Additional knowledge of the disturbance environment through which the vehicle is flying and a better understanding of the physical mechanisms which cause transition will help determine the magnitude of these effects.

(2.f) EFFECT OF THE ENVIRONMENT

The freestream environment and the relationship between the environment and the boundary-layer disturbances responsible for transition are of great significance to boundary-layer transition. The environment provides an extremely important initial condition for any boundary-layer transition problem. The environment provides the mechanism by which boundary-layer disturbance growth is generally initiated and establishes the initial disturbance amplitude at the onset of disturbance growth. Based upon the supposition that transition occurs when some boundary-layer disturbances have obtained the critical amplitude required for breakdown of the laminar flow, a change in the initial amplitude of the dominant disturbances changes the required period of growth to obtain the critical amplitude. Thus, a change of the environment will most likely change the transition Reynolds number. This critical element of the transition problem is often overlooked. Then one or several sets of data are used to make a transition prediction in a new situation, a similarity is implied for not only the geometric and flow parameters, but also the environment. It is assumed that the case in question has the same environment as the data base. Environmental differences provide a reasonable explanation for most of the differences in transition Reynolds numbers obtained in wind tunnels and those obtained in flight. In supersonic and hypersonic wind tunnels the strong acoustical disturbances in the freestream which are generated by the turbulent boundary layer on the wall of the nozzle generally produce transition Reynolds numbers lower than found in flight. Differences in wind tunnel environments can result in significant differences among wind tunnel transition Reynolds numbers, thus presenting problems in correlating only wind tunnel transition data. The data of Schubauer and Skramstad⁴⁹ and Wells⁵⁰ provide an interesting example. The classical experiments of Schubauer and Skramstad were carried out on a sharp, flat plate in a low turbulence, low speed wind tunnel. Turbulence levels in the freestream could be controlled by varying the number of damping screens. Transition Reynolds numbers were found

to be directly related to the freestream turbulence level, with transition Reynolds number increasing as the turbulence level decreased. At low tunnel turbulence levels, the transition Reynolds number obtained a maximum value of 2.8×10^6 and remained at this level with still further reductions in turbulence levels. Wells repeated this experiment in a different wind tunnel. In the Schubauer and Skramstad experiment, control over the damping screens provided control over the velocity fluctuations in the freestream of their wind tunnel but the screens had little effect on the acoustical disturbances which were present. In the Wells experiment, the tunnel was designed so as to minimize the acoustical disturbances as well as to provide control over the velocity fluctuations. Wells found the same trends as obtained by Schubauer and Skramstad, but his maximum transition Reynolds number was approximately 5×10^6 . Both experiments were dealing with the same boundary layer phenomena. What was different was the environment. Fig. 29 (from Ref. 50) contains these results. Wells indicated that most of the freestream energy in his experiment occurred at frequencies below 150 cps with acoustic content less than 10% of the total energy. The tests of Schubauer and Skramstad involved significant energy levels out to 400 cps, and, in addition, the spectrum exhibited large acoustic energy peaks at 60 and 95 cps which accounted for approximately 90% of the total disturbance energy that was measured for intensities less than about 0.05%. Spangler and Wells⁵¹ continued the study by systematically investigating the effects of acoustic noise fields of discrete frequencies. Large effects were found when the acoustic frequencies (or a strong harmonic) fell in the range where Tollmien-Schlichting waves were unstable. It is significant to note that transition prediction methods cannot account for these large differences in transition Reynolds number unless the differences in the freestream environment are somehow taken into account.

Not all freestream disturbances are important to boundary-layer transition. Some disturbances may have frequencies that do not correspond to unstable boundary-layer frequencies. Thus, these disturbances, upon entering the boundary layer, will be stable and attenuate. Other freestream disturbances may influence only slowly growing boundary-layer disturbances which do not grow large enough to affect transition. It is believed that the critical environmental disturbances are those disturbances of the same frequency as the boundary-layer disturbances responsible for transition. Therefore, it is important to identify the dominant boundary-layer disturbances and the amplitudes

of the corresponding environmental disturbances at the same frequency. This requires that consideration be given to the spectral content of the environmental disturbances.

Environmental disturbances are predominantly of low frequency and the most unstable hypersonic boundary-layer disturbances are of relatively high frequency. Thus an important consideration for hypersonic boundary-layer transition is whether or not the disturbance environment will provide a suitable stimulus to excite the most unstable boundary disturbances. Normally one would expect the most unstable disturbances to have the most rapid growth and be the first disturbances to obtain the critical amplitude which produced nonlinear effects and the eventual breakdown of the laminar flow. If transition must wait for disturbances with a smaller growth rate to obtain the critical amplitude, then a delay in transition would be expected. There are many hypersonic flow situations, both in ground test facilities and in flight, where the potentially most unstable boundary-layer disturbances may not be excited. Thus, some transition delay, due to a lack of environmental stimulus of the potentially most unstable disturbances, may be a common hypersonic occurrence. Stetson¹² has pointed out that for a sharp, 7-deg half angle cone in a Mach number 8 wind tunnel at a freestream unit Reynolds number of 20 million, the most unstable boundary-layer disturbances would have frequencies greater than a megahertz. Available instrumentation cannot measure disturbances in this frequency range; however, it seems unlikely that there would be much freestream disturbance energy at such high frequencies to stimulate boundary-layer disturbance growth. Transition under this situation would be expected to be the result of disturbances which were not the theoretically most unstable. This should provide larger transition Reynolds numbers. The Reentry F flight experiment³⁵ reported transition Reynolds numbers as high as 60 million. An estimation of the frequency of the most unstable boundary-layer disturbances indicated they were greater than 500 kHz. There is a possibility that these high transition Reynolds numbers were obtained because the theoretically most unstable disturbances were not present.

Another important aspect of the disturbance environment is the receptivity (Morkovin¹) of the boundary layer to these disturbances. Receptivity relates to the response of the boundary layer to the environmental disturbances and the resulting signature of these disturbances within the boundary layer. Receptivity has long been recognized as an important problem; however, an

understanding of this problem has been slow to develop. Reshotko has discussed the receptivity problem in several papers.^{2,3,52}

The sobering environmental conclusion is that even if we could perform a miracle and obtain an analytical method to calculate exactly the stability characteristics of the boundary layer and the breakdown to turbulence, we would still have problems predicting transition because we would still have to somehow prescribe the external disturbances. The freestream disturbances are a very important initial condition of any boundary-layer transition problem and, unfortunately, they are generally not well known. The uncertainty of the disturbance environment in flight puts an additional uncertainty into any transition prediction.

(2.g) EFFECT OF WALL TEMPERATURE

The temperature of the surface of a vehicle or model can have a large effect on boundary-layer transition. One of the results from the compressible stability theory of Lees¹⁸ was the prediction that cooling the wall would stabilize the boundary layer. Calculations were subsequently made which indicated that, with sufficient cooling, the boundary layer could be made completely stable at any Reynolds number (e.g., Van Driest⁵³). A number of experiments followed to verify the prediction of the stabilizing effect of wall cooling. The results demonstrated one more time the complicated, inter-related involvement of transition parameters. The trend of increasing transition Reynolds numbers with increasing wall cooling was confused by a transition reversal. That is, situations occurred in which the stabilizing trend of wall cooling was reversed and further cooling resulted in a reduction of transition Reynolds number. In very highly cooled cases, there was evidence of a re-reversal, a return to a stabilizing trend. Fig. 30 (from Ref. 33) illustrates some of these results. There were attempts to explain transition reversal on the basis of a surface roughness effect; however, much of the data did not seem to support the roughness argument. The roughness issue for very cold wind tunnel models was considered more recently by Lysenko and Maslov.⁵⁷ They determined that ice crystals on the wind tunnel model could trip the boundary layer. Transition reversal, as a result of wall cooling, has remained a controversial subject.

Hypersonic wind tunnel transition data have provided conflicting results regarding the effects of surface temperature. Fig. 31 contains supersonic and

hypersonic wind tunnel data collected by Potter.⁵⁸ $(Re_{XT})_{AD}$ is the transition Reynolds number obtained under adiabatic conditions and M_e is the Mach number at the edge of the boundary layer. Wall cooling is seen to significantly increase the transition Reynolds number for the lower supersonic Mach numbers, with a lesser effect at hypersonic Mach numbers. The results of Sanator, et al⁵⁹ (not shown in Fig. 31 because the value of $(Re_{XT})_{AD}$ was not known) at $M_e = 8.8$ found no significant change of transition location on a sharp cone with changes of T_w/T_o from 0.08 to 0.4. Some additional data (not shown in Fig. 31) of Stetson and Rushton³³ at $M_\infty = 5.5$ and Mateer⁶⁰ at $M_\infty = 7.4$ report a reduction in transition Reynolds number with a reduction in the temperature ratio.

The hypersonic transition trends shown in Fig. 31 can generate some interesting speculation, since they are in contradiction with theory and boundary-layer stability experiments. The low supersonic boundary layers should contain only first mode disturbances which are stabilized by surface cooling. The low Mach number transition data are compatible with the theoretical trends. The hypersonic boundary layers would be expected to have both first and second mode disturbances, with the second mode disturbances as the dominant disturbances. The fact that the hypersonic boundary-layer transition data have the same trend as the supersonic data raises the question of the dominance of the second mode disturbances. As mentioned previously, it has been speculated that there may be hypersonic flow situations, both in ground test facilities and in flight, where the potentially most unstable second mode disturbances are not excited. The movement of transition location with changes in surface temperature may be a good indication of the role of second mode disturbances. This is an important hypersonic transition issue that needs future attention.

There is agreement among stability theory, stability experiments, and transition experiments which have been conducted in conjunction with stability experiments such that it was evident that second mode disturbances were the major disturbances. When second mode disturbances are known to be the dominant disturbances, cooling the surface significantly reduces the transition Reynolds number.

Surface temperature is seen to have a potentially large effect on hypersonic boundary-layer transition, with wall cooling expected to be stabilizing for first mode disturbances and destabilizing for second mode disturbances.

The problem is that unless the identity of the major disturbances is known (or predictable) one does not even know if the proper trend is increasing or decreasing transition Reynolds number.

(2.h) EFFECT OF SURFACE ROUGHNESS

The physical mechanisms by which roughness effects transition are not well understood. Usually the only parameter measured is the movement of transition location and the details of what is causing the movement are unknown. Small roughness is not believed to generate hypersonic boundary layer disturbances. It was generally believed that small roughness effected transition by changing the mean flow characteristics of the boundary layer in such a manner as to increase the growth rate of disturbances already present in the boundary layer. However, experiments by Reshotko and Leventhal,⁶¹ Corke, Bar-Sever and Morkovin,⁶² and Kendall⁶³ have raised some new issues. All experiments addressed Blasius-like boundary layers for simplicity and standardization. The first two experiments measured the growth of naturally occurring flow fluctuations as the laminar boundary layer passed over sand-paper roughness. Kendall chose to measure the mean velocity profiles. The stability experiments found fluctuation growth rates which exceeded theoretical Tollmien-Schlichting-instability values and observed unexpected low frequency fluctuations below the frequency range of TS instabilities. The increased TS growth rates are speculated to result from profile distortion and possibly unsteady behavior close to the wall and below the roughness element tops. The low frequency disturbances are thought to result from some nonlinear by-pass phenomenon.

Experiments have shown there is a minimum size of roughness elements which will influence transition. Below this minimum the surface is considered to be aerodynamically smooth. If roughness elements are large enough to generate locally separated flow about the roughness elements, they can produce small regions of turbulence which can become a mechanism for exciting new boundary-layer disturbance growth. In this case, roughness not only increases the growth rate of those disturbances already present, but introduces new disturbances. It is speculated that such a mechanism may be responsible for exciting boundary-layer disturbance growth in flight in a frequency range where the freestream environment had not provided the stimulus. Large roughness greatly distorts the boundary layer and further complicates an under-

standing of the phenomena. The relative size of roughness elements is usually determined by comparing it to the boundary layer thickness. Any effect which influences boundary layer thickness can affect the influence of roughness. Therefore, body location, unit Reynolds number, wall temperature, Mach number, and mass addition or removal can all influence the effect of roughness. Wind tunnel experiments have shown there is a strong effect of Mach number on roughness effects. The roughness size required to trip the boundary layer increases rapidly with increasing Mach number and even at low hypersonic Mach numbers the roughness heights required are of the same order as the boundary layer thickness (e.g., see Ref. 64). Part of the problem is trying to understand roughness effects is associated with the many roughness parameters involved. Roughness is usually characterized by its height, but other parameters, such as, configuration and spacing are very important. Also important are whether the roughness elements are two-dimensional or three-dimensional, individual elements or distributed (e.g., sand grain) type. The nosetip of a hypersonic vehicle, where the Mach number is subsonic and the boundary layer is very thin, can be very sensitive to roughness. The frustum of a hypersonic vehicle, where the local Mach number is hypersonic and the boundary layer is relatively thick, is expected to be insensitive to small or moderate roughness.

(2.1) EFFECT OF PRESSURE GRADIENT

The general effects of pressure gradients are well known for situations where transition results from first mode instabilities. Both theory and experiment have shown that favorable pressure gradients stabilize the boundary layer and adverse pressure gradients destabilize the boundary layer. In many cases pressure gradient effects are simultaneously combined with other effects so the resultant effect is not always as expected. Stetson²⁵ has illustrated a hypersonic flow situation (the local Mach number was supersonic) on a sphere-cone where the transition Reynolds number decreased as the favorable pressure gradient increased (moving closer to the nosetip). Apparently the destabilizing effect of the nosetip was more powerful than the stabilizing effect of the pressure gradient. Also, the same paper reports that the adverse pressure gradient on the cone frustum did not have a significant effect on transition.

Surfaces which generate pressure gradients may sometimes generate Görtler vortices, and this further complicates the understanding of transition associ-

ated with pressure gradients. It is then necessary to consider the two competing effects on transition -- the effect of the first and second mode disturbances and the effect of the Görtler vortices. When there exists a concave curvature of the streamlines (not necessarily a concave surface) the associated centrifugal forces result in the formation of pairs of counter-rotating vortices called Görtler vortices, the axes of which are parallel to the principal flow direction (see Fig. 32). The growth of Görtler vortices can be calculated from a linear stability theory (e.g., see the papers of Floryan and Saric,⁶⁵ El-Hady and Verma,⁶⁶ and Spall and Malik⁶⁷). Experimentally, surface visualization techniques, such as oil flow, are believed to show the existence of Görtler vortices. Also, Ginoux⁶⁸ noted that the vortices produce large peaks in the heat transfer rate in the lateral direction. An interesting case has been found in the study of transition on wind tunnel nozzles. Transition was found to occur on Mach 3.5 and 5 nozzle walls earlier than expected.^{69,70} Oil flow studies showed streaks that were believed to result from Görtler vortices. Stability calculations,⁷¹ for the $M = 3.5$ nozzle, indicated that the strong favorable pressure gradient damped the first mode disturbances and the Görtler vortices were the major disturbances.

There is insufficient information available at present to make a prediction of the effect of a specific pressure gradient on hypersonic boundary-layer transition. Stability and transition experiments are being planned to study adverse pressure gradient effects and, hopefully, some guidance is forthcoming.

(2.1) EFFECT OF MASS TRANSFER

As with pressure gradients, mass transfer effects can be described only in a general way. Experiments have shown that suction stabilizes the boundary layer. It produces a "fuller" velocity profile, just as a favorable pressure gradient, and a more stable boundary layer. Blowing destabilizes the boundary layer, analogous to the adverse pressure gradient. Details of the effects of mass flow weights, gas composition, and mass transfer methods are too sketchy to be of much assistance in predicting the effects of mass transfer on hypersonic boundary-layer transition in a specific situation. Mass transfer effects must also be considered in combination with other effects; for example, its effect on roughness and surface cooling.

Wind tunnel experiments by Martellucci⁷² confirmed that mass transfer had a destabilizing effect upon the boundary layer. He noted that the effects of mass transfer were much like surface roughness. When the mass was injected at a subcritical value, no influence on transition was noted; however, at a discrete value of blowing (termed the critical value) transition was affected and moved rapidly forward.

(2.k) EFFECT OF HIGH TEMPERATURE/NONEQUILIBRIUM

This is an area which has only recently been addressed. Using linear stability theory as a guide, any effect which changes the boundary-layer profiles will influence boundary-layer stability. Therefore, high temperature and nonequilibrium effects would be expected to influence transition. Ground test facilities will not be of much help due to their limitations, so flight test results and stability calculations must be relied upon for the answers. Mach 20 reentry vehicle transition data contains some high temperature, equilibrium flow effects. Nonequilibrium flow field effects are generally thought to be associated with the region downstream of a strong shock where the gas temperatures are sufficiently large to produce various dissociations, rearrangements, and ionization reactions (such as, behind a blunt nose) and for low density conditions (high altitudes) such that the chemical reactions are not fast enough to attain an equilibrium condition with the changing flow field. Whether or not nonequilibrium effects will be significant at altitudes relevant for boundary-layer transition presently does not have a general answer and will probably require a judgement for the specific case being considered. Eventually, stability calculations should provide better insight into these problems.

(2.1) EFFECT OF VIBRATION

Vehicle or model vibration is not normally considered to be a major parameter influencing boundary-layer transition. However, for a vehicle which has an operating engine, vibration effects should not be ignored. Intuitively one would expect structural vibrations to be at such a low frequency relative to the most unstable boundary-layer frequencies, that they would be of little consequence.

PART 3: SOME ADDITIONAL GENERAL COMMENTS

There are several disturbance mechanisms which, given the right conditions, can produce boundary-layer disturbances sufficiently large to cause transition to turbulence. Also, flow and vehicle parametric effects have various influences on the growth of the boundary-layer disturbances and, thus, can produce large variations in transition Reynolds numbers. Variations of the freestream disturbance environment can also influence the path to turbulence. Following is an attempt to categorize the disturbance mechanisms under the heading of those described by linear theory and those which are not.

(3.a) MECHANISMS DESCRIBED BY A LINEAR THEORY

For a small-disturbance freestream environment there are four fundamentally different instability mechanisms described by a linear theory which can produce disturbance growth in a hypersonic boundary layer.

First Mode, Tollmien-Schlichting (TS): In an incompressible boundary layer a viscous instability produces low frequency, vorticity disturbances which are most unstable as two-dimensional disturbances. Inviscid instability increases with Mach number and for hypersonic boundary layers much information can be obtained from inviscid theory. Hypersonic first mode disturbances are most unstable as oblique waves and generally are slowly growing disturbances which are not expected to become the dominant disturbances.

Second Mode (Mack Modes): Second mode disturbances are unique to a high Mach number boundary layer since they require a region of the boundary layer near the wall to be supersonic relative to the mean velocity at the generalized inflection point. This instability produces high frequency, acoustical-type disturbances which grow faster than T.S. disturbances, yet may still have relatively slow growth rates compared to other potential disturbances. Second mode disturbances should be the dominant disturbances in situations where there are no major cross-flow, Görtler, or by-pass disturbances.

Crossflow: An inflectional instability of the crossflow velocity profile. Little is known about the characteristics of these disturbances. Experimental transition data imply these disturbances can have rapid growth rates and they may be the dominant disturbances in three-dimensional flow fields.

Görtler: A centrifugal instability due to concave streamline curvature. This instability produces counter-rotating streamwise vortices, which, under some conditions, appear to dominate the transition process. Little is known about Görtler vortices in a hypersonic boundary layer and how they interact with other disturbances, such as, second mode disturbances.

Linear stability theory provides a valuable tool to study parametric effects and has been utilized to describe the features of Tollmien-Schlichting, Mack, and Görtler disturbances. Eventually linear theory can be expected to address the crossflow disturbances.

(3.b) MECHANISMS NOT DESCRIBED BY LINEAR THEORY

Most of our understanding of boundary-layer stability is associated with those phenomena which can be described by a linear theory. Other aspects of stability and transition which are not described by a linear theory are poorly understood. For example, the characteristics of large boundary-layer disturbances (too large for a linear theory) and the features of the final breakdown to turbulence are not known and there is no theory available for guidance. Another class of disturbance phenomena falls under the heading of what Morkovin¹ refers to as a "by-pass," since transition in these cases has by-passed the known linear processes. In some situations, disturbances apparently grow very rapidly by some forcing mechanism and produce transition at very small Reynolds numbers, where linear stability theory would indicate that the boundary layer would be stable for all disturbances.

An example of by-pass transition occurs with high turbulence levels in the freestream. Reshotko³ discussed the classic example of Poiseuille pipe flow. Another case was observed by Kendall⁸ in wind tunnel experiments at a Mach number of 4.5. Disturbances of all frequencies were observed to grow monotonically larger in the region of a boundary layer extending from the flat plate leading edge to the predicted location of instability; i.e., in a region where linear stability theory indicated the boundary layer should be stable for all disturbance frequencies. This early growth of disturbances was attributed to the strong sound field generated by the turbulent boundary layer on the nozzle wall.

In any new transition situation there should be concern about unexpected transition behavior. The ballistic reentry transition problem of the 1950s should be remembered as a example of how wrong we can be. The blunt copper

heat sink reentry vehicles were initially designed on the basis of maintaining a laminar boundary layer throughout reentry, all the way to impact. Having a laminar boundary layer to impact was then a logical conclusion, based upon knowledge available at that time. The stability of Lees¹⁸ had indicated that wall cooling was very stabilizing. Van Driest⁵³ had made calculations which indicated after a certain cooling temperature ratio was exceeded, the boundary layer remained laminar for any Reynolds number. Sternberg's⁷³ V-2 flight had obtained laminar Reynolds numbers up to 90×10^6 (which is still believed to be the highest laminar Reynolds number ever reported), thus supposedly confirming the predictions of the stabilizing effects of cold walls. The heat sink reentry vehicle, in addition to having a highly cooled boundary layer, had a strong favorable pressure gradient which would be expected to provide additional stability. It was easy to conclude that the boundary layer would remain laminar until impact. Subsequent shock tube experiments (these results later appeared in the unclassified literature as Ref. 37) and flight experiments gave surprising results. It was found that a highly cooled blunt body does not maintain a laminar boundary layer to large Reynolds numbers, but, in fact, has very low transition Reynolds numbers. Transition on relatively smooth bodies typically occurred at length Reynolds numbers as low as 0.5×10^6 ($Re_\theta \approx 300$). Surface roughness produced even lower transition Reynolds numbers. It is now more than thirty years later and an explanation of this blunt body paradox is still lacking.

Little is known about by-pass phenomena at this time. Therefore, for new transition situations, the transition predictor should consider the possible consequences of the low transition Reynolds numbers that might result if by-pass transition occurs.

Surface roughness is another mechanism influencing disturbance growth which cannot be described by linear theory. Fortunately, experiments have demonstrated that the hypersonic boundary layer is rather insensitive to surface roughness. However, the nosetip or wing leading edge of a hypersonic vehicle is a different situation. In situations where the boundary layer is thin and the local Mach number is small, surface roughness can be a dominating factor.

(3.c) CONFIGURATION DIFFERENCES

Be aware of the influence of configuration differences on transition.

Most of the available hypersonic transition data base is for conical configura-

tions and these data are being used to estimate transition on non-axisymmetric configurations. The cone vs flat plate issue illustrates the problem. Up until recently, it had generally been assumed that one should obtain higher transition Reynolds numbers on cones than on flat plates, at least between Mach numbers 3 and 8. This trend was consistently evident in wind tunnel data. Pate⁷⁴ made an extensive analysis of this problem and Fig. 33 is taken from his paper. At $M_\infty = 3$, cone transition Reynolds numbers were from 2.2 to 2.5 greater than flat plate transition Reynolds numbers. The value decreased monotonically with increasing Mach number to approximately 1.0 to 1.1 at $M_\infty = 8$.

Early stability analyses were for planar boundary layers. Recently these analyses have been extended to axisymmetric boundary layers. These new axisymmetric results logically led to a comparison of planar vs axisymmetric stability results and papers by Mack^{19,20} and Malik²² addressed this problem. Their numerical results indicated that disturbances begin to grow sooner on a plate (smaller Re_c), but they grow slower than in a cone boundary layer. This result would suggest that, for a quiet environment, thus a long distance of disturbance growth before transition, plate transition Reynolds numbers should be greater than cone transition Reynolds numbers, just the opposite of the wind tunnel results. Subsequently, experiments were performed in the NASA/Langley Research Center Mach 3.5 quiet tunnel to investigate this issue.²³ The ratios of cone-to-flat-plate transition Reynolds numbers were found to vary from about 0.8 for low-noise freestream conditions to about 1.2 for higher noise conditions. These new quiet-tunnel experimental results support the implications of the analytical results obtained using linear stability theory and indicate that the transition data of Fig. 33 was not a general result, but was dominated by wind tunnel freestream noise.

Recently, Mach 8 stability and transition data have been obtained with a 10 inch diameter hollow cylinder with a sharp leading edge (Stetson et al, to be published). These cylinder data should be equivalent to the planar data of a sharp flat plate. The cylinder was water-cooled, thus permitting a comparison with the water-cooled, 7-degree half angle cone data obtained in the same Mach 8 wind tunnel.¹⁴ Heat transfer rate data were used to determine the location of boundary-layer transition and hot-wire data provided details of the boundary-layer disturbances. These transition data were consistent with previous transition results from conventional wind tunnels. The cone transition

Reynolds numbers were approximately 3.2×10^6 and the cylinder transition Reynolds numbers were approximately 2.7×10^6 , resulting in a cone-to-cylinder ratio of 1.19 (this is in close agreement with the data of Fig. 33). Also, the second mode disturbance growth rates obtained from the hot-wire data were consistent with the previously mentioned numerical results. The second mode disturbances in the planar boundary layer were found to have smaller growth rates than second mode disturbances in a conical boundary layer. Thus these new data support the apparent contradiction between stability analytical results and conventional wind tunnel transition data. Details of the cone vs plate issue are still lacking; however, it appears evident that the results of Fig. 33 should not be used for flight applications.

(3.d) SOME PROBLEMS OF WIND TUNNEL TRANSITION DATA

Historically, the wind tunnel has been the major source of boundary-layer transition information. Often these wind tunnel data have become the primary data base used to develop transition correlations and to establish transition criteria for flight. During the late 1950s and the 1960s, the identification and understanding of wind tunnel freestream disturbances provided an explanation for wind tunnel transition Reynolds numbers being smaller than flight transition Reynolds numbers. A quiet wind tunnel (freestream disturbance amplitudes reduced to a small value) was proposed as a way of obtaining wind tunnel transition Reynolds numbers which would be comparable in magnitude to flight values. However, it is important to keep in mind that one should not expect a transition Reynolds number obtained in any wind tunnel, conventional or quiet, to be directly relatable to flight.

Only in a few isolated cases can one expect to duplicate hypersonic flight conditions in a wind tunnel. Furthermore, even though the configuration can be duplicated, it is usually of a relatively small scale. Thus, one must rely on similarity parameters and extrapolation procedures in order to use wind tunnel data for flight vehicle design and performance predictions. For wind tunnel transition experiments, in addition to similarity in terms of Mach number and Reynolds number, one must also be concerned with similarity of freestream environments and similarity of boundary-layer profiles.

An internal flow system, such as a wind tunnel, has a number of sources to generate velocity, temperature, and acoustical fluctuations not present within the atmosphere. It is well known that the freestream of a wind tunnel

is a different environment than found in the atmosphere. One can reduce the amplitude of these disturbances, as in a quiet tunnel, but it is unrealistic to think of duplicating the atmospheric environment in a wind tunnel. The flight environment is mostly unknown and is probably time-dependent. So one must live with a wind tunnel environment which is different than flight.

For most situations the transition Reynolds numbers obtained in wind tunnels are lower than corresponding flight transition Reynolds numbers. It should be remembered that the differences between wind tunnel and flight transition Reynolds numbers are not the same throughout the Mach number range. The largest differences are generally at supersonic Mach numbers and the smallest differences are at subsonic and large hypersonic Mach numbers. Figs. 16 and 17 illustrate these differences. Also, the specific configuration is a factor. In some cases, a transition parameter may be dominant enough to overshadow the difference in the freestream environment (e.g., bluntness or surface roughness). The wind tunnel transition Reynolds numbers obtained on the shuttle configuration were not much less than found in flight.

One may be able to duplicate a flight Mach number and Reynolds number, but generally in hypersonic wind tunnels it will not be possible to duplicate velocity or temperature. Therefore, it is not possible to maintain similarity of boundary-layer profiles between wind tunnel and flight. Since the boundary-layer stability characteristics are very sensitive to the profiles, differences in transition Reynolds number must be expected as a result of profile differences. The sensitivity of boundary-layer transition to changes in boundary-layer profiles is presently not well enough understood to evaluate this effect. However, stability calculations of Mack¹⁹ suggest that the effects are significant. Mack made stability calculations corresponding to wind tunnel conditions and stagnation temperatures of 922°R and 1310°R. He noted that, "increasing the stagnation temperature has a considerable stabilizing influence at $M_e = 6.8$. The amplification rate is lowered at almost all frequencies and the unstable frequency band is narrowed by about 15%." A reduction in second mode amplification rates would be expected to increase the transition Reynolds number. If this is a consistent trend, then the larger stagnation temperatures in flight should produce larger transition Reynolds numbers than found in wind tunnels, independent of the environmental effects. Also, the larger stagnation temperatures of a shock tunnel should produce larger transition Reynolds numbers than the long duration, conventional hypersonic wind tunnel.

It is difficult to even speculate how transition in cold helium flow should relate to other situations.

The bottom line is that a hypersonic wind tunnel cannot duplicate the atmospheric environment or the boundary-layer profiles; therefore, there is no reason to expect the wind tunnel to duplicate flight transition Reynolds numbers. A possible approach to obtain a solution to this dilemma is to take the same approach as being used for other aspects of hypersonic aerodynamics - through a combination of analytical and experimental studies. To the extent possible, experiments should be conducted to define the instability phenomena, to compare with theory, to assist in the modelling of the instabilities for computation, to check the computational methods, and to evaluate the differences that occur because the environment and boundary-layer profiles have not been duplicated. The experimental requirements defined above require stability experiments, not transition experiments. When the only information obtained is the location of transition it is impossible to know the disturbance mechanisms which caused the transition or any details of the transition phenomena. A basic question that needs to be answered is whether or not the transition phenomena are the same in wind tunnels and in flight. If the transition phenomena are the same and the difference in transition Reynolds number are only the result of a difference in the freestream disturbance environments and the boundary-layer profiles, then the situation is promising. Compatibility of conventional wind tunnel, quiet wind tunnel, and flight transition Reynolds numbers becomes a matter of properly accounting for the environmental boundary condition and the boundary-layer profiles.

(3.e) LENGTH OF THE TRANSITION REGION

As a rule-of-thumb, it has been customary in the past to assume that the length of the transition region was the same as the length of the laminar region. The end of transition is not as well documented as the onset; however, there is a reasonable amount of data to support this conclusion. For example, the sharp cone and sharp plate correlations of Masaki and Yakura⁷⁵ and the extensive work of Pate⁷⁴ support this reasoning. Pate found $(Re_{XT})_B / (Re_{XT})_E \approx 0.5$ for a range of local Mach numbers from 3 to 8. There may be some variations in the reported transition lengths due to the method of detecting transition onset. The location of transition onset has been found to vary depending upon the method of detection; whereas, the end of transition

was essentially independent of the method used. For example, transition onset detected optically is consistently further downstream than onset detected by heat transfer rate or surface total pressure. These findings prompted Pate to make his correlations based upon the end of transition, rather than onset. Harvey and Bobbitt⁷⁶ have reported that in low noise wind tunnels and flight the transition region can be much shorter than the laminar region, with $(Re_{XT})_B / (Re_{XT})_E$ varying from about 0.5 to 0.9. Most flight experiments have added uncertainties due to the inability to control the flow conditions and vehicle altitude, coupled with more restrictions on vehicle instrumentation. An exception was the carefully controlled flight experiments of Dougherty and Fisher.³⁰ A 5-deg. half angle cone, which has been extensively tested in transonic and supersonic wind tunnels, was mounted on the nose boom of an F-15 aircraft and flight tested. The same instrumentation, primarily a surface pitot probe, detected transition both in flight and in the wind tunnels. The flight experiments, up to a Mach number of 2.0, measured a very short transition region, with $(Re_{XT})_B / (Re_{XT})_E$ being between 0.8 and 0.9. Mach 6 wind tunnel experiments⁴⁵ (see Figures 24 and 26), on a 8-deg. half angle cone with both a sharp tip and small nosetip bluntness, found X_{TB} / X_{TE} to be approximately 0.75. With larger nosetip bluntness, which produced early frustum transition, there was typically a very long transition region. Usually the transition region extended to the end of the model so that the end of transition could not be measured, with the transition length being several times as long as the laminar length. The Reentry F flight test data showed large variations in the length of the transition region. At 84,000 feet, $(Re_{XT})_B / (Re_{XT})_E = 0.64$ and at 60,000 feet, the value reduced to 0.19. These results very likely reflect the coupling of several effects and are difficult to interpret.

It can be seen that the length of a transition region to be expected in hypersonic flight is not well defined and predictable. The Reentry F flight results would support long transitional regions; whereas, several other results indicated that short transitional regions should be expected. There is clearly a large uncertainty associated with a prediction of the transition length.

(3.f) SOME PROBLEMS WITH FLOW FIELD CALCULATIONS

Remember that boundary-layer properties are an important element in the interpretation and analysis of transition results. Uncertainty in flow field

calculations directly influence the uncertainty in the transition estimates. This is an important point to keep in mind when using transition data. The uncertainty of an author's flow field calculations are often overlooked when studying his results and comparing his data with the data of others. In this regard, much of the available hypersonic transition data were obtained 20 or more years ago. The techniques used to generate the boundary-layer properties for the analyses of these results may have been primitive by today's standards. Also, currently much detailed flow field information is obtained from Parabolized Navier-Stokes (PNS) codes. Characteristically, the boundary-layer edge conditions derived from PNS results differ significantly from boundary-layer code results. Unfortunately, these differences have not been adequately investigated and documented, making it difficult to account for code differences in transition problems. Fig. 34 illustrates this problem by comparing PNS code, boundary-layer code, and experimental results. This example points out that, not only are there differences between PNS code and boundary-layer code results, but these differences are very sensitive to the grid density utilized in the PNS code. The experimental data were obtained with a multi-probe system which had major interference effects near the surface. The outer portion of the boundary layer is believed to be a reasonable representation. The velocity was calculated from the total pressure data, assuming a constant static pressure through the boundary layer. The boundary-layer code results were obtained from the Patankar-Spalding code.⁷⁷ The agreement with experiment is good near the outer portion of the boundary layer and the boundary-layer edge defined by the code was close to that obtained by experiment. As a check, PNS results were obtained for these same conditions, using the AFWAL PNS code.²⁷ The initial run used 60 grid points, between the surface and the shock. A definition of the boundary-layer edge as the height above the surface where the enthalpy ratio (h_T/h_{T_∞}) reached 0.999 is shown. The profiles and the definition of the boundary-layer edge are significantly different than the boundary-layer code results and the experimental data. The PNS calculations were repeated, doubling the grid points to 120, and the PNS profile became much closer to the boundary-layer code profile, but there were still differences in the outer part of the boundary layer. A third PNS calculation was made, still with 120 grid points, but increasing the density of grid points in the boundary layer. These results (not shown) were only slightly different, moving the profile in the direction of closer agreement

with the boundary-layer code results and the experimental data. There seems to be several messages from the information on this figure which warrant further investigation to see if they represent an isolated or the general case.

(1) PNS and boundary-layer codes give different boundary-layer profiles and different edge conditions.

(2) PNS codes can give a variety of profiles, depending upon the grid density used. It appears that PNS profiles may generally require an iteration procedure. A recent paper by Neumann and Patterson⁷⁸ discusses PNS computational strategy to obtain an efficient, good solution.

(3) For boundary-layer profiles on relatively simple configurations, perhaps the old boundary-layer codes have been too quickly abandoned.

(4) There is particular concern in the generation of mean profiles for stability calculations (e.g., the e^N method). Boundary-layer stability analyses are sensitive to the mean profiles that are used. If these profiles are generated with a PNS code, the code-related influence could be a problem.

Calculations of the boundary-layer properties are a very important part of the transition problem. Close attention should be given to the flow field properties.

PART 4: COMMENTS ON SOME PREDICTION METHODS

(4.a) INTRODUCTION

There are no good, general empirical transition correlations. The extreme complexity of the transition process requires that any technique make serious compromises. As previously discussed, transition is influenced by many parameters. Some parameters have a large effect and others have little or no effect. Several parameters are often competing for the dominant role, and, for a given situation, it is not always possible to predict the outcome. Even if one were successful in identifying the major parameters, it would not be possible to account for their individual effects in a transition correlation technique. Usually an empirical correlation is based upon a dominant parameter and the others are neglected. Many effects become hidden in the empirical relationship. As long as the transition correlation is being applied to a configuration and flow condition similar to those of the data base used to establish the correlation, the hidden effect may not be greatly dissimilar. A problem exists, however, when one wants to apply a transition correlation to a configuration or flow condition unlike those of the data base. A change in the outcome of the competition of the various factors, or a change in the contribution of the various hidden effects, can greatly reduce the accuracy of the transition prediction.

One should always keep in mind that empirical transition correlations are always tailored to emphasize certain effects on a special class of configurations and flow conditions. When using a particular correlation it is important to have knowledge of how the correlation was developed and the data based used in the development. It is important to consider how well the case in point corresponds to the data base of the correlation and make an allowance for the fact that the hidden effects might cause a surprise. All transition predictions have an uncertainty associated with them. It would seem desirable to try to estimate the uncertainty of a transition estimate and to indicate the degree of confidence in the prediction.

Since all transition prediction methods are empirical, an experimental data base is a necessary requirement in establishing a transition prediction method. The availability of a data base, per se, is not a problem since much experimental transition data have been obtained over the past years. The problem is that one seldom has the right data available. Transition experi-

ments document the location of the breakdown of laminar flow and how some flow or geometric parameter causes that location to move. The specific details of the phenomena involved are usually lacking and the interpretation of the transition data becomes difficult and speculative. If an attempt is made to utilize a variety of results in a single transition plot, the large variations of results will generally make it impossible to establish a meaningful empirical relationship. Fig. 35 (from Ref. 79) illustrates the problem. It becomes essential to be selective in the data used and to include only those data which most nearly correspond to the problem in question. The decision of what data to use in the establishment of a empirical relationship and the transition criteria is always a difficult choice since it can have a large effect on the resulting transition predictions. Such a procedure then limits the generality of the prediction method. The trend seems to be that improvements to the prediction method are made only at the expense of greater limitations on the application of the method. It is clear that one should always know what data were used to establish the transition prediction method being considered.

When it becomes necessary to predict transition on a new configuration or at new flow conditions empirical prediction methods have problems. The data base can only be used as a guide and any transition prediction for such a situation will have a large uncertainty associated with it.

(4.b) $Re_{\theta_T}/M_e = \text{CONSTANT}$

One of the most commonly used transition prediction methods is to use $Re_{\theta_T}/M_e = \text{constant}$. This technique was used for the Space Shuttle, and this prior usage has seemed to make it a prime candidate for future transition predictions. The fact that it worked reasonably well for the Shuttle was due to the uniqueness of that situation and this should not be interpreted as verification of the technique in general. The Shuttle's very blunt nosetip, high angle-of-attack, rough surface, and locally supersonic flow (with little variation) always produced relatively low transition Reynolds numbers which were not much larger than obtained in wind tunnels. It can easily be shown $Re_{\theta}/M_e = \text{constant}$ should not be expected to have a general application. Fig. 36 schematically shows the trend of transition Reynolds number vs Mach number variation for sharp cones. When a cone with nosetip bluntness is considered, a whole family of curves result, with a separate curve for each freestream Mach number. When we say $Re_{\theta}/M_e = \text{constant}$, we are trying to represent all of

these data by a single slope. There is only one region where a single slope appears to provide a reasonable representation of the data. For a sharp cone and $Me > 8$, a slope of about 100 seems to be reasonable. Note that for subsonic Mach numbers the constant can exceed 1000. Therefore, for Mach numbers up to 8, the constant is varying by a factor of 10. When consideration is given to entropy layer effects generated by a nosetip, there is no region where a constant slope has any credibility. The best that can be done is to use some average slope. The fact that Space Shuttle flight transition data gave a slope in the range of 200-400 : $Me \approx 2$ is of no value in predicting transition on a hypersonic vehicle with large local Mach numbers.

It should be remembered that Re_θ is proportional to $(Re_x)^{1/2}$. Therefore, plots of Re_θ , and the variations in Re_θ , must be viewed in this perspective. It was thought to be informative to show a comparison of Re_θ and Re_x . Fig. 37 shows approximate calculations for sharp cones. Note the large variations in Re_x at large local Mach numbers that result from changes in the Re_θ/Me constant. For example, at $Me = 15$:

| Re_θ/Me | Re_x |
|----------------|--------------------|
| 100 | 36.9×10^6 |
| 200 | 148×10^6 |
| 300 | 332×10^6 |
| 400 | 590×10^6 |

Considering that the Reentry F flight data indicated a sharp cone transition Reynolds number of approximately 40×10^6 , which corresponds to an Re_θ/Me just over 100, there seems to be no rationale for using large values of Re_θ/Me for this case.

Using $Re_\theta/Me = \text{constant}$, and using the same constant for a range of local Mach numbers, is not likely to result in good transition predictions.

(4.c) $Re_{\theta T}$ vs X/R_N

Probably the most extensive transition correlation study ever made was performed by Martellucci and associates. Some of these results are presented in Ref. 80. They considered approximately 200 reentry vehicle ($M_\infty \approx 20$) cases and selected those which met the following criteria:

- Small angles of attack at transition onset, $\alpha/\theta_c \leq 0.1$
- The trajectory could be determined

- c. Sphere - cone configurations
- d. On-board sensors
- e. Redundant transition altitude sensors

This resulted in the consideration of 72 reentry vehicles and 149 data points. In order to obtain a consistent set of boundary layer properties they performed the following calculations:

- a. Utilization of engineering methods to determine thermochemical shape change of ablative nosetips throughout reentry - the results of which were used as inputs to the inviscid flow field and boundary layer codes.
- b. A numerical solution of the inviscid shock layer for axisymmetric bodies, to provide shock shape and surface pressure distributions.
- c. A numerical solution of the heat conduction equation to define in-depth material response, frustum ablation, and surface temperature characteristics.
- d. A numerical implicit finite difference solution of the boundary layer equations which included mass addition effects.

The resulting data were correlated against over 50 different transition correlation techniques ($Re_\theta / M_e = \text{constant}$, was one). A significant, although not surprising, result was that none of the correlation techniques did a good job of correlating the data. Re_θ vs X_T/R_N correlations were considered to be the best and further improvements could be made by using sub-sets of data for like heat shield materials. Fig. 38 (from Ref. 80) shows some of the results. Like all transition correlations, many effects are not accounted for. This correlation applies only to Mach 20 reentry vehicles and should not be used, as is, for other Mach numbers since the relationship is Mach number dependent. Bluntness effects are only partially included, but as long as only slender reentry vehicles with small nosetip bluntness are considered, bluntness effects are nearly similar. That is, using Rotta's³⁴ similarity approach for highly cooled sphere-cones, the boundary layer properties within the entropy layer resulting from the nosetip are a function of

$$\frac{S/R_N}{K(Re_\infty/FT, R_N)^{1/3}}$$

where the constant K is primarily a function of cone angle and Mach number and can be obtained from Fig. 20. Thus, for situations where $K(Re_\infty/FT, R_N)^{1/3}$ does not vary significantly, S/R_N , by itself, adequately accounts for the variation of boundary layer properties within the entropy layer. Note, also that it is the product of these terms that is important, not their individual

values. Thus, if the freestream unit Reynolds number is decreased an order of magnitude (increasing altitude by approximately 50K feet) and the nosetip radius is increased an order of magnitude, the entropy layer, in terms of S/R_n is unchanged.

This Re_{6T} vs X/R_N transition correlation was not meant to be a general correlation and should not be used as such. Like all correlations, it should be used only where it is appropriate.

(4.d) e^N

Empirical correlations address only the resultant effect of many parameters. The net effect of all of the involved parameters is represented by a single curve. Thus, it is impossible to know the individual contributions of the various parameters or the generality of the correlation. It is desirable to have an analytical method which can account for the history of the boundary-layer disturbances in the laminar boundary layer prior to transition. Within the limits of the theory being used an analytical method can be used to study the influence of the various parameters on transition, as well as the combined effect. This would provide valuable opportunities to study parametric effects. Also, an analytical method has the potential of handling new situations, provided the appropriate stability theory and mean flow calculations can be obtained.

Presently, the most common analytical approach to predicting transition follows the method of Smith⁸¹ and Van Ingen.⁸² Linear stability theory is utilized to calculate amplitude ratios. Transition is presumed to occur with the earliest attainment of some preassigned amplitude ratio, usually expressed as e^N . The solutions of the linear stability equations yield the disturbance growth rate $(-\alpha_i)$ which can be integrated to compute the exponent N :

$$N = \ln(A/A_0) = \int_{s_0}^s -\alpha_i ds.$$

s_0 is the location of the onset of instability (at Re_c) and A_0 is the disturbance amplitude at Re_c . This method is often criticized as having no theoretical justification for predicting transition since all it does is compute an amplitude ratio (A/A_0) . It ignores the environment (A_0) and the actual transition process. The value of N must be input, based upon available experimental data, and transition is predicted to occur when N reaches the preassigned value. In spite of such criticisms, it is presently the best analytical transition prediction method in general use and Bushnell and his associates at NASA/Langley Research Center have reported

rather remarkable results for subsonic, supersonic, and low hypersonic situations. Their results account for first mode, second mode, Görtler, and cross-flow disturbances and have been applied to cones, flat plates, airfoils, bodies of revolution, swept wings, swept cylinders, a rotating disk, and a wind tunnel nozzle wall. Ref. 83 contains a list of the references describing these results. Some recent results of Malik²² contain some hypersonic results. His computations for sharp cones, using a N-factor of 10, showed that first mode disturbances were responsible for transition at adiabatic wall conditions for freestream Mach numbers up to 7. For cold walls, second mode disturbances dominated the transition process at lower hypersonic Mach numbers due to the destabilizing effect of cooling on the second mode. Malik's results also show that a favorable pressure gradient and suction are stabilizing for second mode disturbances.

Verification of the e^N method for hypersonic, three-dimensional, high temperature flows with entropy layers will be an extremely difficult task. Of course, verification of other aspects of such flows will face similar difficulties. Obtaining valid mean profiles to input the stability calculations and obtaining reliable flight transition data to determine the proper N-factors are seen as particularly difficult tasks.

PART 5: COMMENTS ON PREDICTION METHODOLOGY

As previously mentioned, there may be several disturbance mechanisms which are competing for the dominant role in the transition process. The transition prediction method selected should be appropriate to deal with the dominant disturbances in the boundary layer. For example, it would make little sense to use a transition prediction method based upon second-mode disturbance transition when the case in point was dominated by Görtler vortices. Therefore, the first step is to make an initial assessment of the boundary-layer disturbances to determine the dominant disturbances which are controlling transition. Calculate the critical transition parameter for each class of disturbance to see if this condition is exceeded.

(5.a) NOSETIP

Hypersonic configurations, through necessity, will have some degree of nosetip bluntness. Due to the fact that nosetip transition Reynolds numbers are very low, possibly being two orders of magnitude less than frustum transition length Reynolds numbers, it is necessary to consider nosetip transition independently from the rest of the configuration. This is a Morkovin "by-pass" situation which cannot be explained theoretically, but sufficient experimental data have been obtained to provide guidance in predicting transition. This basically requires a calculation of the Reynolds number at the sonic point, along with an allowance for the surface roughness and the temperature ratio across the boundary layer, also at the sonic point. If transition does occur on the nosetip, all flow downstream can be expected to be transitional or turbulent. Nosetip transition is insensitive to free-stream Mach number and very dependent upon nosetip radius, surface roughness, and the temperature ratio across the boundary layer (the local Reynolds number at the sonic point is dependent upon the nosetip radius and the boundary-layer is very thin, making roughness more effective). Fig. 22 contains some nosetip transition data. For a "smooth" nosetip, Re_{θ} 's greater than about 300 can result in transition on the nosetip. A rough nosetip significantly reduces the transition Reynolds number. Ref. 84 contains a review and evaluation of nosetip transition experiments.

(5.b) EARLY FRUSTUM:

Early frustum is defined as the region just downstream of the nosetip, extending for several nose radii. Early frustum transition is a subject which has only recently been identified. The transition experiments reported in Ref. 25 clearly identified the early cone frustum as a region with its own transition criteria. This region, which extended for several nose radii down the frustum, had very low transition Reynolds numbers. It was determined that transition on the early part of the frustum could be related to conditions on the nosetip. Early frustum transition could be related to the Reynolds number at the sonic point and the nosetip surface roughness, analogous to the nosetip transition criteria. Therefore, calculations of Re_θ at the nosetip sonic point can also be used to predict early frustum transition. For a sphere-cone at a Mach number of 6, Re_θ 's of 120, or greater, at the sonic point of a smooth nosetip produced transition on the early portion of the frustum. That is, for Re_θ 's at the sonic point of less than 120, both the nosetip and the early portion of the frustum had a laminar boundary layer. For Re_θ 's from 120 to about 300, the nosetip had a laminar boundary layer and transition occurred on the early region of the frustum. For Re_θ 's of about 300 or greater, transition occurred on the nosetip. Fig. 22 gives a criterion for both early frustum transition and nosetip transition. Unfortunately, not enough information is known about early frustum transition to determine the generality of these results. It appears that the results are sensitive to the favorable pressure gradient. Increasing the pressure gradient, as would result from increasing the freestream Mach number, is expected to increase the threshold value of Re_θ above 120. Likewise, decreasing the pressure gradient is expected to reduce the threshold value.

(5.c) CROSSFLOWS

There is little guidance available for estimating the effects of crossflow on hypersonic transition. Experimental data are available for the leeward side of cones at angle-of-attack (samples are shown in Figures 23-27) and indicate low transition Reynolds numbers in this region. If the cone configuration is relevant to the problem at hand, transition estimates may be based upon the cone data. A more general method would be to base crossflow influenced transition upon a crossflow Reynolds number. The laminar boundary-layer profile in a three-dimensional, viscous flow has a twisted profile that

can be resolved into tangential (u) and crossflow (w) velocity components. The crossflow component of the velocity is used for the computation of crossflow Reynolds number. Owen and Randall⁴³ performed subsonic experiments with swept wings and found there was a critical crossflow Reynolds number that caused transition to make an instantaneous jump from the trailing edge to near the leading edge. Using a length dimension of nine-tenths of the boundary-layer thickness, the critical crossflow Reynolds number was 150 to 175. Higher subsonic laminar crossflow Reynolds numbers have been reported, so the generality of the Owen and Randall data is not known. Pate^{44,74} has indicated that the Owen and Randall results appear to be valid for supersonic flows. If the boundary-layer thickness is used as the length dimension, a value of 200 seems like a reasonable conservative guess for hypersonic flows. The procedure would be to make calculations of crossflow Reynolds numbers and see if any condition resulted in a number which exceeded 200. For those conditions where the crossflow Reynolds number exceeded 200, it could be expected that crossflow instabilities would dominate and cause transition. The crossflow Reynolds number is defined as:

$$Re_{CF} = \frac{\rho_e w_{max} \delta}{\mu_e}$$

(5.d) LEADING EDGE CONTAMINATION

A cylinder normal to the flow has a stagnation line. However, if the cylinder is swept, one can think in terms of the normal component of velocity as stagnating, but there is no true stagnation line since the tangential velocity component remains unchanged in passing through the bow shock wave. The line of maximum pressure (usually called the attachment line or the leading line) corresponds to the line which divides the upper surface flow from the lower surface flow. The existence of the tangential velocity along the attachment line requires that the attachment line have a boundary layer (one can also think in terms of the windward meridian of a cylinder at angle-of-attack). The attachment line boundary layer can be laminar, transitional, or turbulent, depending upon the values of the pertinent parameters. However, the boundary layer on the attachment line of an infinite swept cylinder is unique in that it is invariant with position on the cylinder. Thus, in the absence of any parameter variations, the state of the attachment line boundary layer (e.g., laminar or transitional) is invariant with position on the cylinder. (A swept wing with a constant leading edge radius can be considered analogous to a cylinder.)

In addition to crossflow instabilities, there is another important mechanism that can dominate transition in the leading edge region of swept wings. This mechanism is referred to as "leading edge contamination". If the beginning of the leading edge of a swept wing is in contact with a solid surface (e.g., a fuselage or a wind tunnel wall), the turbulence which is present in the boundary layer of the adjoining surface will contaminate the leading edge boundary of the swept wing. Such turbulence contamination has a significant effect on the state of the leading edge boundary layer and can dominate the transition process on the wing.

Bushnell and Huffman⁸⁵ correlated a large amount of data for Mach numbers up to 10 and sweep angles from 10 to 80 deg. and found that when no end disturbances were present, the attachment line flow was always laminar up to values of $Re_{\infty D} \approx 8 \times 10^5$ (a Reynolds number based upon freestream conditions and the leading edge diameter), which was the upper limit for data available at that time. When large end disturbances were present, transition was generally observed for $Re_{\infty D} \gtrsim 2 \times 10^5$. Creel, et al⁸⁶ investigated transition on 45 and 60 deg swept cylinders in the Mach 3.5 Quiet Wind Tunnel. They found that end plates or large trips near the upstream end of the cylinders caused transition along the entire attachment line of the models for $Re_{\infty D} \gtrsim 1.0 \times 10^5$. When all end disturbance sources were removed, transition occurred on the attachment lines at $Re_{\infty D} \approx 7-8 \times 10^5$.

Poll has made an extensive investigation of the effects of turbulence contamination upon leading edge transition, including both incompressible and compressible flows (see, for example, References 40, 87, and 88). Fig. 39 (from Ref. 87) indicates the conditions for attachment line transition on an infinite swept cylinder in terms of momentum thickness Reynolds number, boundary-layer edge Mach number, and wall-to-recovery temperature. For Reynolds numbers less than the critical value, turbulence contamination in the attachment line boundary layer is damped and the boundary layer remains laminar. Remember that since the attachment line boundary layer on a cylinder is not growing, it remains laminar regardless of the length of the cylinder. When the critical Reynolds number is exceeded, the disturbances grow and cause transition on the attachment line.

In the check for dominant mechanisms, first make a judgement as to whether or not the leading edge boundary layer will be contaminated with turbulence from an adjoining surface. If the leading edge boundary is contam-

inated, calculate the attachment line momentum thickness Reynolds number to see if it is greater than or less than the critical value given in Fig. 39. If the Reynolds number exceeds the critical value, transition can be expected on the leading edge.

(5.e) ADVERSE PRESSURE GRADIENTS/GÖRTLER INSTABILITIES

There is insufficient data available to establish a general criterion to determine when adverse pressure gradient effects and Görtler instabilities will dominate and produce an early transition. A limited amount of transition data on concave surfaces has been correlated with the Görtler number; $G = \text{Re}_\theta \sqrt{\frac{\theta}{R_c}}$, where Re_θ is the momentum thickness Reynolds number, θ is the momentum thickness and R_c is the radius of curvature of the boundary-layer streamlines (see, for example, Ref. 89). Transition was found to occur for Görtler numbers between 6 and 10.

Linear stability theory (the e^N method) has been used to predict the effects of Görtler instabilities on transition of boundary layers on wind tunnel nozzle walls.^{71, 90}

(5.f) SECOND MODE

There is no simple criterion to use to estimate second mode disturbance transition. A starting point could be to utilize a collection of cone transition data (such as Fig. 17) or by a correlation technique such as discussed in Part 4. Remember that flight data such as contained in Fig. 17 already contain effects such as small nosetip bluntness, small angles-of-attack, and some surface temperature variations. Some of the flow and geometric parameters which influence the instabilities mentioned in 5a through 5e also influence the growth of second mode disturbances (e.g., nosetip bluntness and surface curvature). Therefore, it is necessary to consider how second mode disturbance growth is modified by parametric effects. The parametric trends such as discussed in Part 2 can be used as a guide. Most of the parametric trends come from wind tunnel data. The influence of the wind tunnel noise may present some uncertainty in the trends; however, they are generally thought to be correct. A possible exception is the effects of unit Reynolds number. The wind tunnel freestream environment can produce a unit Reynolds number effect not expected in flight. However, it is speculated that unit Reynolds number effects boundary-layer transition in several ways,

therefore a unit Reynolds number effect in flight should not be ruled out. Until the situation is clarified, it is suggested that a unit Reynolds number effect be applied to flight data, if such an adjustment would be a more conservative estimate.

Ericsson⁹¹ stated that the delay of transition caused by small nosetip bluntness is attenuated by the wind tunnel noise, but in flight an order of magnitude increase in transition Reynolds number can be obtained for "optimum nose bluntness." However, there is no evidence to support his statement. In fact, a comparison of Mach 6 wind tunnel data with Mach 20 flight data shows a remarkable similarity between wind tunnel and flight. Fig. 40 presents these results. The Mach 6 wind tunnel data is from Ref. 25 and the Mach 20 flight data is from References 35 and 36. The change in transition Reynolds number as a function of location within the entropy layer is shown. The extent of the entropy layer was estimated by the method of Rotta³⁴ (Fig. 20). Although the magnitude of the transition Reynolds numbers differed significantly, the percentage changes were very similar (the Mach 6 transition Reynolds numbers, for a unit Reynolds number of $11.2 \times 10^6/\text{ft.}$, varied from about 6.4×10^6 (sharp) to about 10.3×10^6 ($R_n/R_B = 0.03$). The Mach 20 flight data varied from about 40×10^6 (sharp) to about 68×10^6). There are obvious risks in drawing conclusions from a single comparison, but, unfortunately, there are presently no other data for such comparisons. Until further information becomes available, it is suggested that small nosetip bluntness be assumed to increase the transition Reynolds number by a factor less than two, as shown in Fig. 40. An order of magnitude increase, as predicted by Ericsson,⁹¹ would suggest that optimum nosetip bluntness for the Reentry F vehicle should produce transition Reynolds numbers of about 400×10^6 , an unrealistic prediction.

In making a judgement as to whether or not small nosetip bluntness will be significant, keep in mind that small bluntness can influence boundary-layer transition for large distances downstream of the nosetip. For example, a one inch nosetip radius can influence transition for more than 100 feet downstream of the tip, far beyond what one might intuitively estimate. Fig. 41 was prepared to illustrate this point. For a 5-deg. half angle cone at zero angle-of-attack traveling on the altitude vs Mach number trajectory indicated, the extent of the nosetip influence on boundary-layer transition is shown for three nosetip radii. Wind tunnel data, and a limited amount of flight data,

have indicated that the nosetip history in the boundary layer persists to a distance downstream which is approximately three times the distance required to swallow the entropy layer. That is, for distances greater than three times the entropy-layer-swallowing distance, transition Reynolds numbers may be considered to be those of a sharp configuration. For distances less than three times the entropy-layer-swallowing distance, nosetip bluntness influences the transition Reynolds number. The lines shown are the distances which correspond to three times the entropy-layer-swallowing distance, where the entropy-layer-swallowing distances were estimated by the method of Rotta.³⁴

All parameters which are judged to be significant should be accounted for, to the extent possible. Even a good guess should help keep the final estimate realistic and help avoid surprises.

(5.g) DOMINANT MECHANISMS

Any of the instabilities mentioned in 5.a through 5.f has the potential, given the appropriate circumstances, to produce rapidly growing disturbances which dominate the transition process. For the particular case in point, compare all the possible disturbance mechanisms and make a judgement as to which one will dominate. Having decided upon the dominant disturbance mechanism, use what you consider to be the best available transition method and criterion for that instability to estimate the location of boundary-layer transition.

(5.h) ESTIMATE UPPER AND LOWER BOUNDS

All transition estimates will have an uncertainty associated with them. Even if all parameters could be precisely accounted for, unknown variations in the freestream environment would introduce an uncertainty into the estimate. Even a guess at the uncertainty could be useful in judging the confidence level of the transition estimate and the establishment of conservative and optimistic estimates, if desired.

PART 6: CONCLUDING REMARKS

With so many complicated and often unknown instability mechanisms, modified by many interrelated flow and geometric parameters, all competing for the dominate role in the transition process, it is not surprising that there is often a large uncertainty in estimating the location of boundary-layer transition. New knowledge of these complex phenomena are steadily being obtained; however, progress is slow and much remains to be learned. Since all current transition prediction methods are empirical, confidence is acquired only through having accumulated a suitable data base of similar flight vehicles and similar flight situations. The reality of the current transition prediction situation is that it is not possible to make a confident prediction of transition for a new vehicle configuration flying in a new flight environment. Vehicle designers must accept the fact that there will always be an uncertainty associated with estimating the location of boundary-layer transition. The magnitude of the uncertainty and the consequences of the uncertainty should always be a consideration. Future research will, hopefully, reduce the magnitude of the uncertainty.

In closing, a quotation from two stability and transition leaders, Morkovin and Reshotko,⁵ seems appropriate: "It is of utmost importance that our continuing work proceed with open eyes and open mind; that new knowledge be subject to the tests of the U. S. Transition Study Group (Reshotko²), especially the generalized guideline number four: 'Experiments (and computations) where possible should involve more than one facility. Tests should have ranges of overlapping parameters, and where possible, redundancy in transition measurements'. Only in this way will our efforts avoid inferences based on insufficient evidence and yield a furthering of our understanding of laminar-turbulent transition."

REFERENCES

1. Morkovin, M. V., "Critical Evaluation of Transition From Laminar to Turbulent Shear Layers with Emphasis on Hypersonically Traveling Bodies," AFFDL TR-68-149, March 1969. (Also, see "Instability, Transition to Turbulence and Predictability," AGARDograph No. 236, July 1978.)
2. Reshotko, Eli, "Boundary Layer Stability and Transition," Annual Review of Fluid Mechanics, Vol. 8, pp 311-350, 1976.
3. Reshotko, Eli, "Stability and Transition, How Much Do We Know?," paper presented at Tenth U. S. National Congress of Applied Mechanics, The University of Texas at Austin, Austin, Texas, June 1986.
4. Arnal, D., "Laminar-Turbulent Transition Problems in Supersonic and Hypersonic Flows," AGARD/FDP/VKI Special Course, Aerothermodynamics of Hypersonic Vehicles, 30 May - 3 June, 1988.
5. Morkovin, M. V. and Reshotko, E., "Dialogue on Progress and Issues in Stability and Transition Research," Third IUTAM Symposium on Laminar Turbulent Transition, Toulouse, France, September 1989.
6. Mack, L. M., "Linear Stability Theory and the Problem of Supersonic Boundary-Layer Transition," AIAA Journal, Vol. 13, No. 3, pp 278-289, March 1975.
7. Mack, L. M., "Boundary Layer Linear Stability Theory," AGARD Report No. 709, June 1984.
8. Kendall, J. M., "Wind Tunnel Experiments Relating to Supersonic and Hypersonic Boundary Layer Transition," AIAA Journal, Vol. 13, No. 3, pp 290-299, March 1975.
9. Demetriades, A., "New Experiments on Hypersonic Boundary Layer Stability Including wall Temperature Effects," Proceedings of the Heat Transfer and Fluid Mechanics Institute, pp. 39-54, 1978.
10. Stetson, K. F., Thompson, E. R., Donaldson, J. C., and Siler, L. G., "Laminar Boundary Layer Stability Experiments on a Cone at Mach 8, Part 1: Sharp Cone," AIAA Paper No. 83-1761, July 1983.
11. Stetson, K. F., Thompson, E. R., Donaldson, J. C., and Siler, L. G., "Laminar Boundary Layer Stability Experiments on a Cone at Mach 8, Part 2: Blunt Cone," AIAA Paper No. 84-0006, January 1984.
12. Stetson, K. F., Thompson, E. R., Donaldson, J. C., and Siler, L. G., "Laminar Boundary Layer Stability Experiments on a Cone at Mach 8, Part 3: Sharp Cone at Angle of Attack," AIAA Paper No. 85-7492, January 1985.
13. Stetson, K. F., Thompson, E. R., Donaldson, J. C., and Siler, L. G., "Laminar Boundary Layer Stability Experiments on a Cone at Mach 8, Part 4: On Unit Reynolds Number and Environmental Effects," AIAA Paper No. 86-1087, May 1986.

14. Stetson, K. F., Thompson, E. R., Donaldson, J. C., and Siler, L. G., "Laminar Boundary Layer Stability Experiments on a Cone at Mach 8, Part 5: Tests With a Cooled Model," AIAA Paper No. 89-1895, June 1989.
15. Dryden, H. L., "Air Flow in the Boundary Layer Near a Plate," NACA Report No. 562, 1936.
16. Schubauer, G. B. and Skramstad, H. K., "Laminar Boundary Oscillations and Transition on a Flat Plate," NACA Adv. Conf. Report, April 1943.
17. Stetson, K. F., Thompson, E. R., Donaldson, J. C., and Siler, L. G., "On Hypersonic Transition Testing and Prediction," AIAA Paper No. 88-2007, May 1988.
18. Lees, L., "The Stability of the Laminar Boundary Layer in a Compressible Fluid," NACA Report No. 876, 1947.
19. Mack, L. M., "Boundary-Layer Stability Analysis for Sharp Cones at Zero Angle of Attack," AFWAL TR-86-3022, August 1986.
20. Mack, L. M., "Stability of Axisymmetric Boundary Layers on Sharp Cones at Hypersonic Mach Numbers," AIAA Paper No. 87-1413, June 1987.
21. Gasperas, G., "The Stability of the Compressible Boundary Layer on a Sharp Cone at Zero Angle of Attack," AIAA Paper No. 87-0494, January 1987.
22. Malik, M. R., "Prediction and Control of Transition in Hypersonic Boundary Layers," AIAA Paper No. 87-1414, June 1987. (Also, AIAA Journal, Vol 27, No. 11, pp 1487-1493, November 1989).
23. Chen, F.-J., Malik, M. R., and Beckwith, I. E., "Comparison of Boundary Layer Transition on a Cone and Flat Plate at Mach 3.5," AIAA Paper No. 88-0411, January 1988. (Also, AIAA Journal, Vol 27, No. 6, pp 687-693, June 1989).
24. Malik, M. R., Spall, R. E., and Chang, C.-L., "Effect of Nose Bluntness on Boundary Layer Stability and Transition," AIAA Paper No. 90-0112, January 1990.
25. Stetson, K. F., "Nosetip Bluntness Effects on Cone Frustum Boundary Layer Transition in Hypersonic Flow," AIAA Paper No. 83-1763, July 1983.
26. Helliwell, W. S. and Lubard, S. C., "An Implicit Method for Three-Dimensional Viscous Flow with Application to Cones at Angle of Attack," RDA-TR-150, February 1973.
27. Kaul, W. K. and Chaussee, D. S., "AFWAL Parabolized Navier-Stokes Code: 1983 AFWAL/NASA Merged Baseline Version," AFWAL-TR-83-3118, May 1984.
28. Stetson, K. F., "On Nonlinear Aspects of Hypersonic Boundary-Layer Stability," AIAA Jour., Vol. 26, No. 7, pp 883-885, July 1988.
29. White, C. O., "Boundary Layer Transition for Sharp and Slight Blunted Cones Under Hypersonic Entry Conditions," Philco-Ford Corp., Mechanical Engineering, TN 110, October 1966.

30. Dougherty, N. S., Jr., and Fisher, D. F., "Boundary-Layer Transition Correlations on a Slender Cone in Wind Tunnels and Flight for Indications of Flow Quality," AEDC-TR-81-26, February 1982 (also AIAA 80-0154, January 1980).
31. Beckwith, I. E., "Development of a High Reynolds Number Quiet Tunnel for Transition Research," AIAA Journal, Vol. 13, No. 3, pp 300-306, March 1975.
32. Muir, J. R. and Trujillo, A. A., "Experimental Investigation of the Effects of Nose Bluntness, Free-Stream Unit Reynolds Number, and Angle of Attack on Cone Boundary Layer Transition at a Mach Number of 6," AIAA Paper No. 72-216, January 1972.
33. Sretson, K. F., and Rushton, G. H., "Shock Tunnel Investigation of Boundary Layer Transition at $M = 5.5$," AIAA Journal, Vol. 5, pp 899-906, May 1967.
34. Rotta, N. R., "Effects of Nose Bluntness on the Boundary Layer Characteristics of Conical Bodies at Hypersonic Speeds," NYU-AA-66-66, November 1966. (Also, Astronautics Acta, Vol. 13, pp 507-516, 1968).
35. Wright, R. L. and Zoby, E. V., "Flight Boundary Layer Transition Measurements on a Slender Cone at Mach 20," AIAA Paper No. 77-719, June 1977.
36. Johnson, C. B., Stainback, P. C., Wicker, K. C., and Boney, L. R., "Boundary Layer Edge Conditions and Transition Reynolds Number Data for a Flight Test at Mach 20 (Reentry F)," NASA TM-X-2584, July 1972.
37. Stetson, K. F., "Boundary Layer Transition on Blunt Bodies with Highly Cooled Boundary Layers," J. A. S., Vol. 27, pp 31-91, February 1960. (Also, IAS Report No. 59-36, January 1959).
38. Anderson, A. D., "Interim Report, Passive Nosetip Technology (PANT) Program, Vol. X, Appendix, Boundary Layer Transition on Nosetips with Rough Surfaces," SAMSO-TR-74-86, January 1975.
39. Demetriades, A., "Nosetip Transition Experimentation Program, Final Report, Vol. II," SAMSO-TR-76-120, July 1977.
40. Poll, D. I. A., "Transition Description and Prediction in Three-Dimensional Flows," ACARD Report No. 709, 1984.
41. Arnal, D., "Three-Dimensional Boundary Layers: Laminar-Turbulent Transition," ACARD Report No. 741, 1986.
42. Saric, W. S. and Reed, H. L., "Three-Dimensional Stability of Boundary Layers. Perspective in Turbulence Studies," Springer-Verlag, 1987.
43. Owen, P. R. and Randall, D. G., "Boundary-Layer Transition on a Swept-Back Wind," RAE Tech. Memo Aero 277, June 1952.
44. Pate, S. M., "Effects of Wind Tunnel Disturbances on Boundary-Layer Transition with Emphasis on Radiated Noise: A Review," AIAA Paper No. 80-0431, March 1980.

45. Stetson, K. F., "Mach 6 Experiments of Transition on a Cone at Angle of Attack," *Journal of Spacecraft and Rockets*, Vol. 19, No. 5, pp 397-403, Sept-Oct 1982.
46. Potter, J. L., "Boundary-Layer Transition on Supersonic Cones in an Aeroballistic Range," *AIAA Journal*, Vol. 13, No. 3, pp 270-277, March 1975.
47. Potter, J. L., "The Unit Reynolds Number Effect on Boundary Layer Transition," Dissertation submitted in partial fulfillment of the requirements for the degree of Doctor of Philosophy, Vanderbilt University, May 1974.
48. Reshotko, E., "Stability Theory as a Guide to the Evaluation of Transition Data," *AIAA Journal*, Vol. 7, No. 6, pp 1086-1091, June 1969.
49. Schubauer, G. B. and Skramstad, H. K., "Laminar Boundary Layer Oscillations and Transition on a Flat Plate," *NACA Report No. 909*, 1948.
50. Wells, C. D., Jr., "Effects of Freestream Turbulence on Boundary Layer Transition," *AIAA Journal*, Vol. 5, No. 1, pp 172-174, January 1967.
51. Spangler, J. G. and Wells, C. S., Jr., "Effects of Free Stream Disturbances on Boundary Layer Transition," *AIAA Journal*, Vol. 6, No. 3, pp 543-545, March 1968.
52. Reshotko, E., "Environment and Receptivity," *AGARD Report No. 709*, pp 4-1 to 4-11, 1984.
53. Van Driest, E. R., "Calculations of the Stability of the Laminar Boundary Layer in a Compressible Fluid on a Flat Plate with Heat Transfer," *JAS*, Vol. 19, No. 10, pp 801-812, December 1952.
54. Jack, J. R., Wisniewski, R. J., and Diaconis, N. S., "Effects of Extreme Surface Cooling on Boundary Layer Transition," *NACA TN 4094*, October 1957.
55. Sheetz, N. W., Jr., "Free-Flight Boundary Layer Transition Investigation at Hypersonic Speeds," *AIAA Paper No. 65-127*, January 1965.
56. Van Driest, E. R., and Boison, J. C., "Experiments on Boundary Layer Transition at Supersonic Speeds," *JAS*, Vol. 24, pp 885-889, 1957.
57. Lysenko, V. I., and Maslov, A. A., "The Effect of Cooling on the Supersonic Boundary Layer Stability and Transition," *IUTAM Symposium on Laminar Turbulent Transition*, Novosibirsk, 1984.
58. Potter, J. L., "Review of the Influence of Cooled Walls on Boundary Layer Transition," *AIAA Journal*, Vol. 18, No. 8, 1980.
59. Sanator, R. J., DeCarlo, J. P., and Torrillo, D. T., "Hypersonic Boundary Layer Transition Data for a Cold-Wall Slender Cone," *AIAA Journal*, Vol. 3, No. 4, 1965.
60. Mateer, G. G., "Effects of Wall Cooling and Angle of Attack on Boundary Layer Transition on Sharp Cones at $M = 7.4$," *NASA TN D-6908*, August 1972.

61. Reshotko, E. and Leventhal, L., "Preliminary Experimental Study of Disturbances in a Laminar Boundary Layer due to Distributed Surface Roughness," AIAA Paper No. 81-1224.
62. Corke, T. C., Bar-Sever, A., and Morkovin, M. V., "Experiments on Transition Enhancement by Distributed Roughness," Phys. Fluids, Vol. 29, No. 10, pp. 3199-3213, 1986.
63. Kendall, J. M., "Laminar Boundary Layer Velocity Distortion by Surface Roughness: Effect Upon Stability," AIAA Paper No. 81-0195, January 1981.
64. Boudreau, A. H., "Artificially Induced Boundary Layer Transition on Blunt-Slender Cones at Hypersonic Speeds," Journal of Spacecraft and Rockets, Vol. 16, pp 245-251, July - August 1979.
65. Floryan, J. M. and Saric, W. S., "Stability of Gortler Vortices in Boundary Layers," AIAA Journal, Vol. 20, No. 3, 1982.
66. El-Hady, N. M. and Verma, A. K., "Growth of Gortler Vortices in Compressible Boundary Layers Along Curved Surfaces," Journal of Eng. and Appl. Sciences, Vol. 2, 1983.
67. Spall, R. E. and Malik, M. R., "Gortler Vortices in Supersonic Boundary Layers," AIAA Paper No. 88-3678, July 1988.
68. Ginoux, J. J., "Streamwise Vortices in Laminar Flow," AGARDograph 97, 1965.
69. Beckwith, I. E., and Holley, B. B., "Gortler Vortices and Transition in the Wall Boundary Layers of Two Mach 5 Nozzles," NASA TP-1869, 1981.
70. Beckwith, I. E., Creel, T. R., and Chen, F.-J., "Freestream Noise and Transition Measurements in a Mach 3.5 Pilot Quiet Tunnel," AIAA Paper No. 83-0042, 1983.
71. Chen, F.-J., Malik, M.R., and Beckwith, I. E., "Instabilities and Transition in the Wall Boundary Layers of Low Disturbance Supersonic Nozzles," AIAA Paper No. 85-1573, 1985.
72. Martellucci, A., Neff, R. S., and Rittenhouse, C., "Mass Addition Effects on Vehicle Forces and Moments - Comparison Between Theory and Experiment," General Electric Document 69SD934, September 1969.
73. Sternberg, J., "A Free Flight Investigation of the Possibility of High Reynolds Number Supersonic Laminar Boundary Layers," Journal Aero. Sci., Vol. 19, November 1952.
74. Pate, S. R., "Dominance of Radiated Aerodynamic Noise on Boundary Layer Transition in Supersonic-Hypersonic Wind Tunnels, Theory and Application," AEDC-TR-77-107, March 1978.
75. Masaki, M. and Yakura, J. K., "Transitional Boundary Layer Considerations for the Heating Analysis of Lifting Reentry Vehicles," Journal of Spacecraft and Rockets, Vol. 6, No. 9, pp 1048-1059, September 1969.

76. Harvey, W. D., and Bobbitt, P. J., "Some Anomalies Between Wind Tunnel and Flight Transition Results," AIAA Paper No. 81-1225, June 1981.
77. Patankar, S. V., and Spalding, D. B., Heat and Mass Transfer in Boundary Layers, CRC Press, Cleveland, Ohio, 1968.
78. Neumann, R. D., and Patterson, J. L., "Results of an Industry Representative Study of Code to Code Validation of Axisymmetric Configurations at Hypervelocity Flight Conditions," AIAA Paper No. 88-2691, June 1988.
79. Beckwith, J. E., and Bertram, M. H., "A Survey of NASA Langley Studies on High-Speed Transition and the Quiet Tunnel," NASA TM X-2566, July 1972.
80. Berkowitz, A. M., Kriss, C. L., and Martellucci, A., "Boundary Layer Transition Flight Test Observations," AIAA Paper No. 77-125, January 1977.
81. Smith, A. M. O., and Camberoni, N., "Transition, Pressure Gradient and Stability Theory," Douglas Aircraft Co. Report No. ED 26388, 1956.
82. Van Ingen, J. L., "A Suggested Semi-Empirical Method for the Calculation of the Boundary Layer Transition Region," Dept. of Aero. Eng., Delft, Reports VTH-71 and VTH-74, 1956.
83. Bushnell, D. M., Malik, M. R., and Harvey, W. D., "Transition Prediction in External Flows Via Linear Stability Theory," Presented at IUTAM Symposium Transsonicum III, Goettingen, West Germany, May 1988.
84. Batt, R. G., and Legner, H. H., "A Review of Roughness Induced Nosedip Transition," AIAA Paper No. 81-1223, June 1981.
85. Bushnell, D. M., and Huffman, J. K., "Investigation of Heat Transfer to a Leading Edge of a 76° Swept Fin With and Without Chordwise Slots and Correlations of Swept-Leading-Edge Transition Data for Mach 2 to 8," NASA TMX-1475, December 1967.
86. Creel, T. R., Jr., Beckwith, J. E., and Chen, F.-J., "Transition on Swept Leading Edges at Mach 3.5," Journal Aircraft, Vol. 24, No. 10, December 1987.
87. Poll, D. I. A., "The Development of Intermittent Turbulence on a Swept Attachment Line Including the Effects of Compressibility," The Aeronautical Quarterly, Vol. XXXIV, 1983.
88. Poll, D. I. A., "Boundary Layer Transition on the Windward Face of Space Shuttle During Reentry," AIAA Paper No. 85-0899, 1985.
89. Forest, A. E., "Engineering Predictions of Transitional Boundary Layers," AGARD-CP-224, 1977.
90. Beckwith, J. E., Chen, F.-J., and Malik, M. R., "Design and Fabrication Requirements for Low-Noise Supersonic/Hypersonic Wind Tunnels," AIAA Paper No. 88-0143, January 1988.
91. Ericsson, L. E., "Effect of Nose Bluntness and Cone Angle on Slender Vehicle Transition," AIAA Paper No. 87-1415, June 1987.

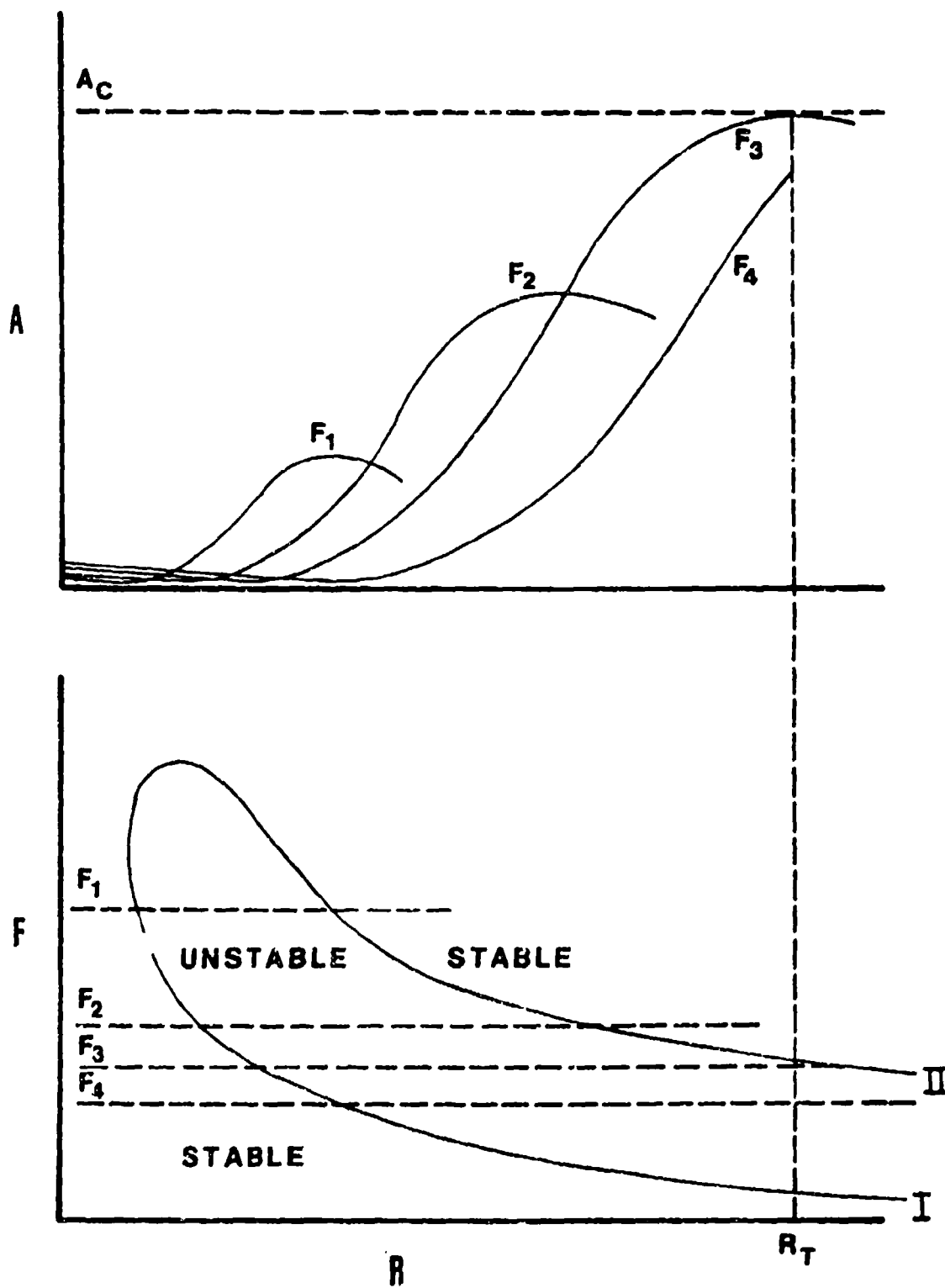


FIG. 1 A Schematic of a Stability Diagram

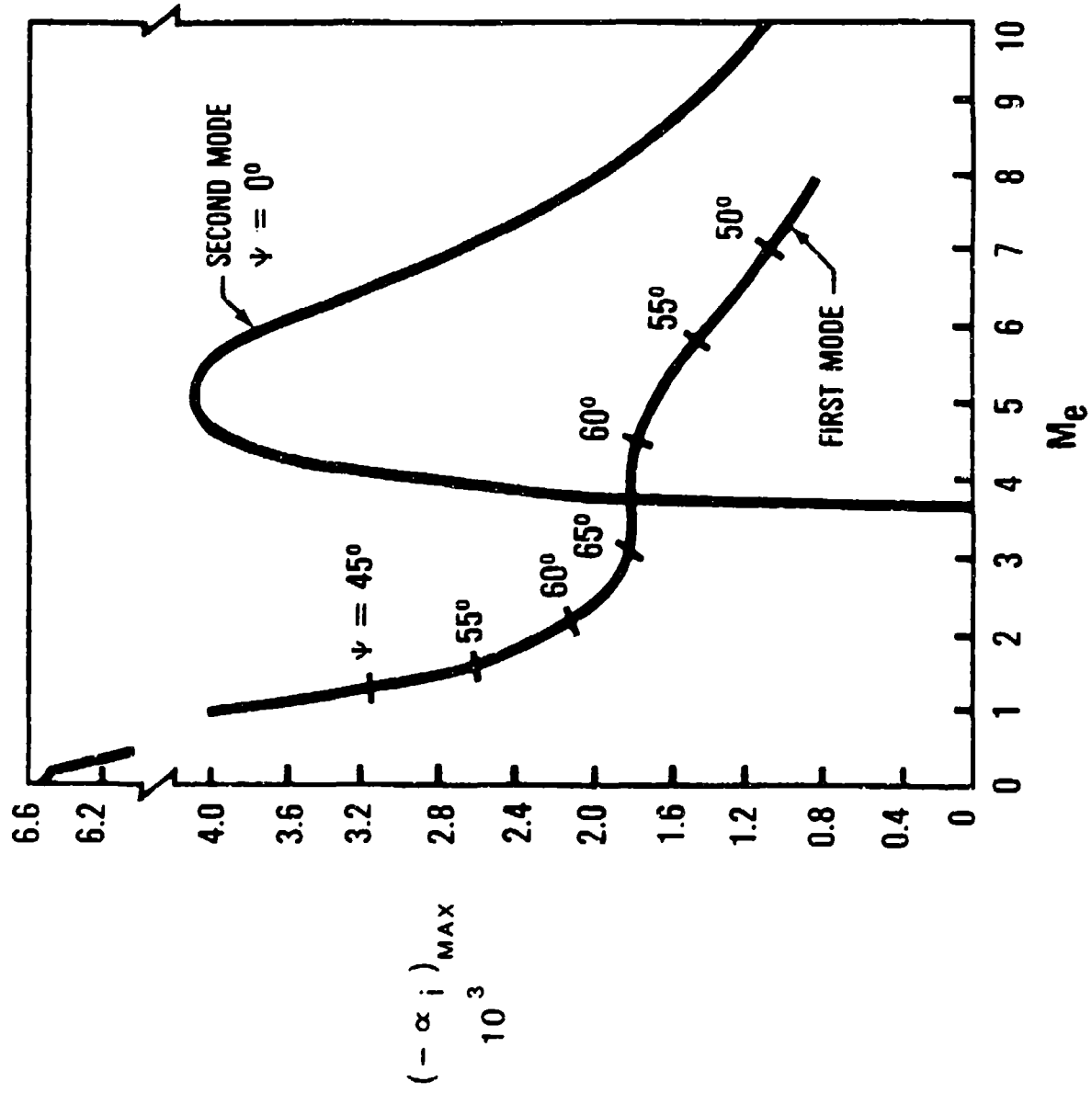


FIG. 2 Maximum First and Second Mode Spatial Amplification Rates at $R = 1500$

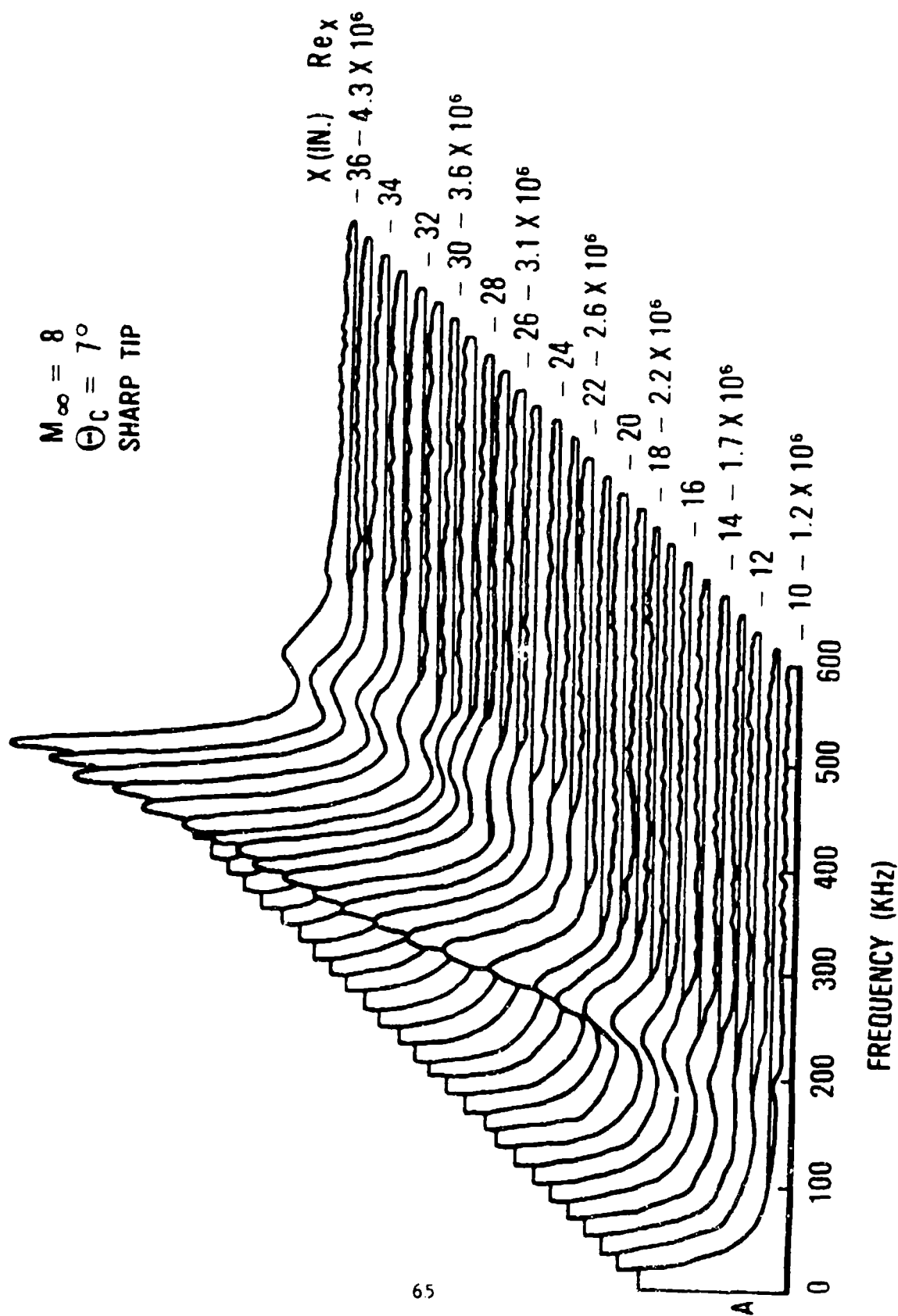


FIG. 3 Boundary-Layer Fluctuation Spectra

$M_{\infty} = 8$
 $\Theta_c = 7^\circ$
 SHARP TIP

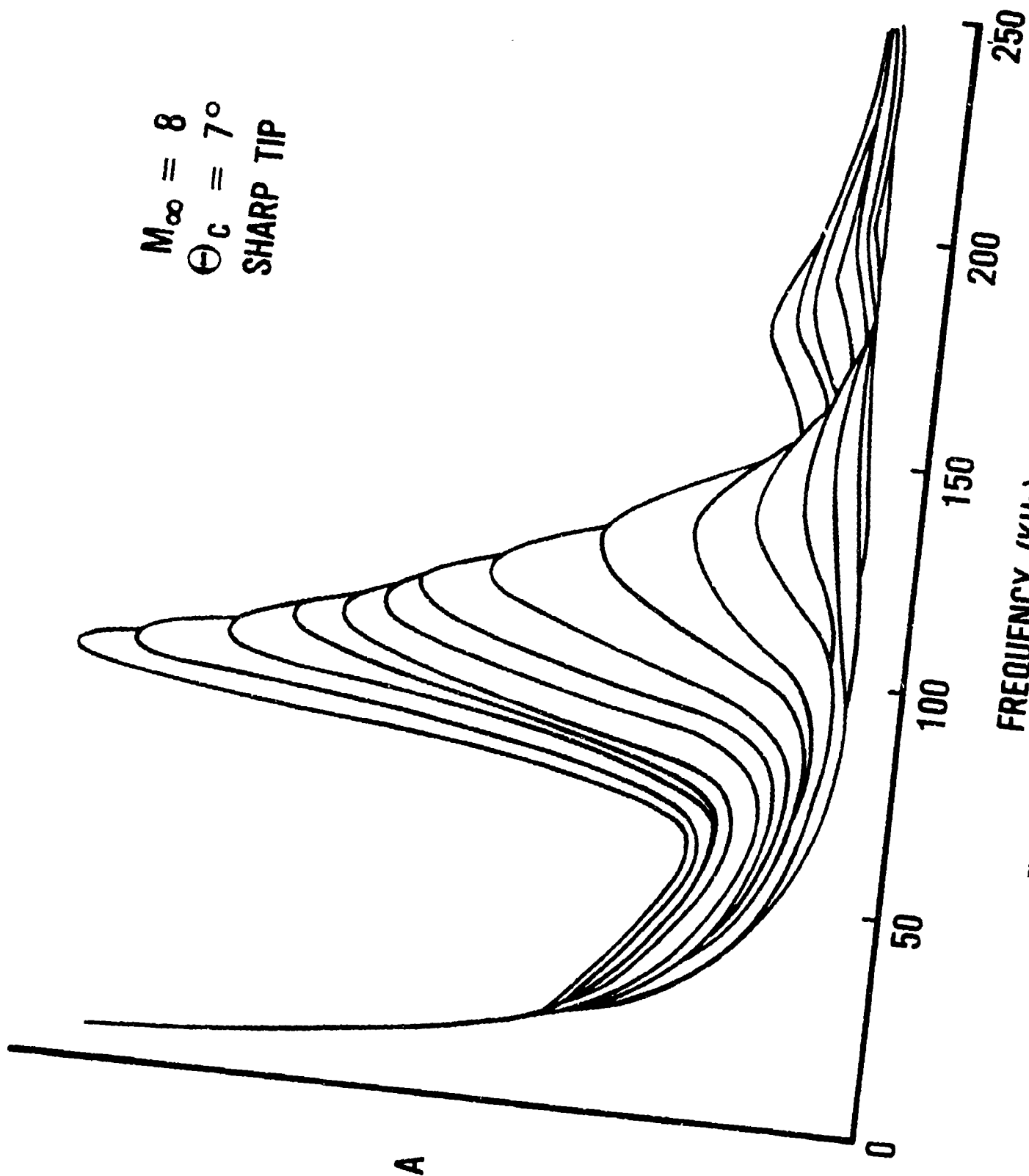


FIG. 4 Fluctuation Spectra Overlaid

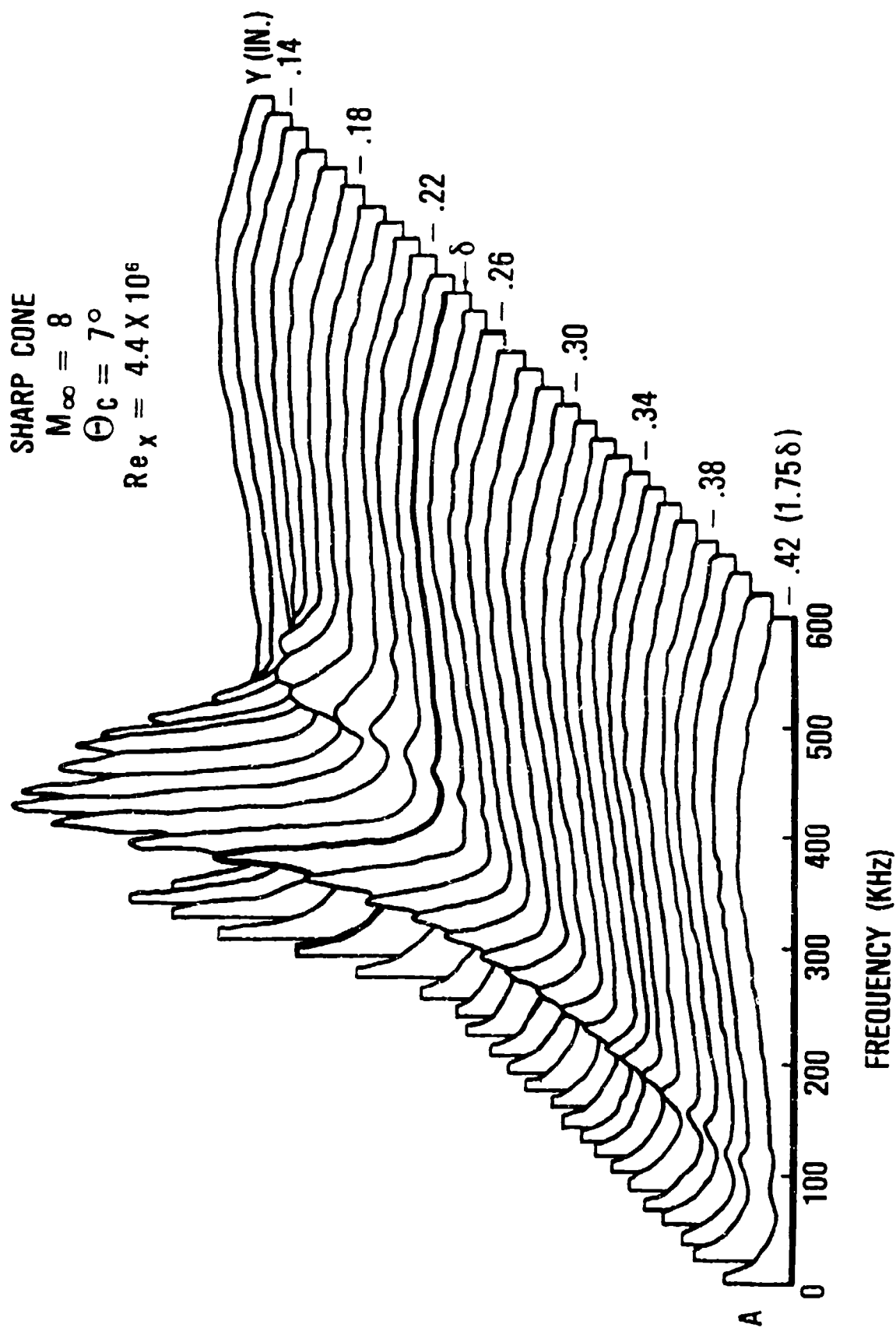


FIG. 5a Fluctuation Spectra, Normal to the Surface. Outside the Boundary Layer. Looking in.

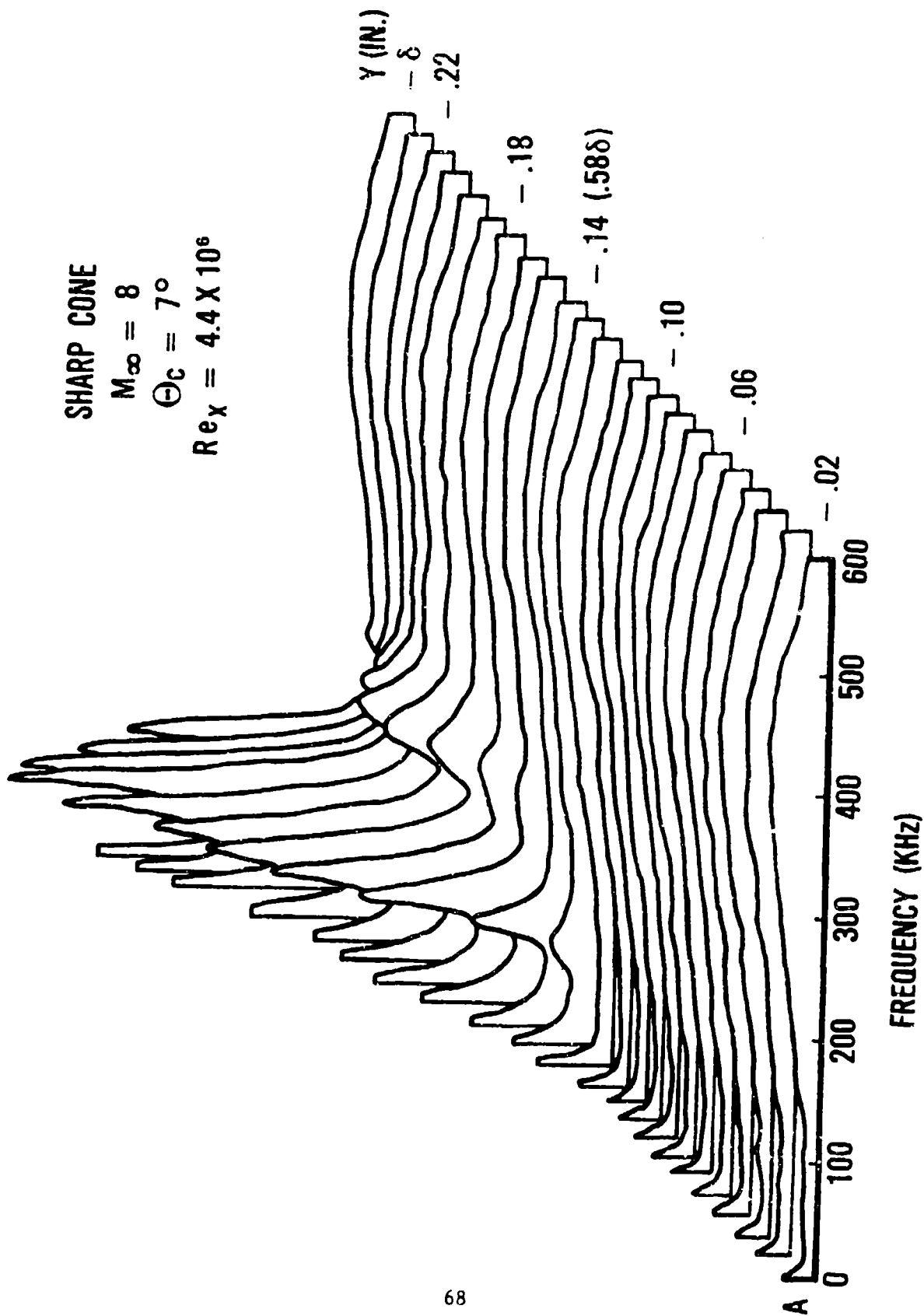


FIG. 5b Fluctuation Spectra, Normal to the Surface.
 From the Surface, Looking Out.

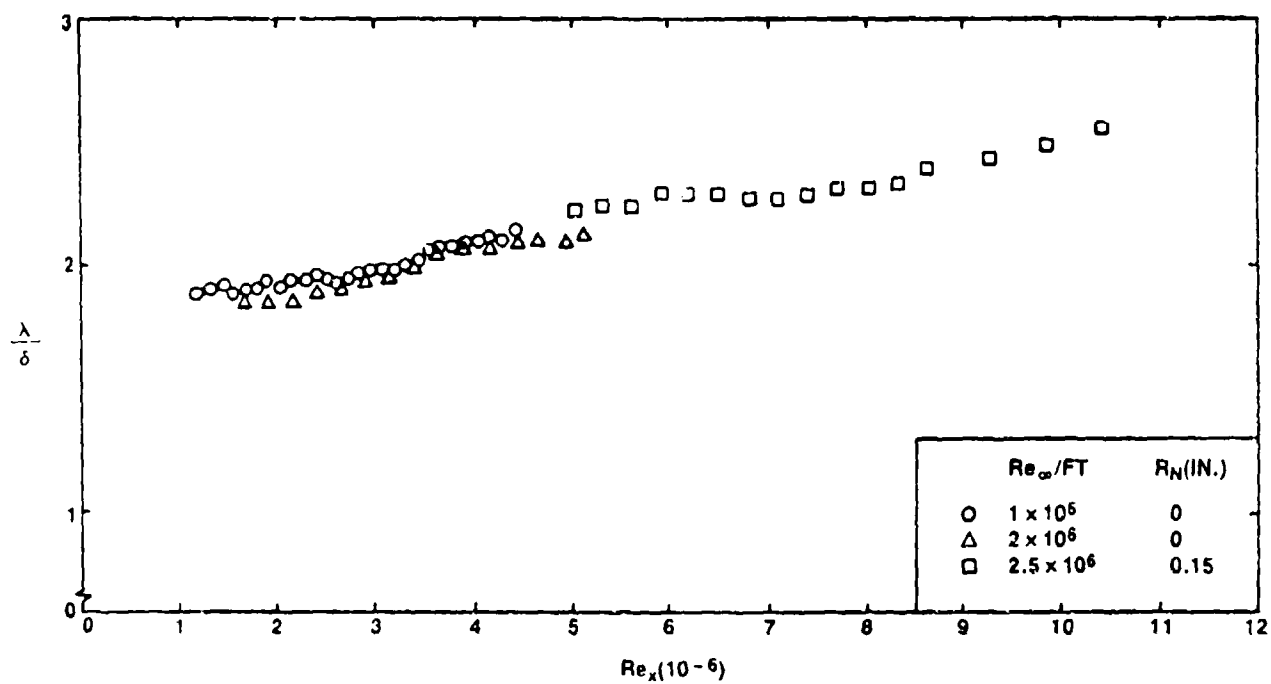


FIG. 6 Wavelengths of the Most Unstable Second Mode Disturbances

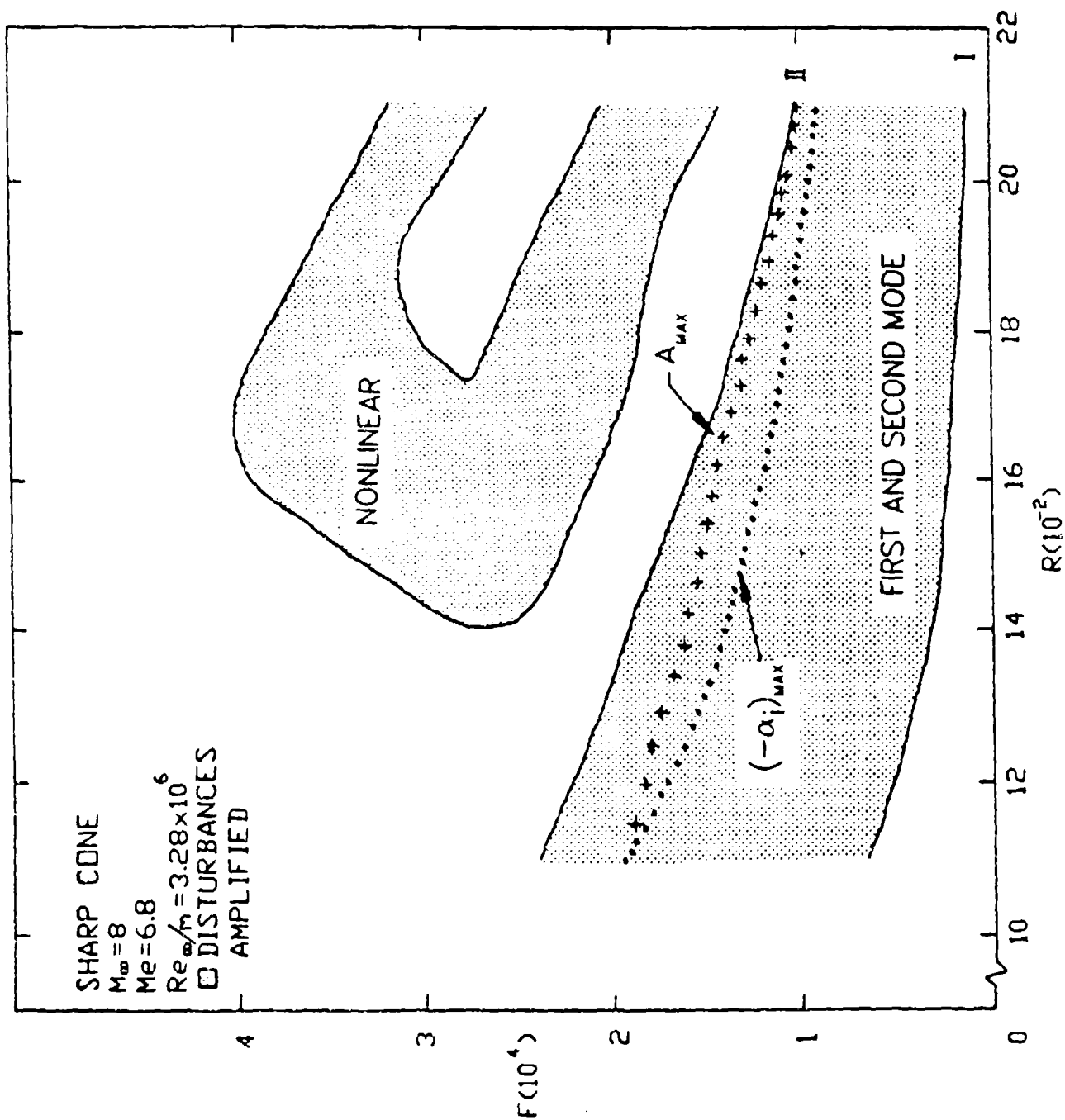
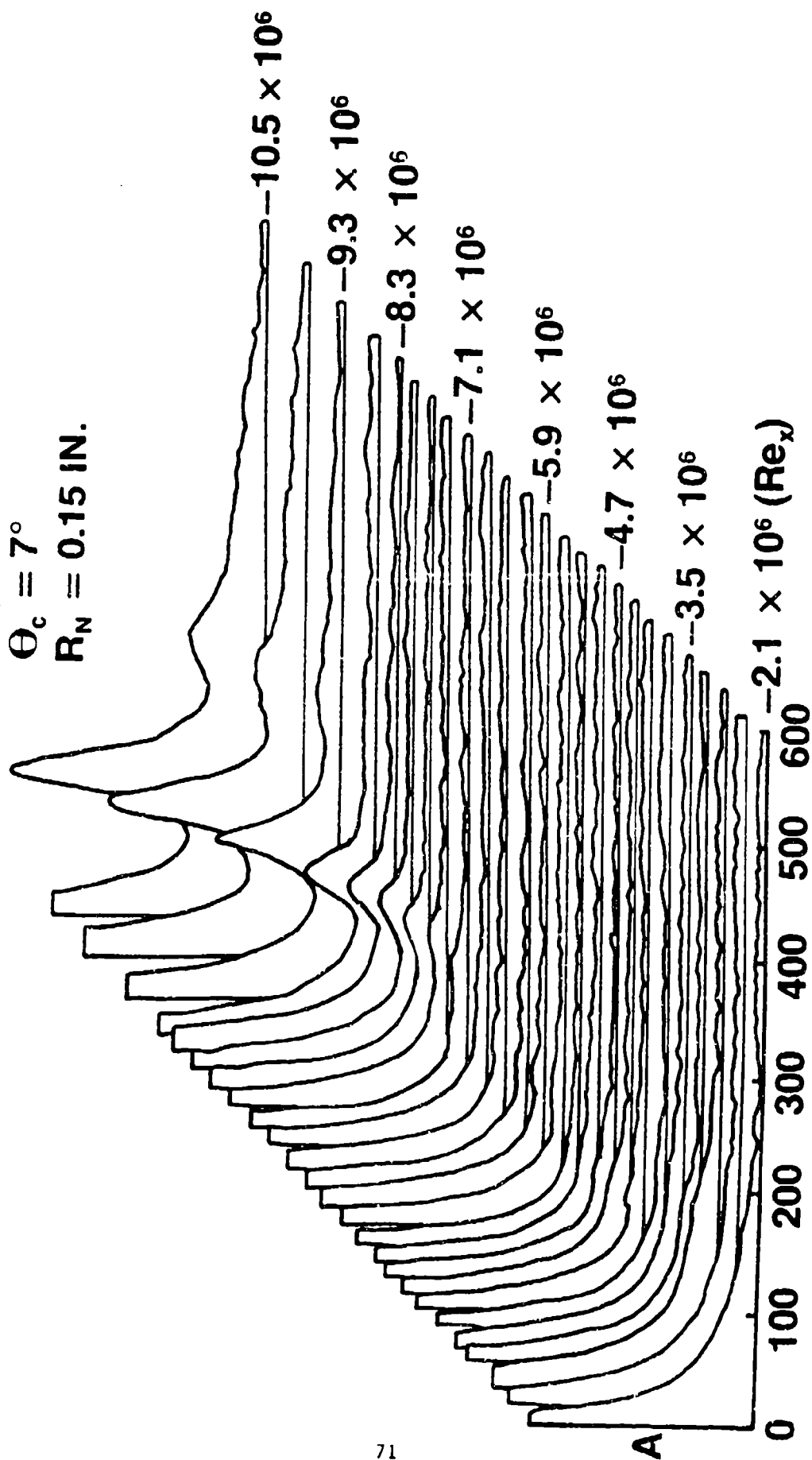


FIG. 7 Experimentally Derived Stability Diagram

$M_{\infty} = 8$
 $\Theta_c = 7^\circ$
 $R_N = 0.15 \text{ IN.}$



$f(\text{kHz})$

FIG. 8 Fluctuation Spectra

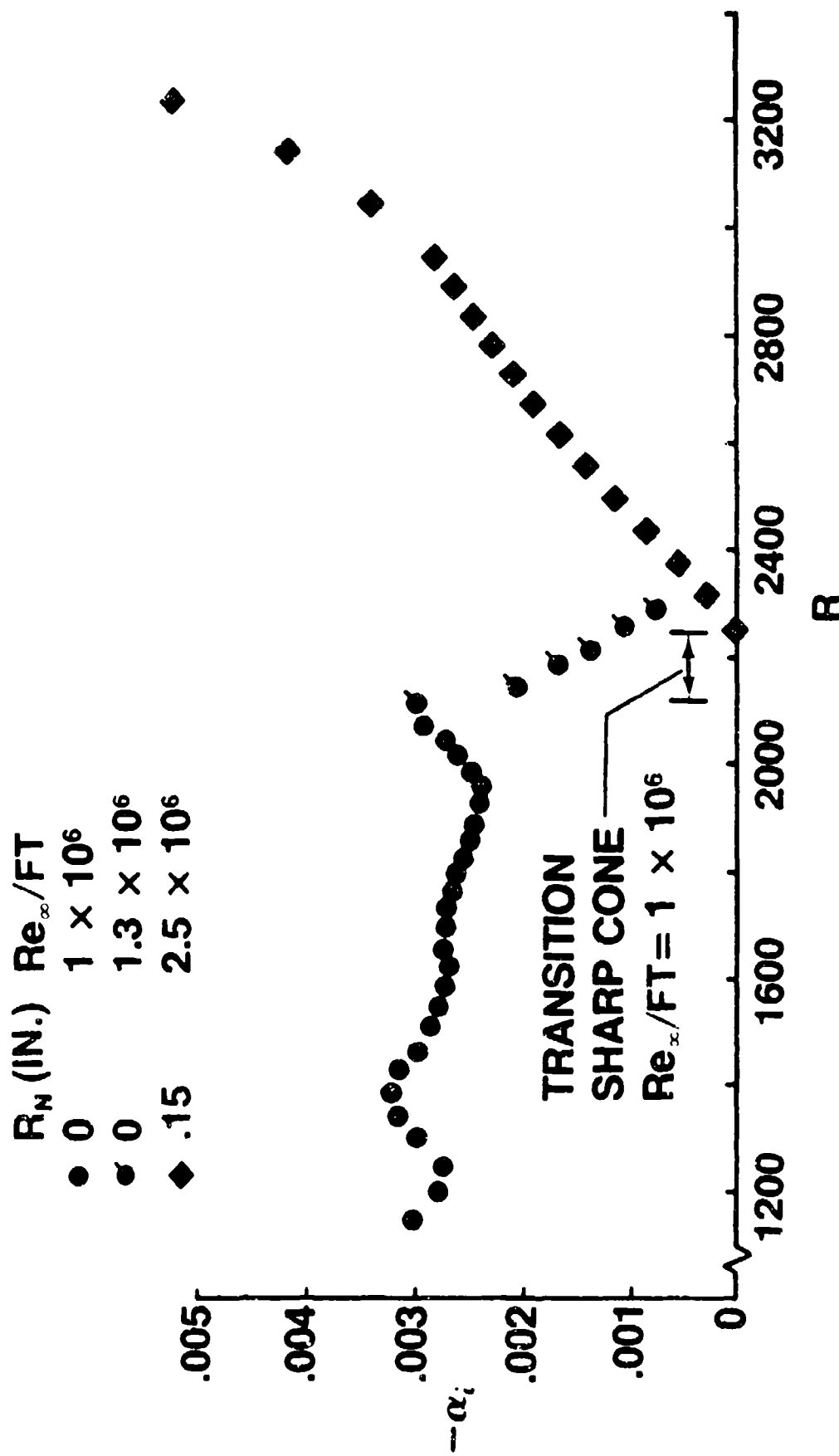


FIG. 9 Maximum Amplification Rates Associated with the Second Mode

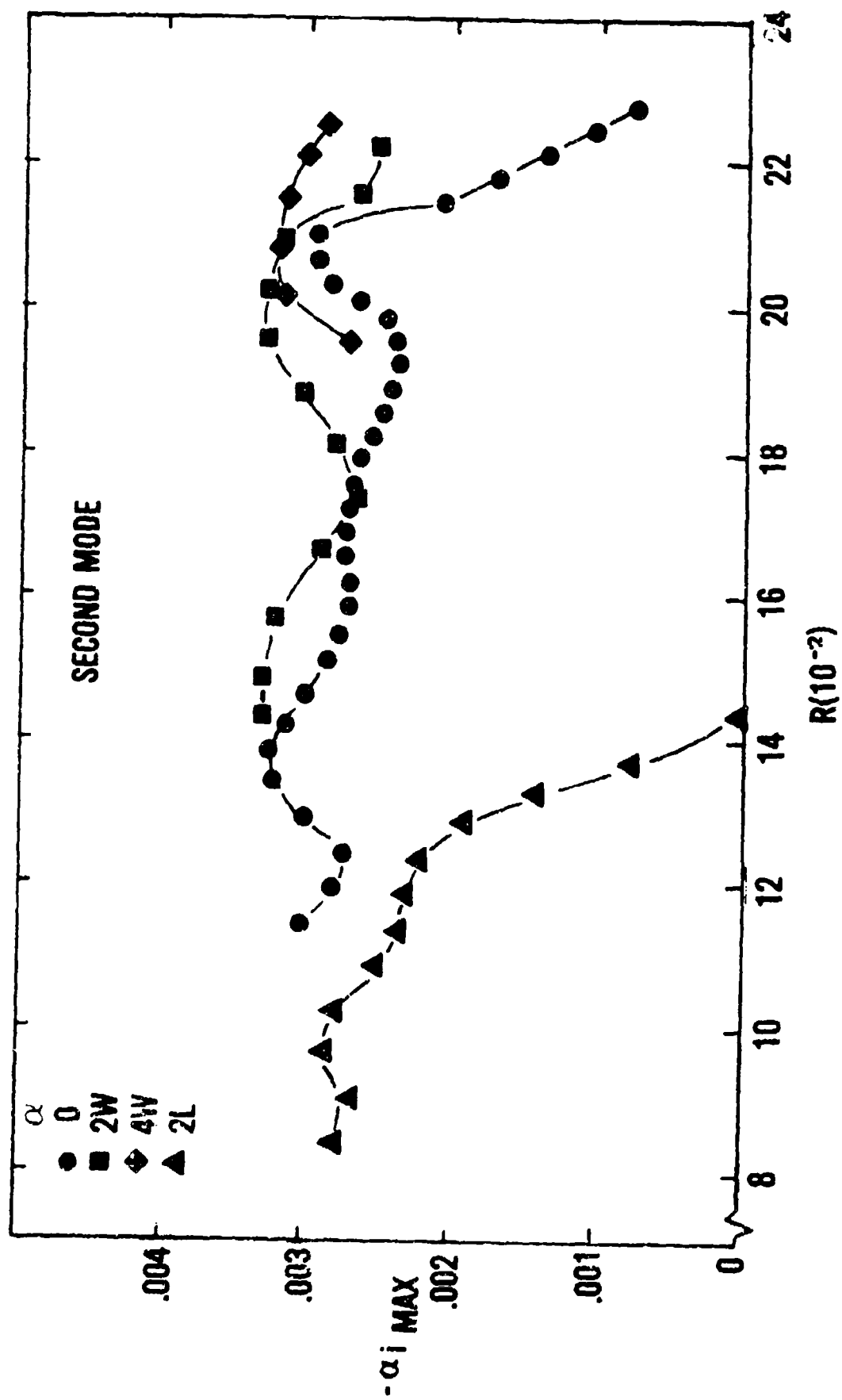


FIG. 10 Second Mode Maximum Amplification Rates

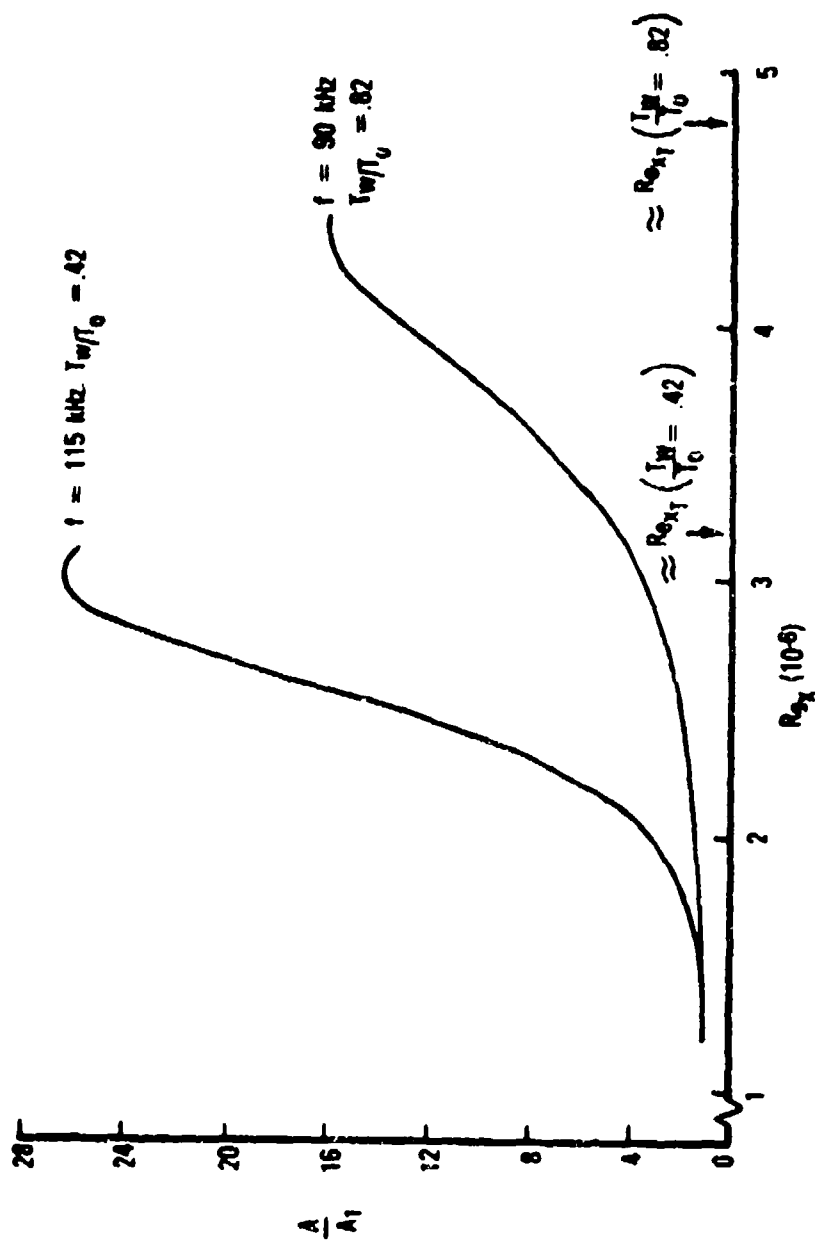


FIG. 11 Second Mode Disturbance Growth

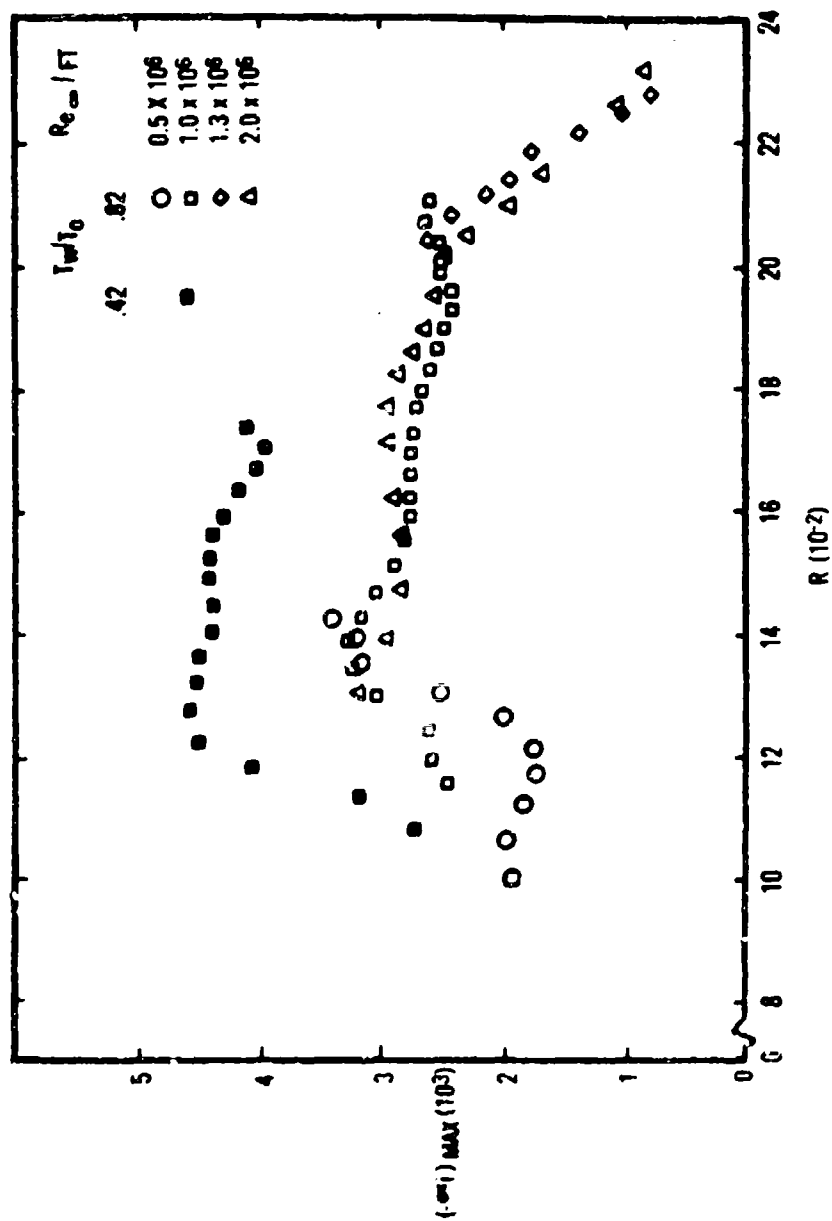


FIG. 12 Maximum Growth Rates for Second Mode Disturbances

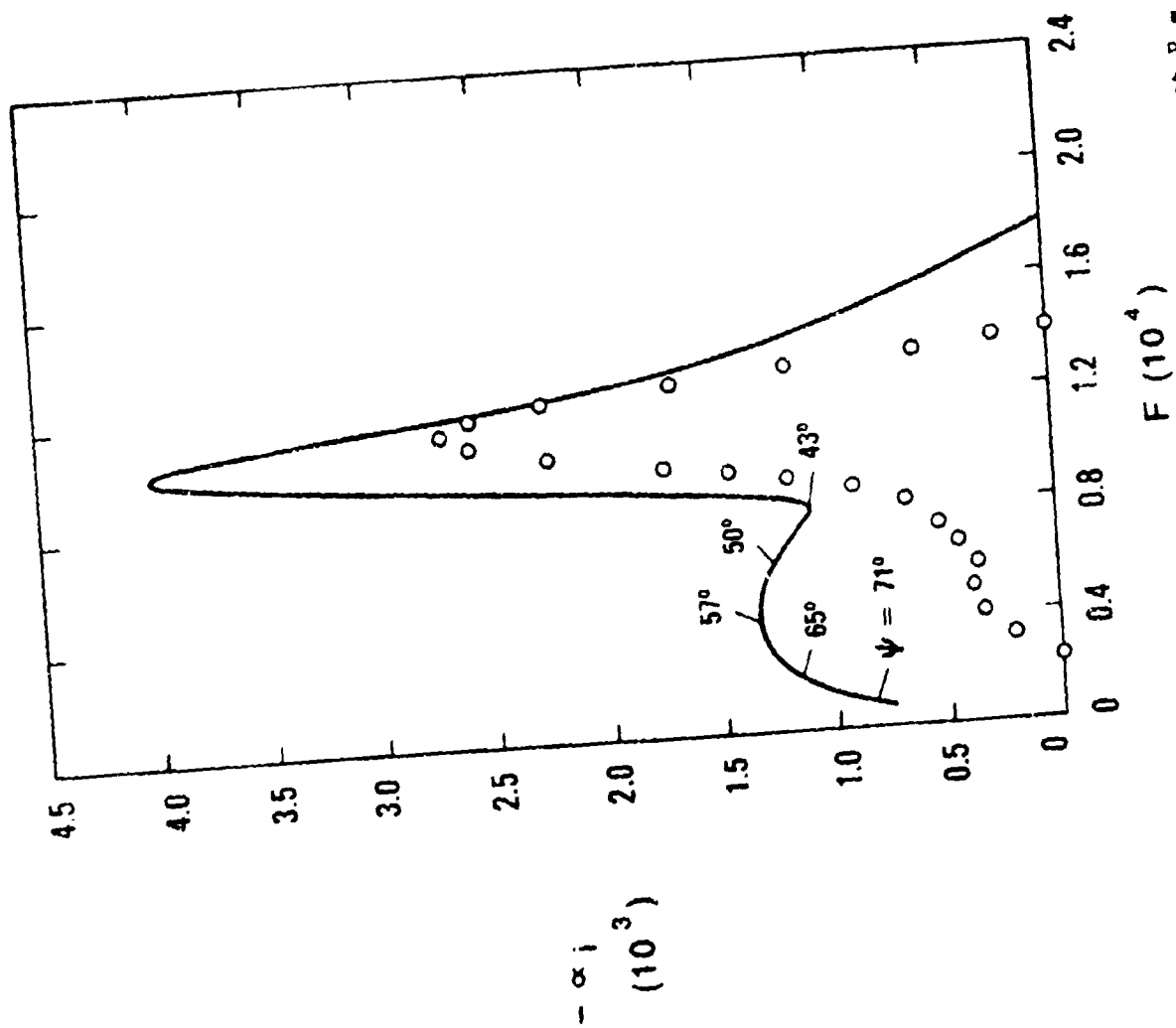


FIG. 13 Spatial Amplification Rate vs. Frequency at $R = 1731$.
Points are From Experimental Data

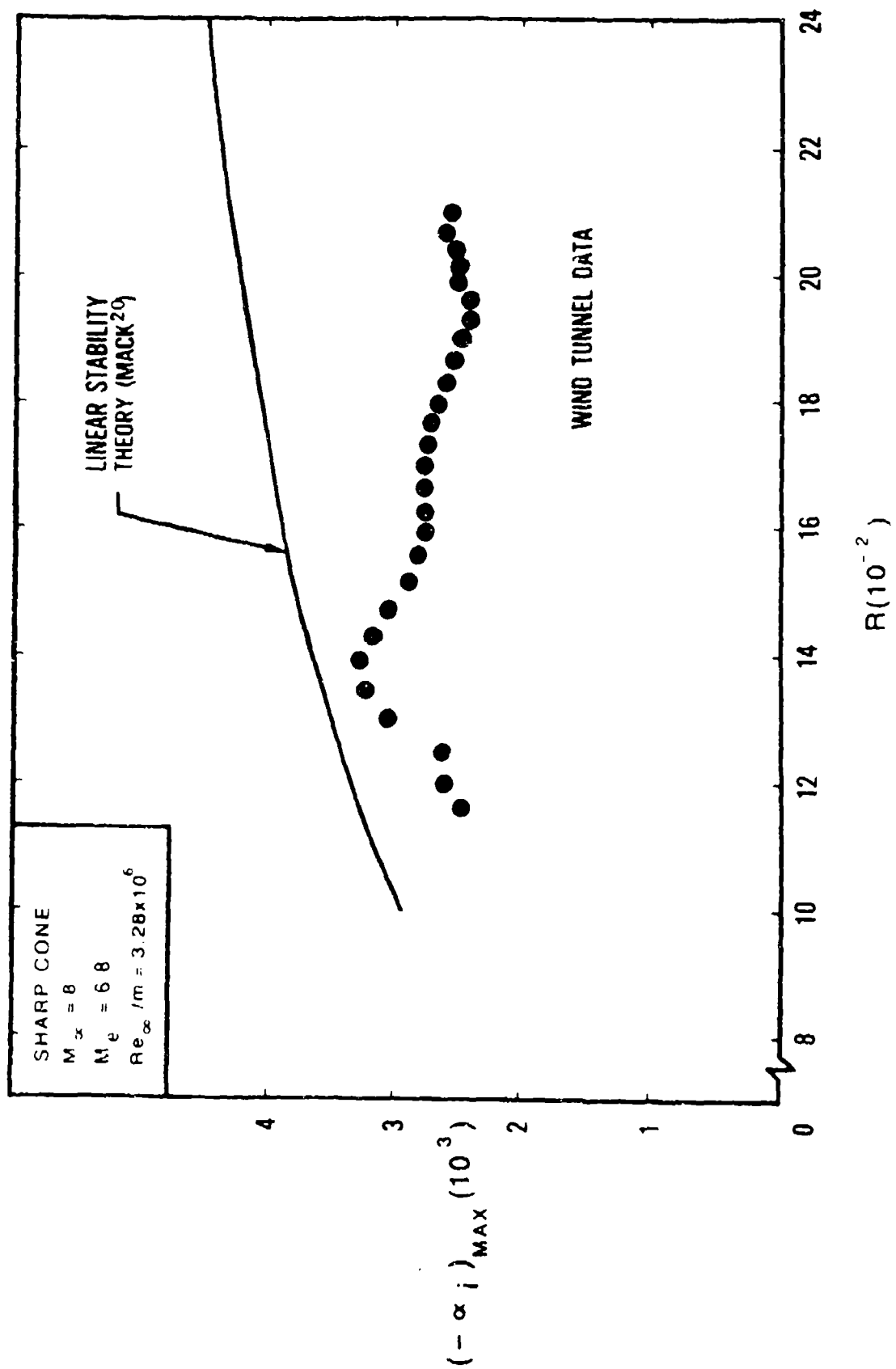


FIG. 14 Second Mode Maximum Amplification Rates

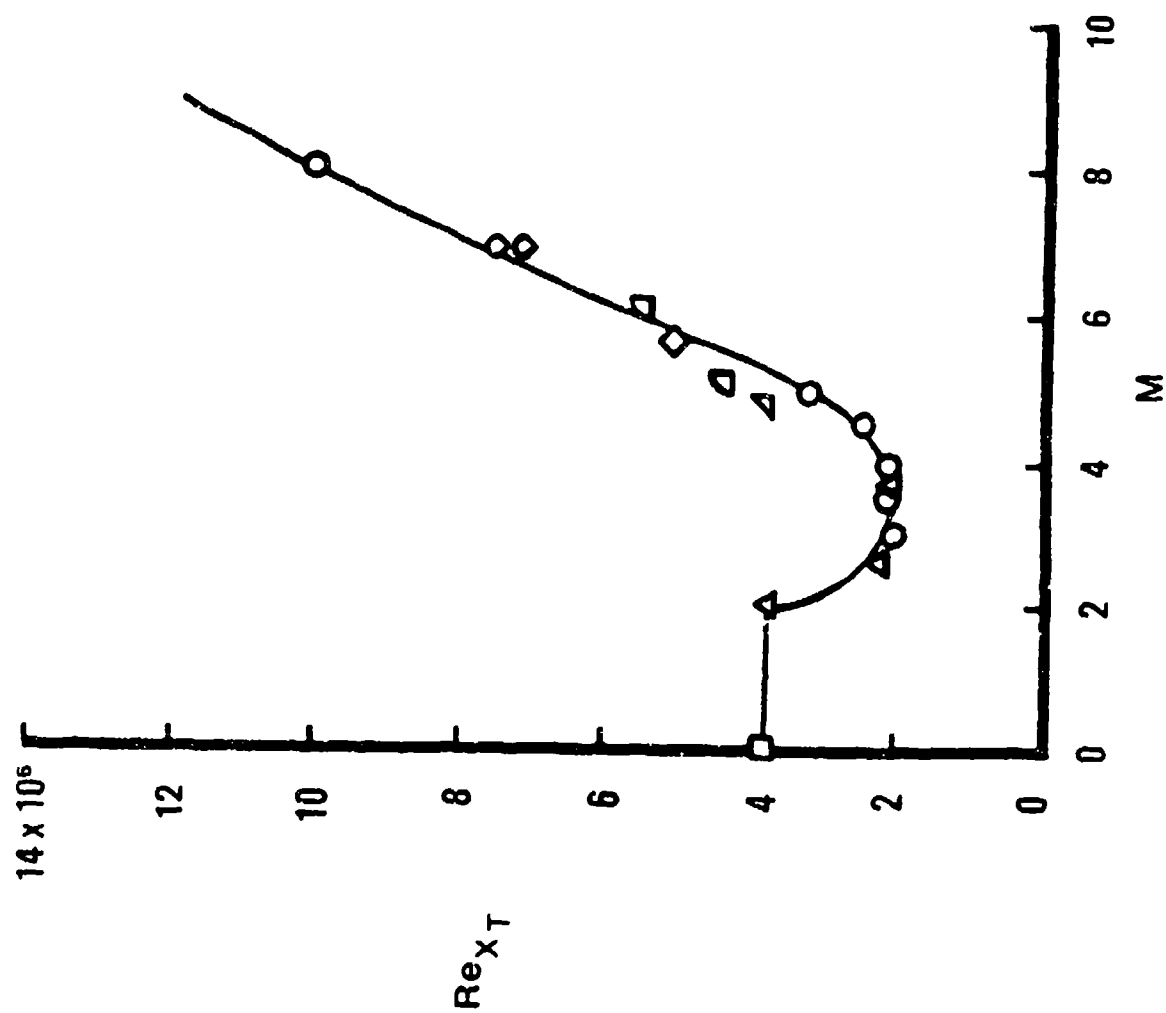


FIG. 15 Effect of Mach Number on Transition

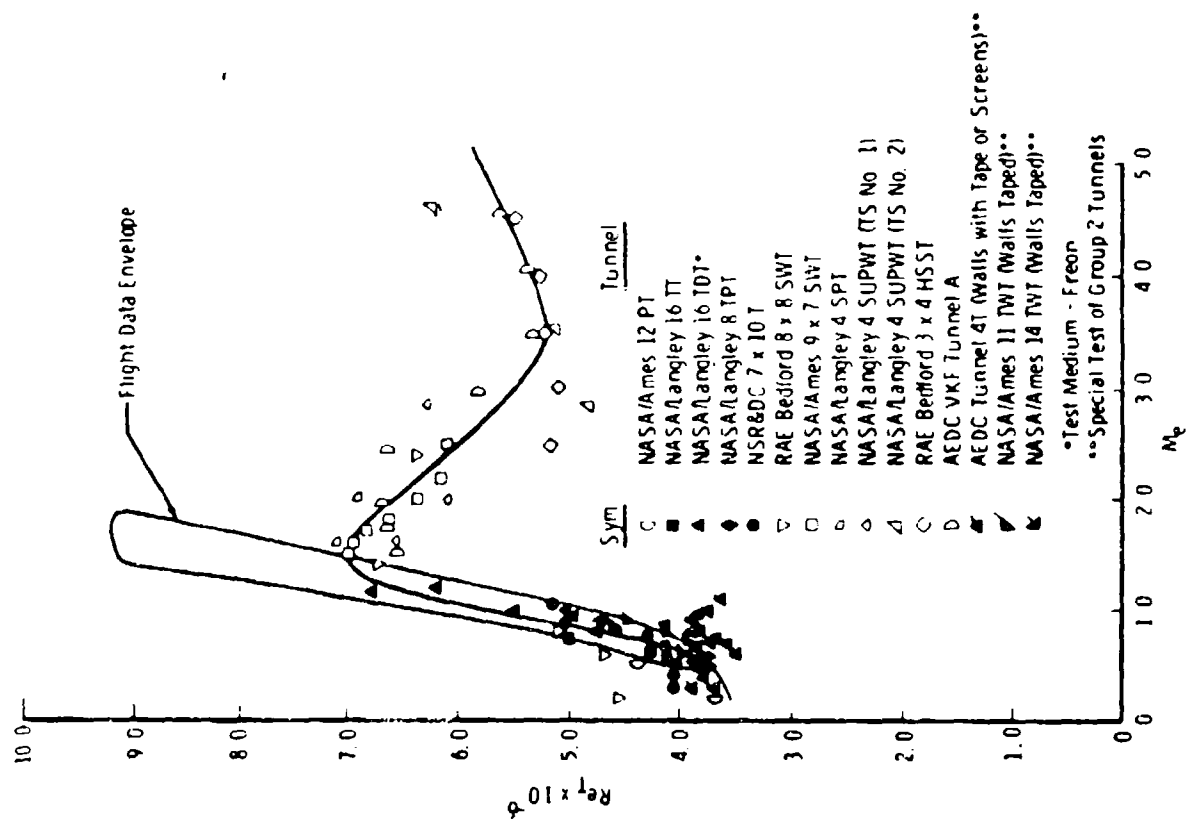


FIG. 16 Wind Tunnel and Flight Transition Results

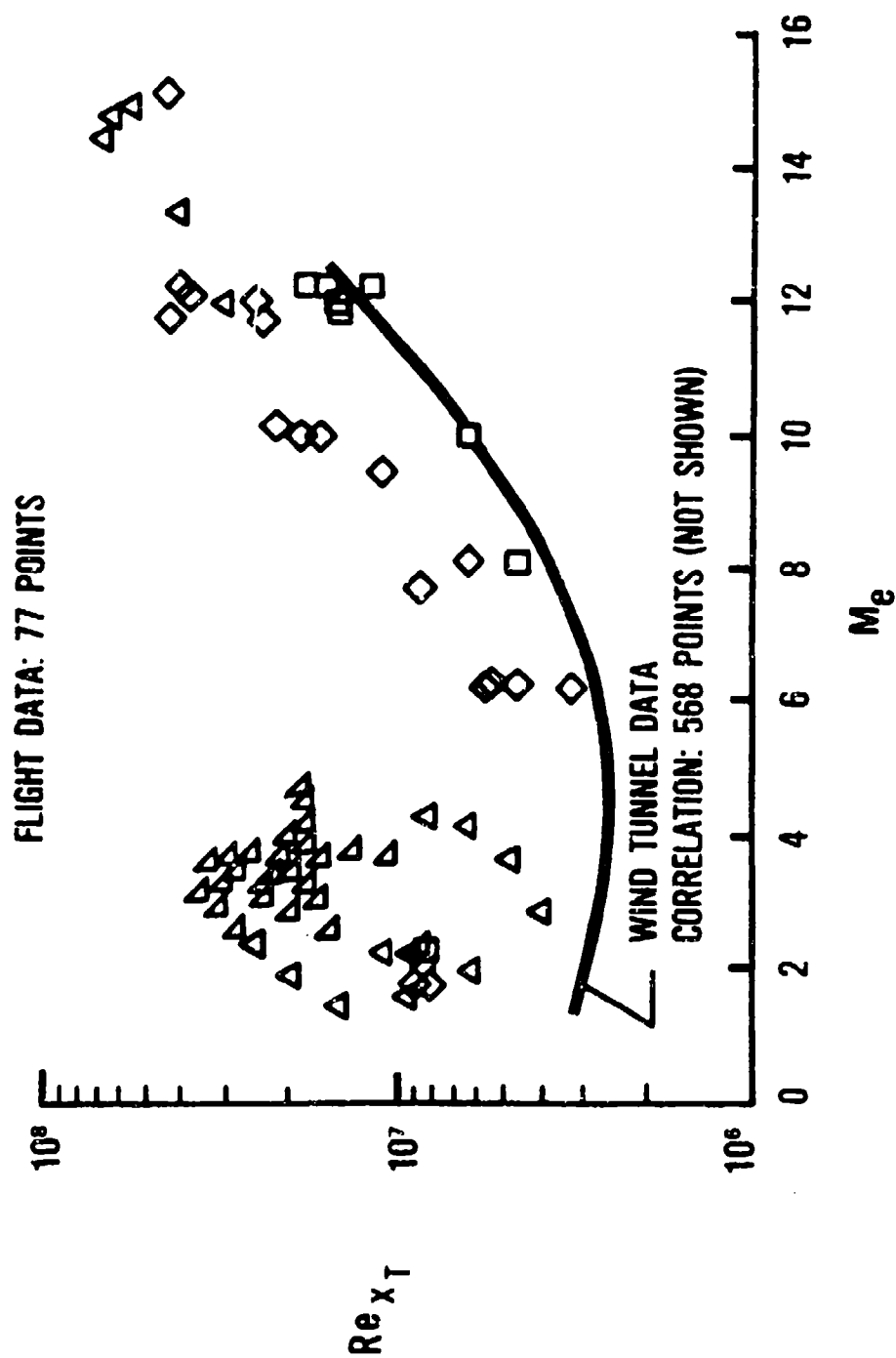


FIG. 17 Cone Transition Reynolds Number Data for Wind Tunnels and Flight

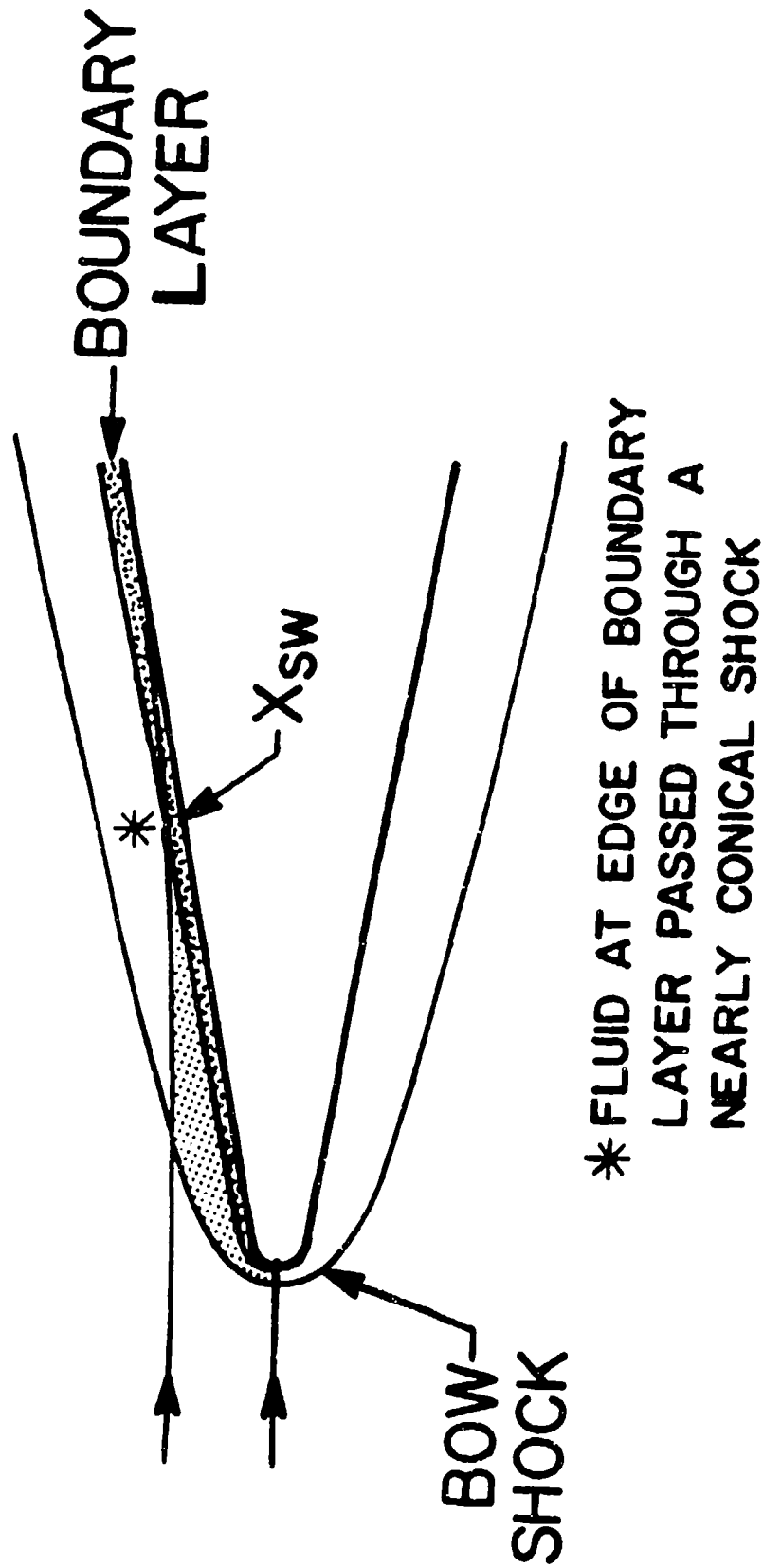


FIG. 18 A Schematic of Flow Over
A Slender Blunt Cone

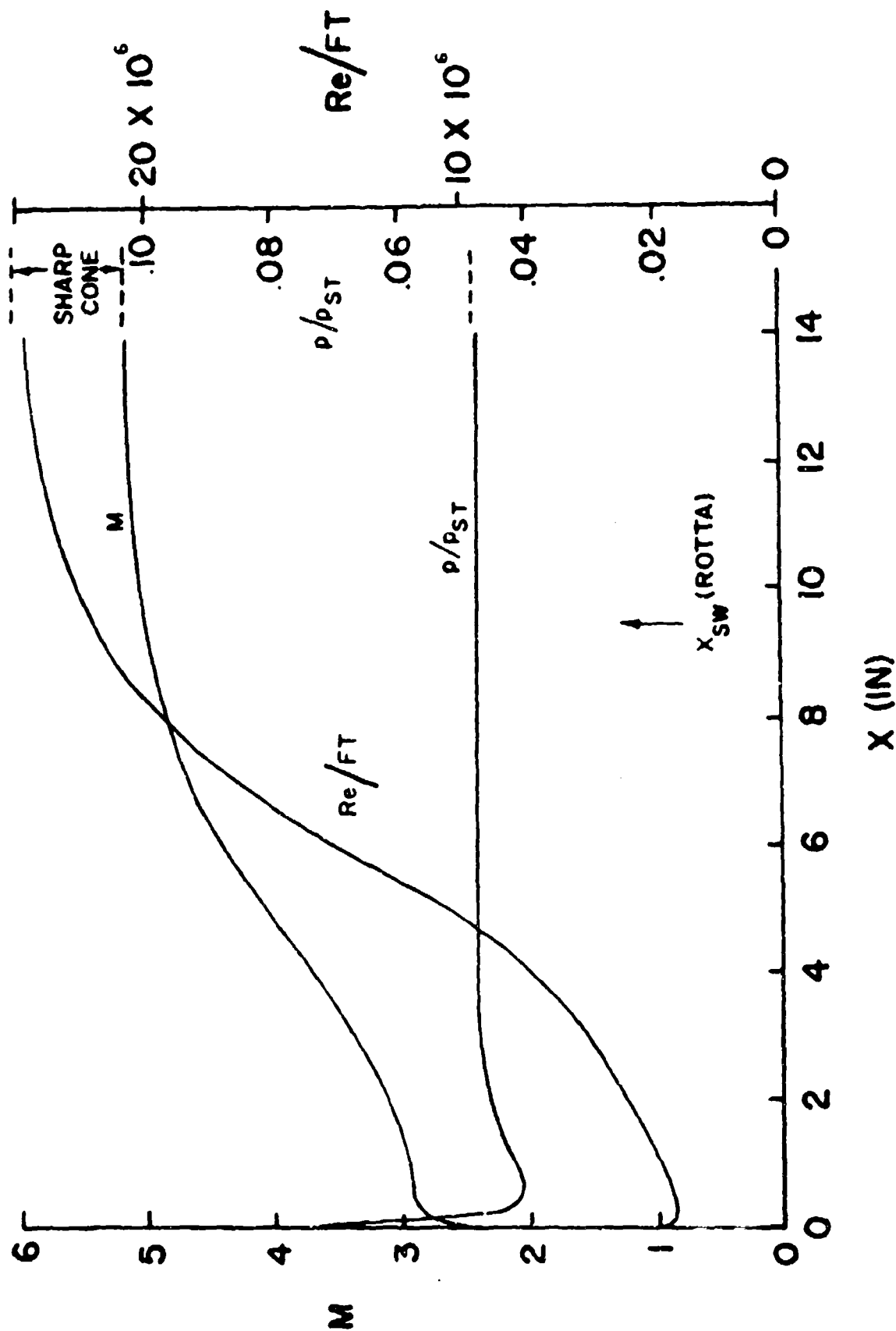


FIG. 19 Calculations of Local Flow Properties on an 8-Deg. Half Angle Cone with 2% Bluntness at $M = 5.9$

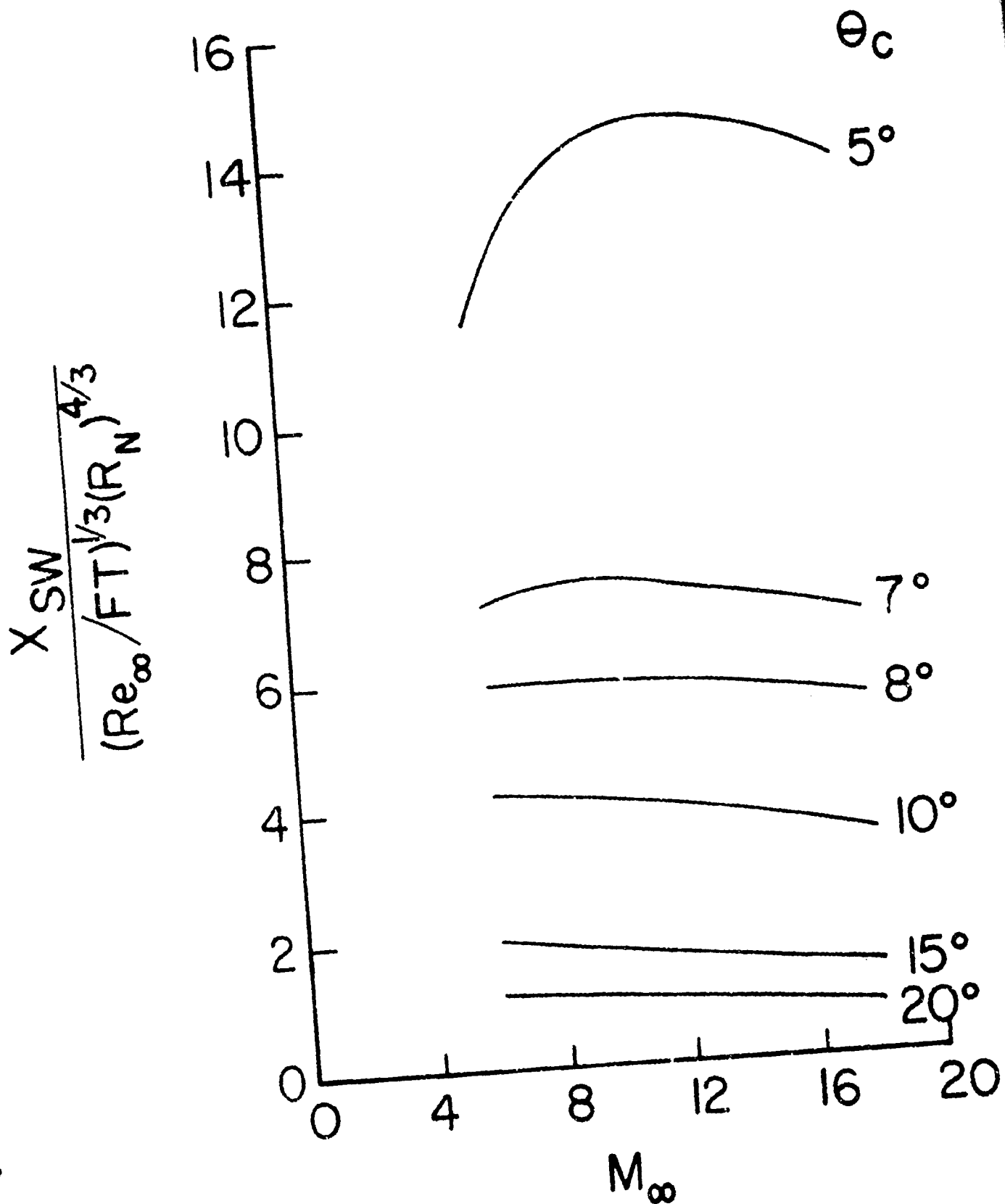


FIG. 20 Entropy-Layer-Swallowing Distance Parameter

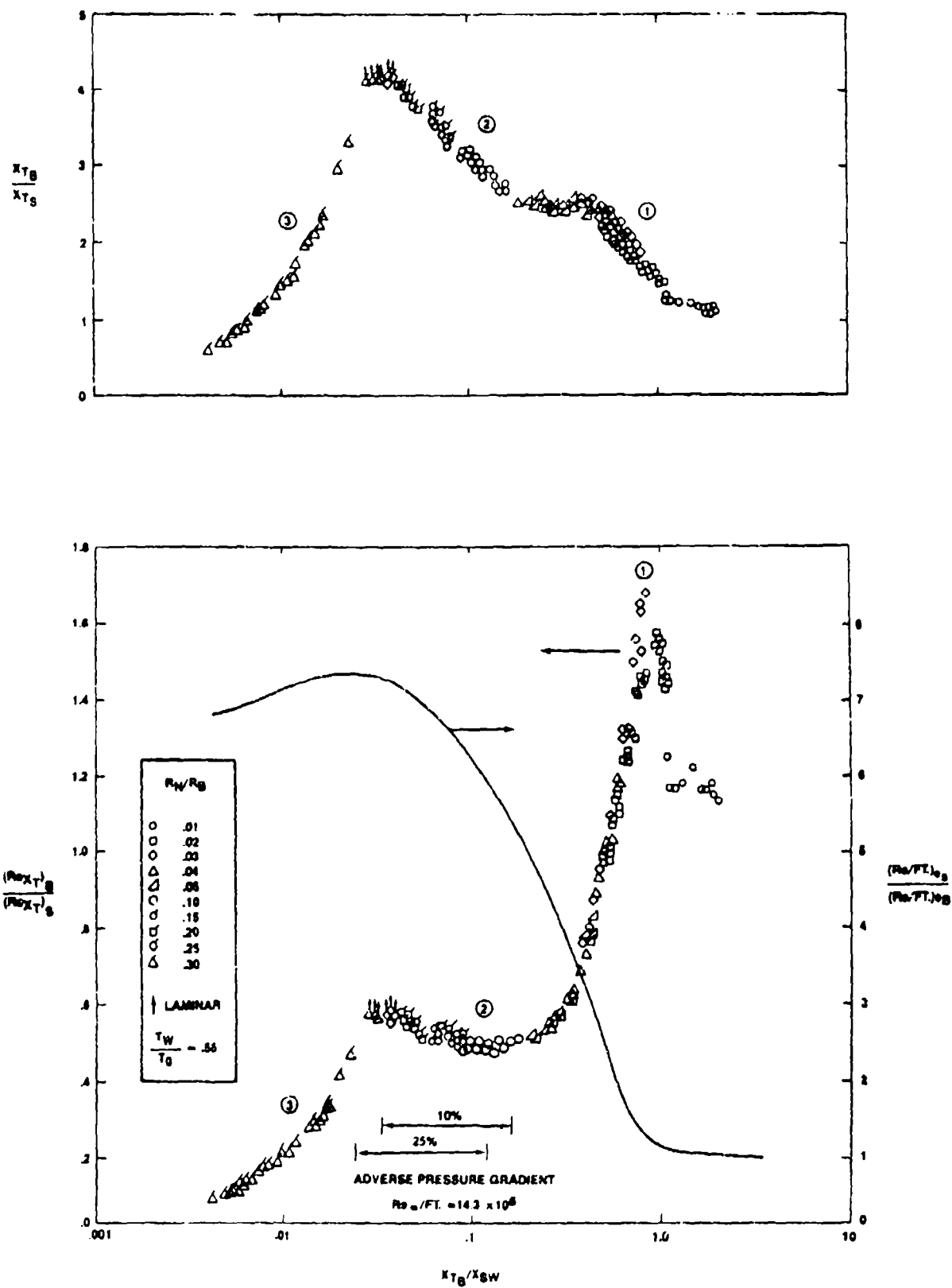


FIG. 21 Effect of Nosetip Bluntness on Cone Frustum Transition at $M_\infty = 5.9$

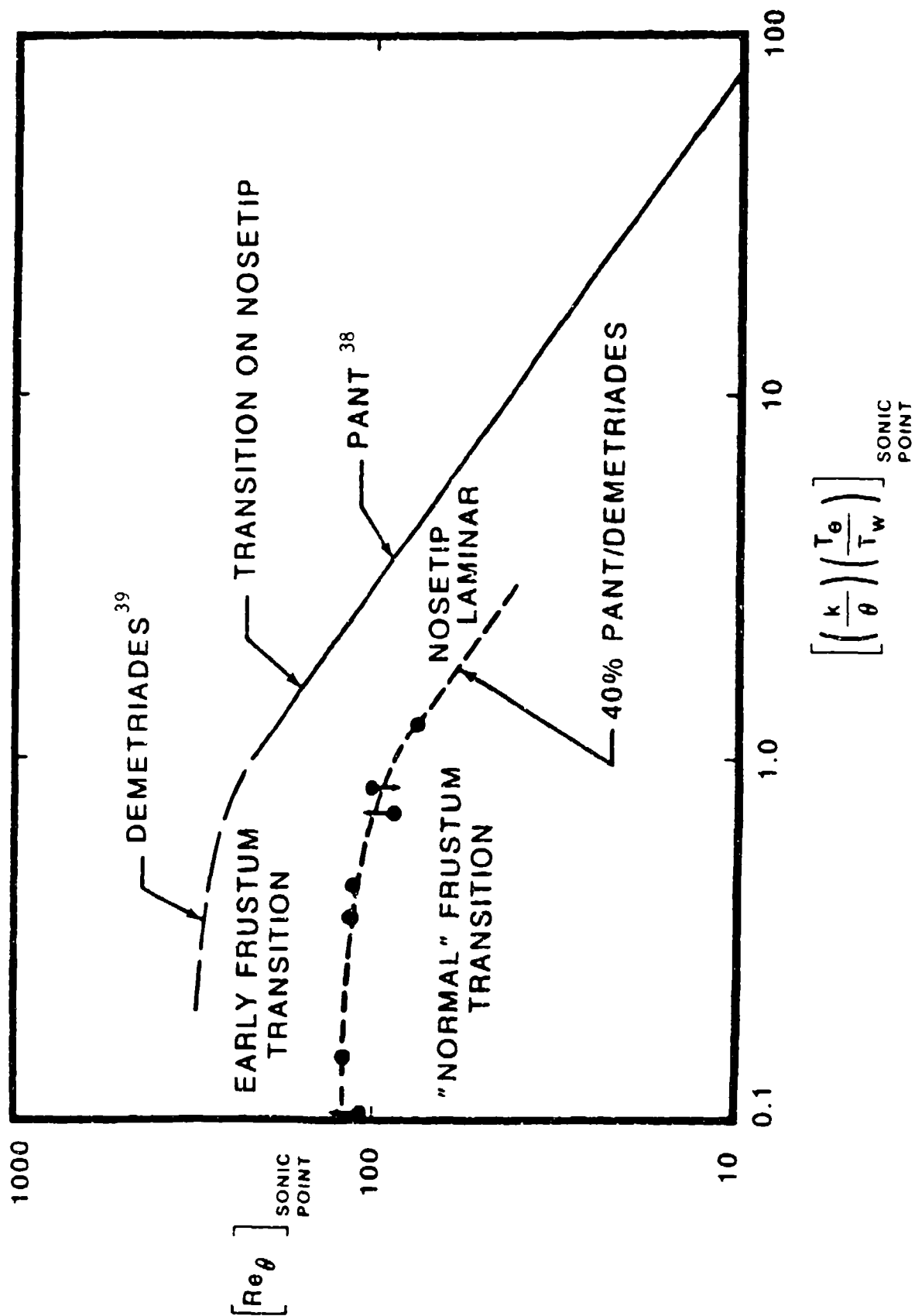


FIG. 22 Nosedip Instability Effects on Cone Frustum Transition

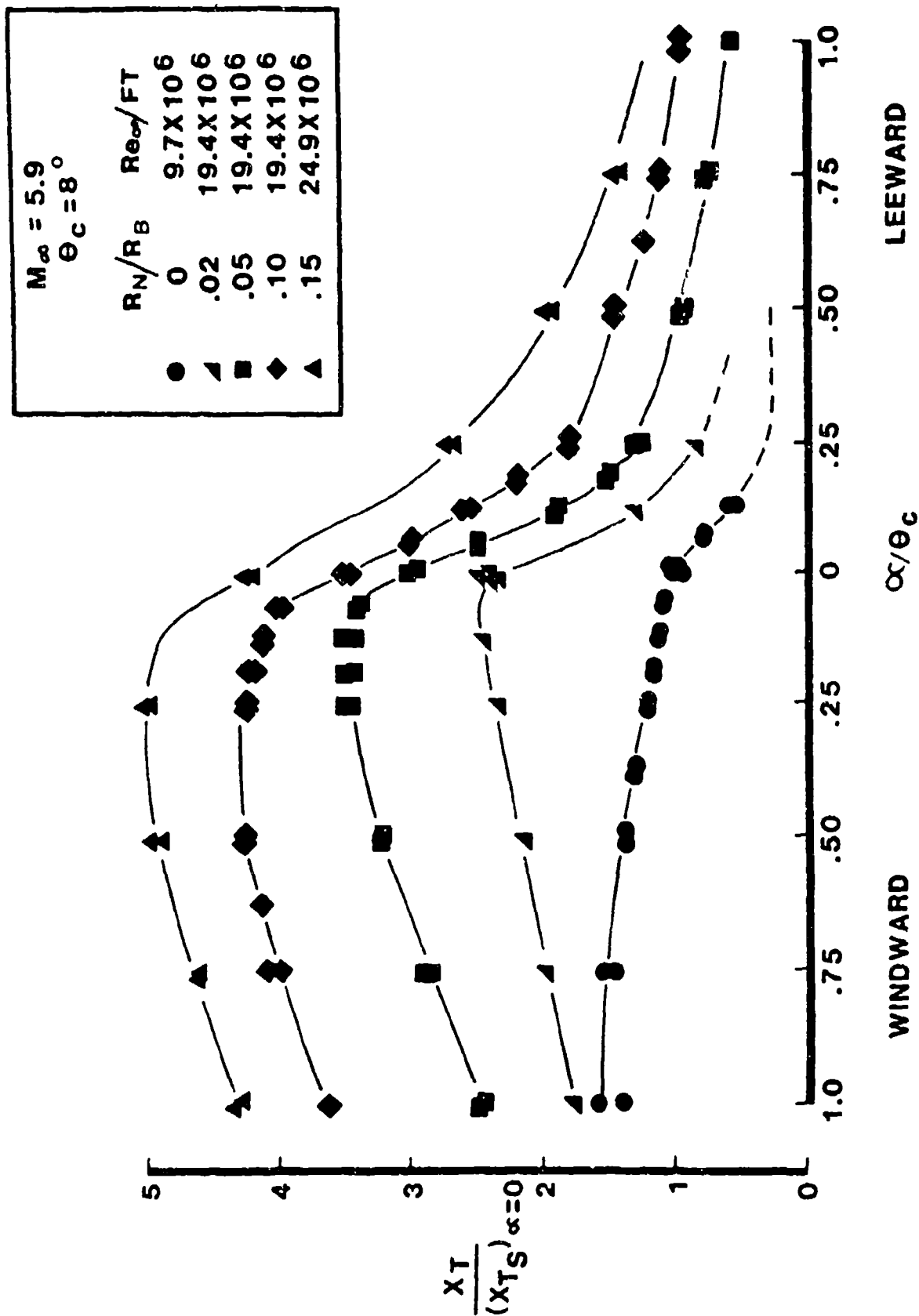


FIG. 23 Transition Movement with Angle of Attack

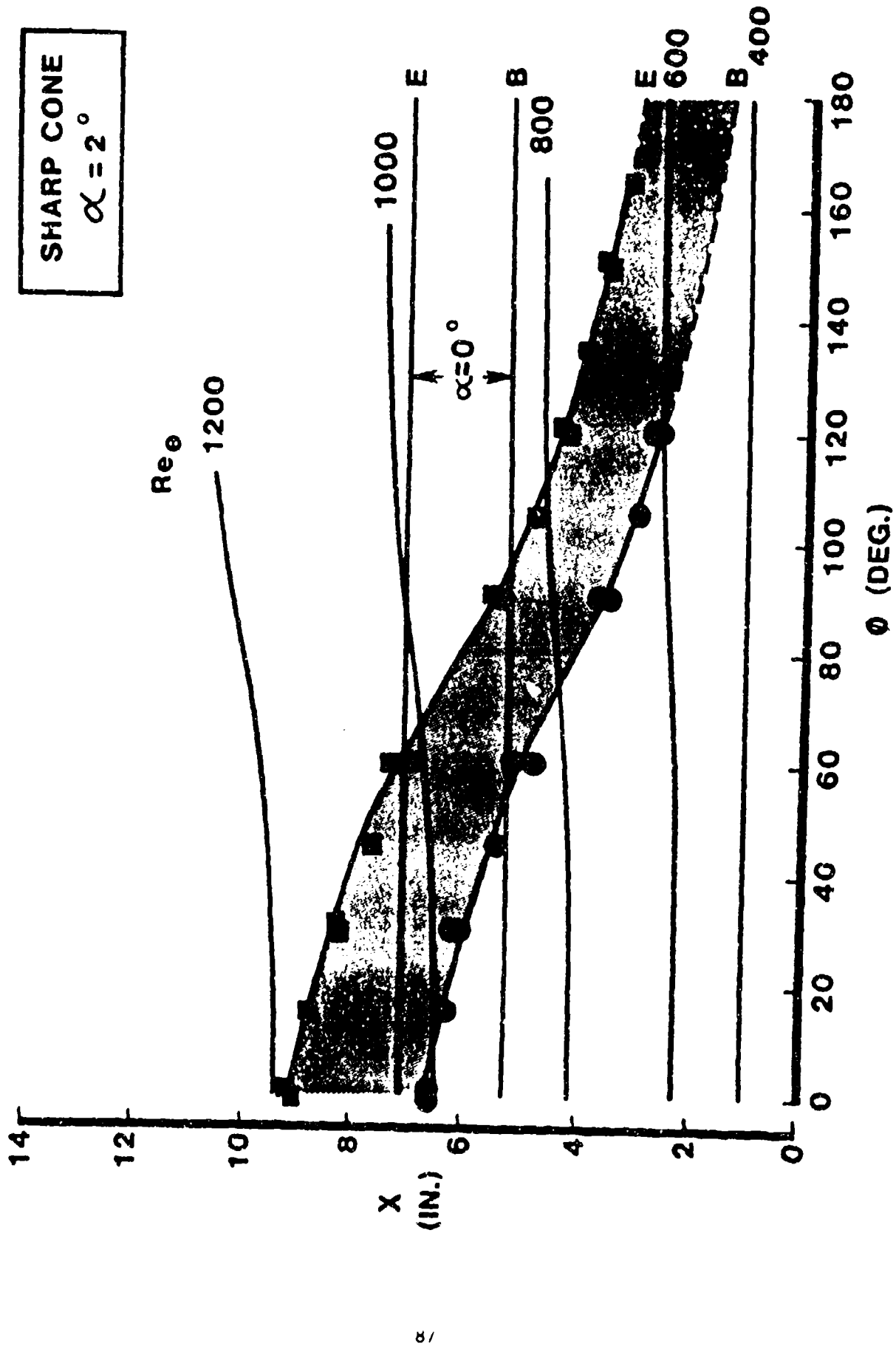


FIG. 24 Transition Pattern on a Sharp Cone at $\alpha = 2^\circ$ Deg.

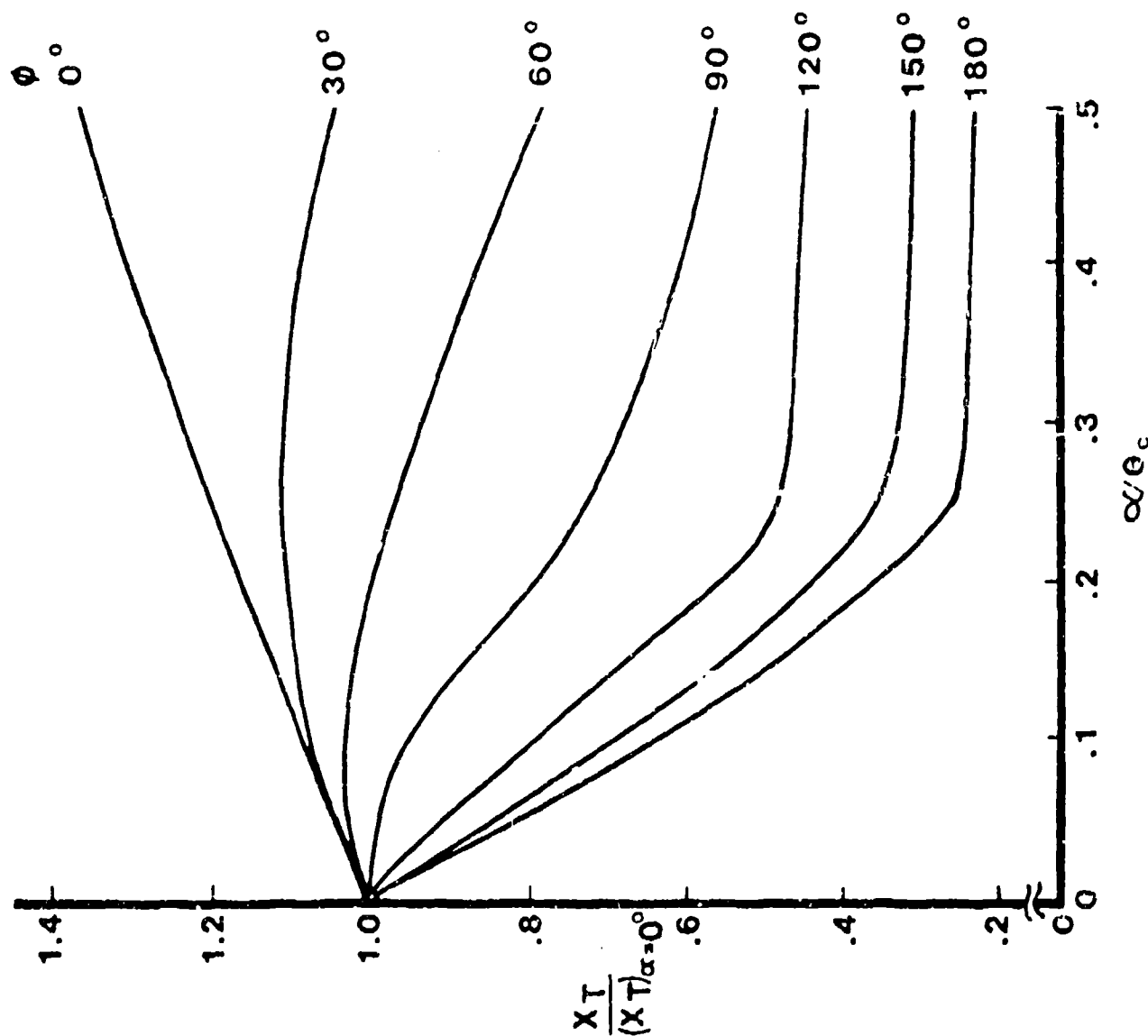


FIG. 25 Transition Asymmetry with Angle of Attack for a Sharp Cone

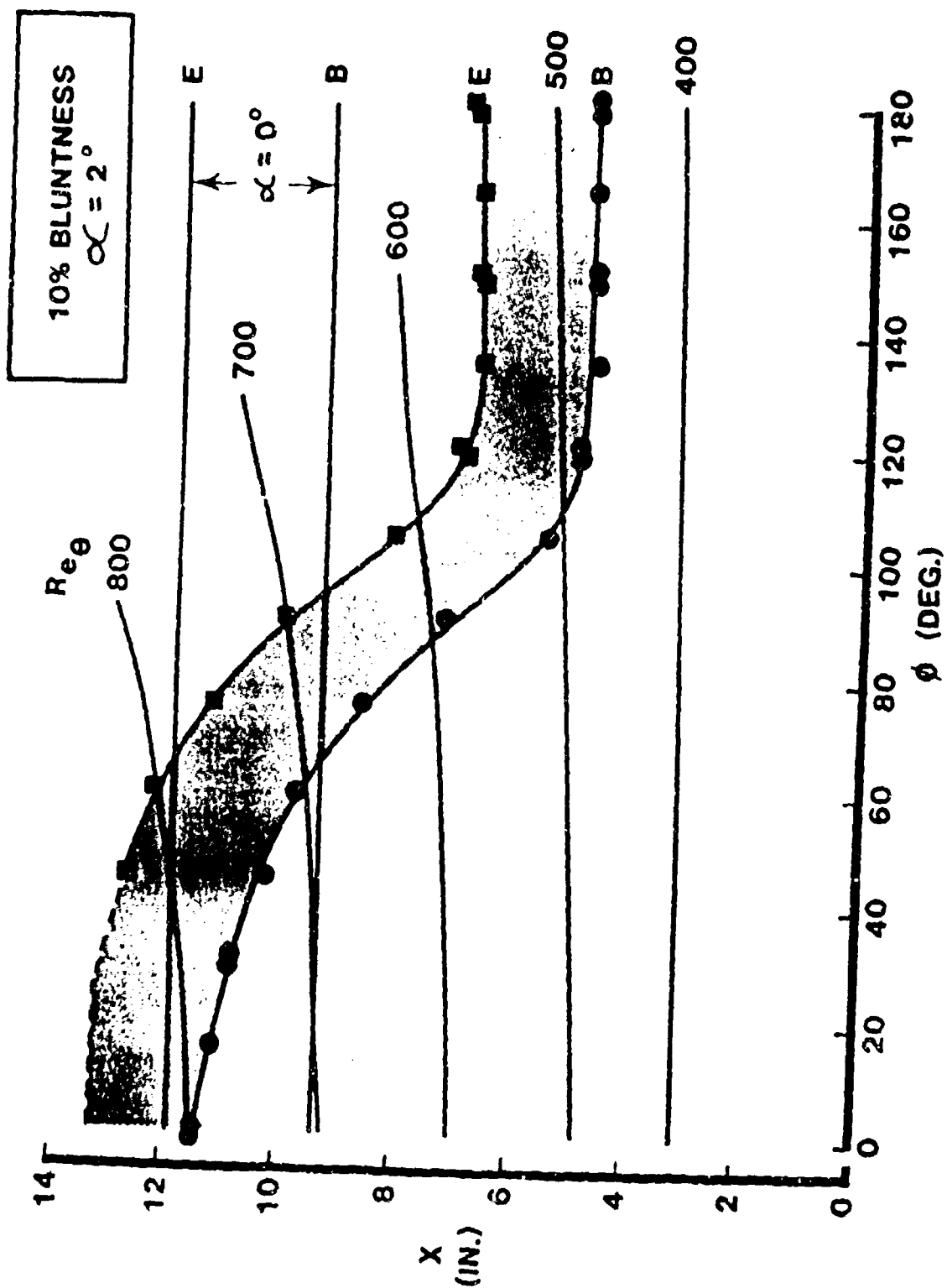


FIG. 26 Transition Pattern on a Blunt Cone at $\alpha = 2^\circ$ Deg.

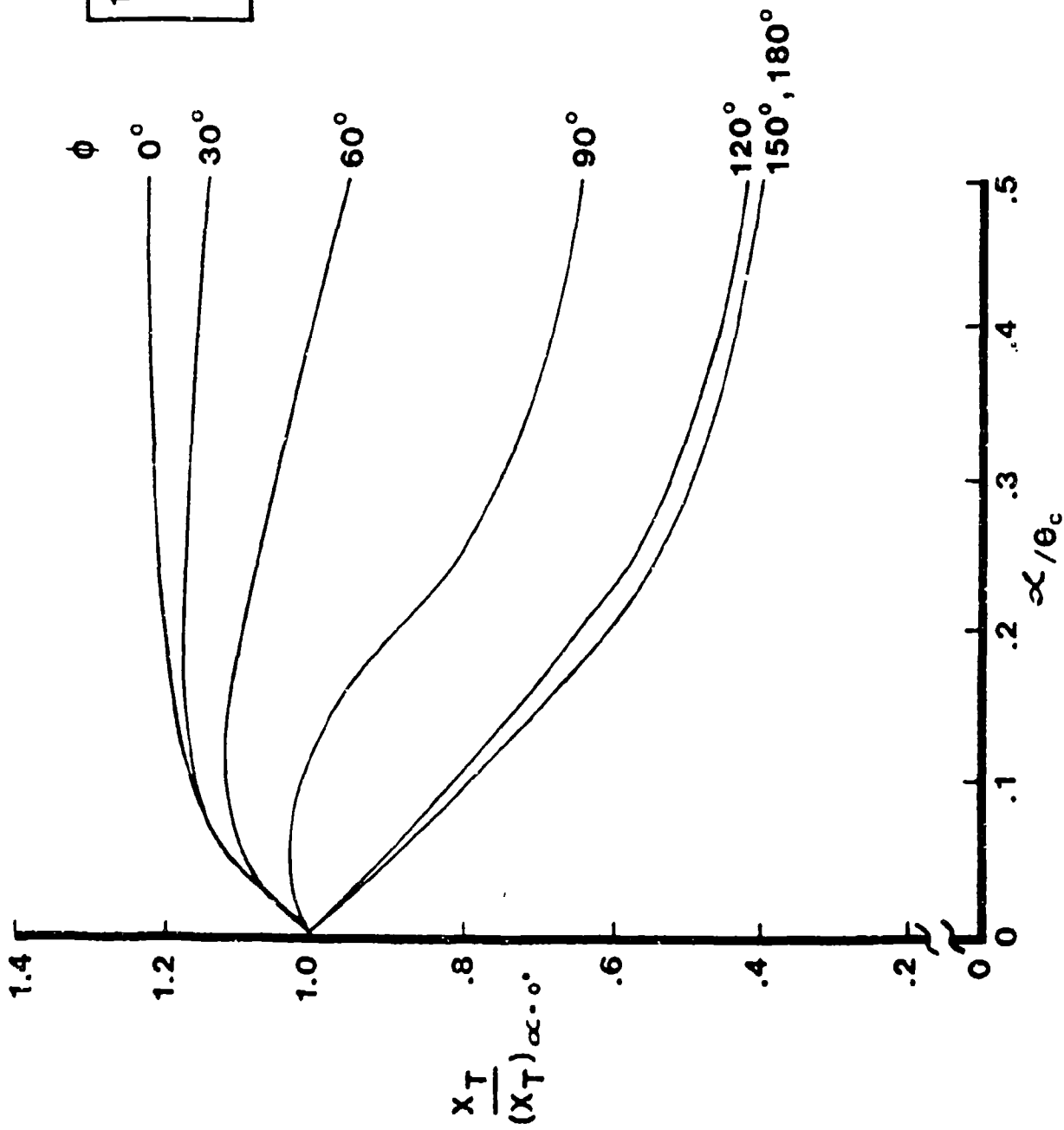


FIG. 27 Transition Asymmetry with Angle of Attack for 10% Nosedip Bluntness

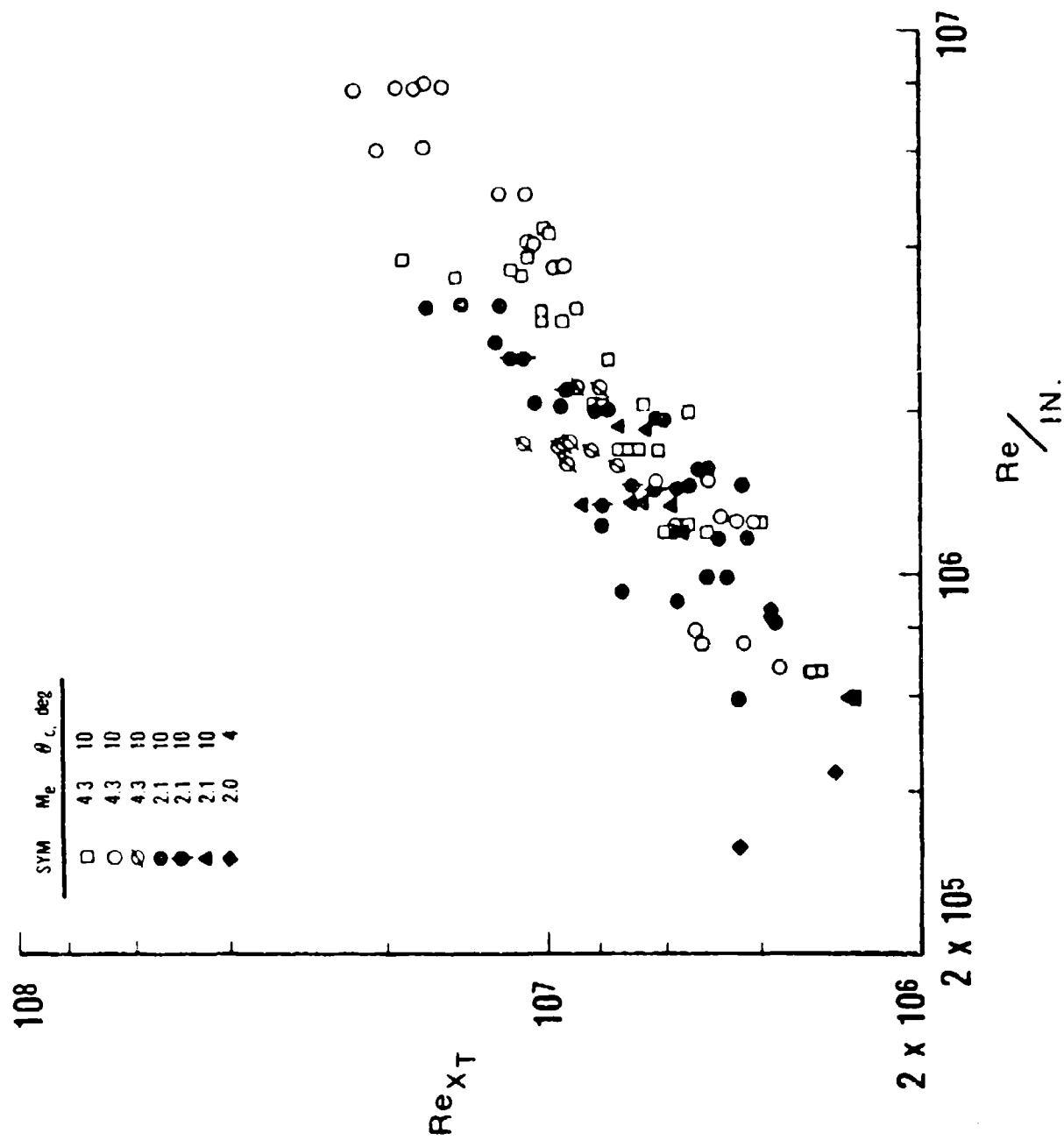


FIG. 28 Unit Reynolds Number Effect in a Ballistic Range

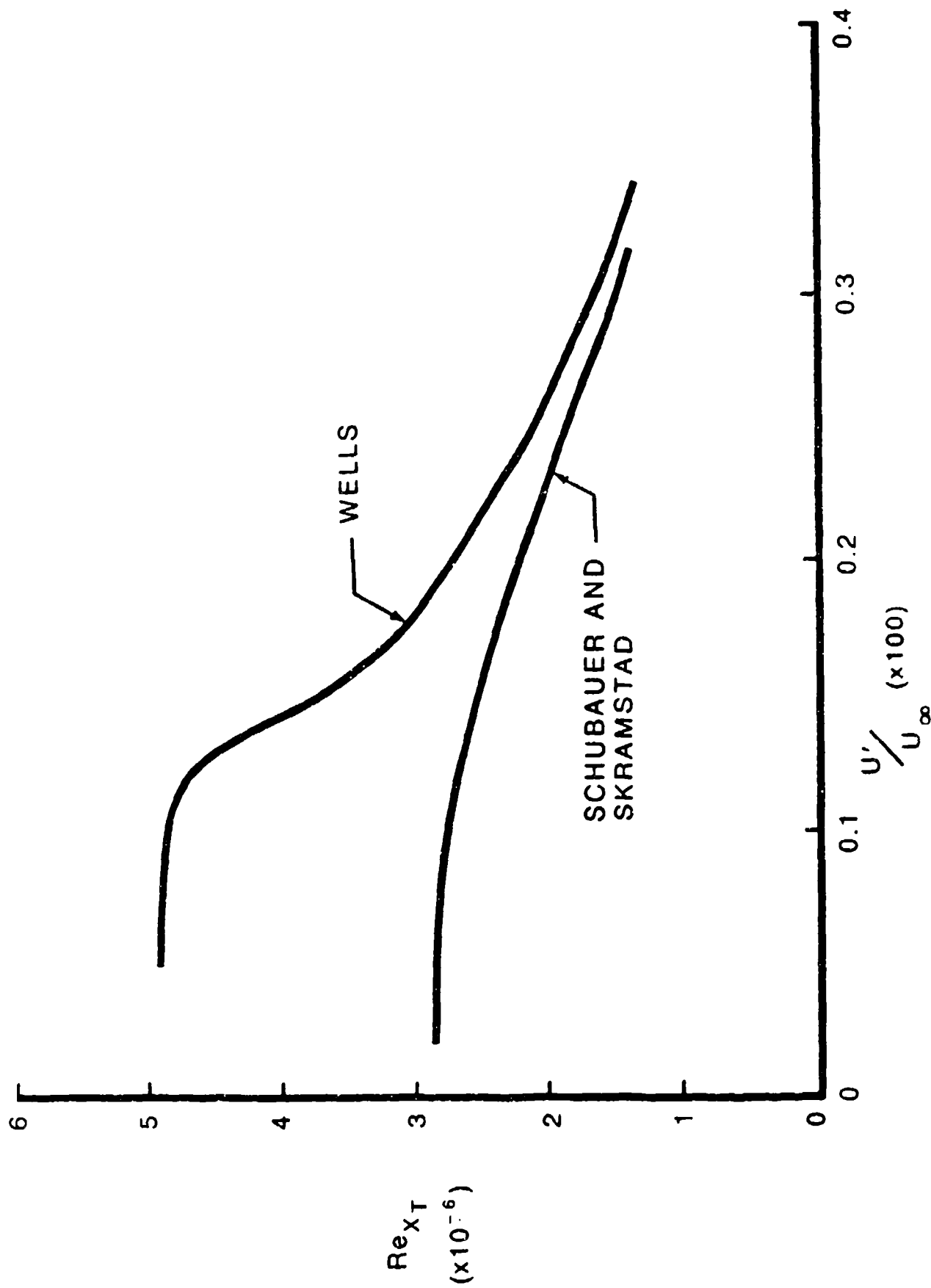


FIG. 29 Effect of Freestream Disturbances on Transition Reynolds Number

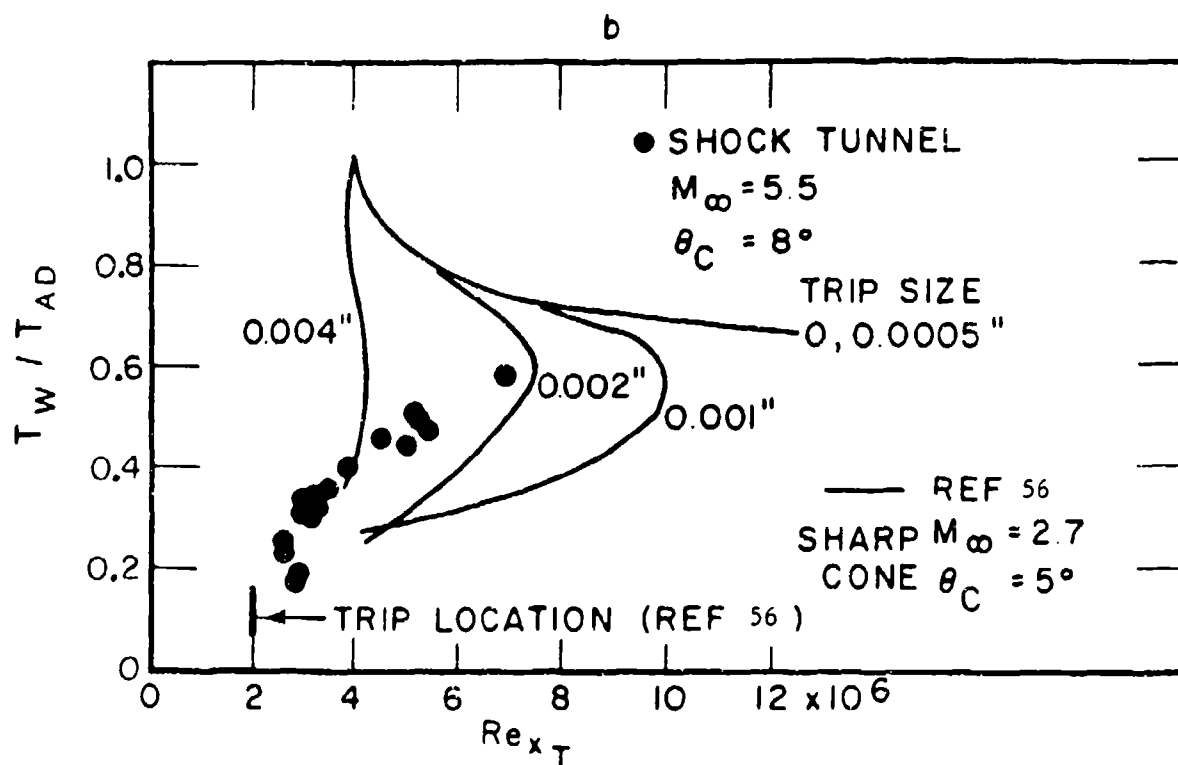
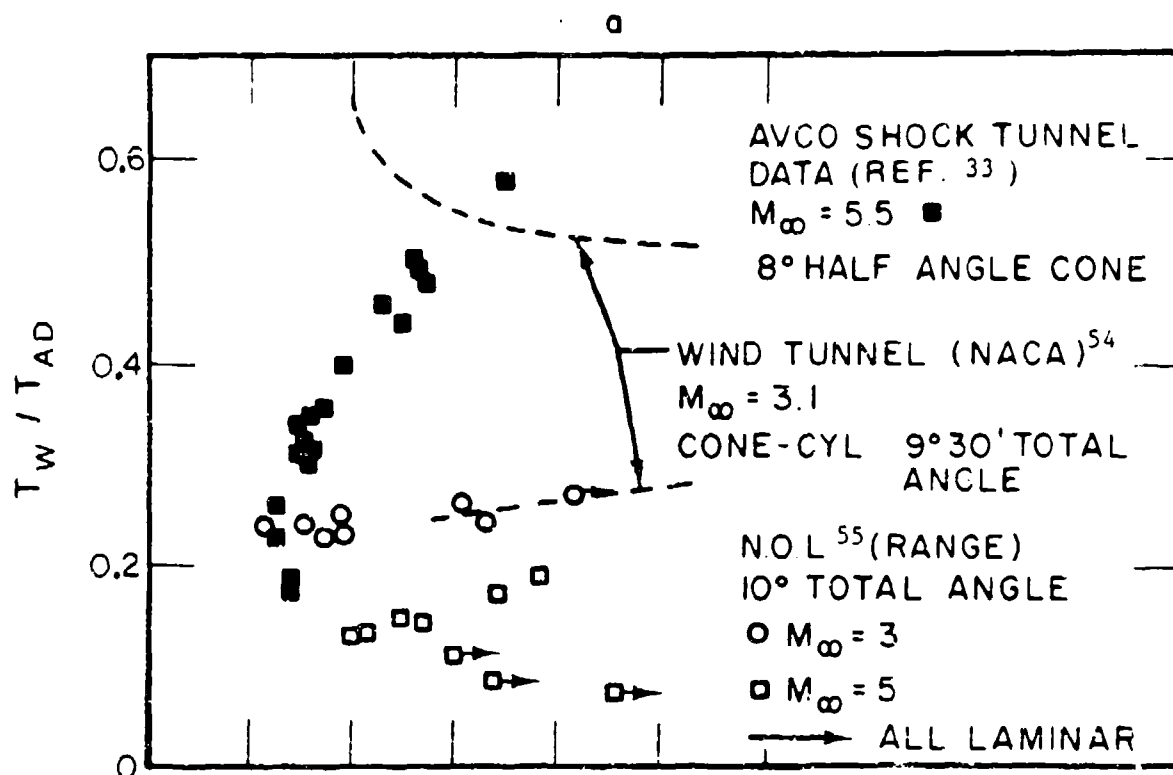


FIG. 30 Effect of Boundary-Layer Cooling on Transition

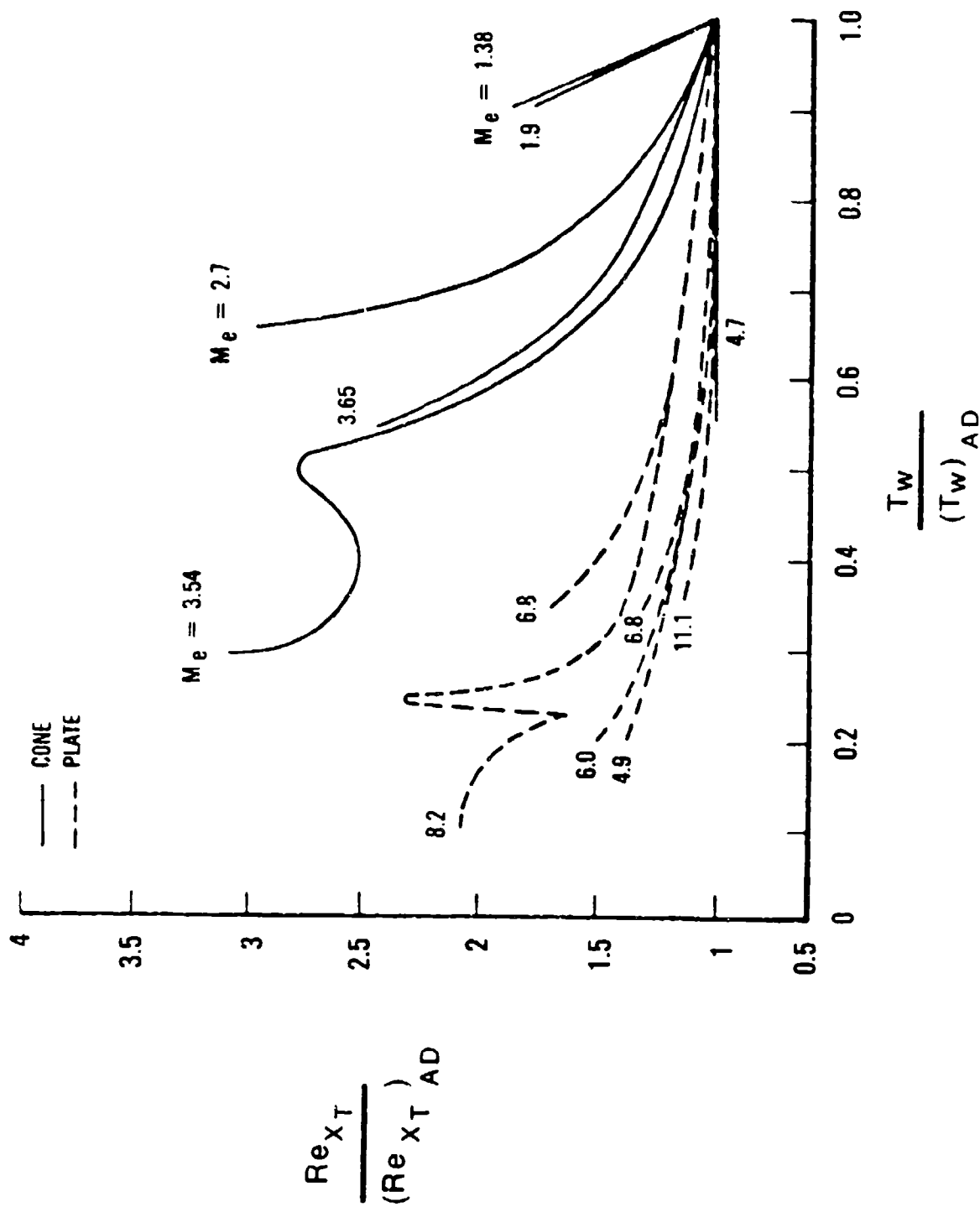


FIG. 31 Effect of Wall Cooling on Transition Reynolds Numbers

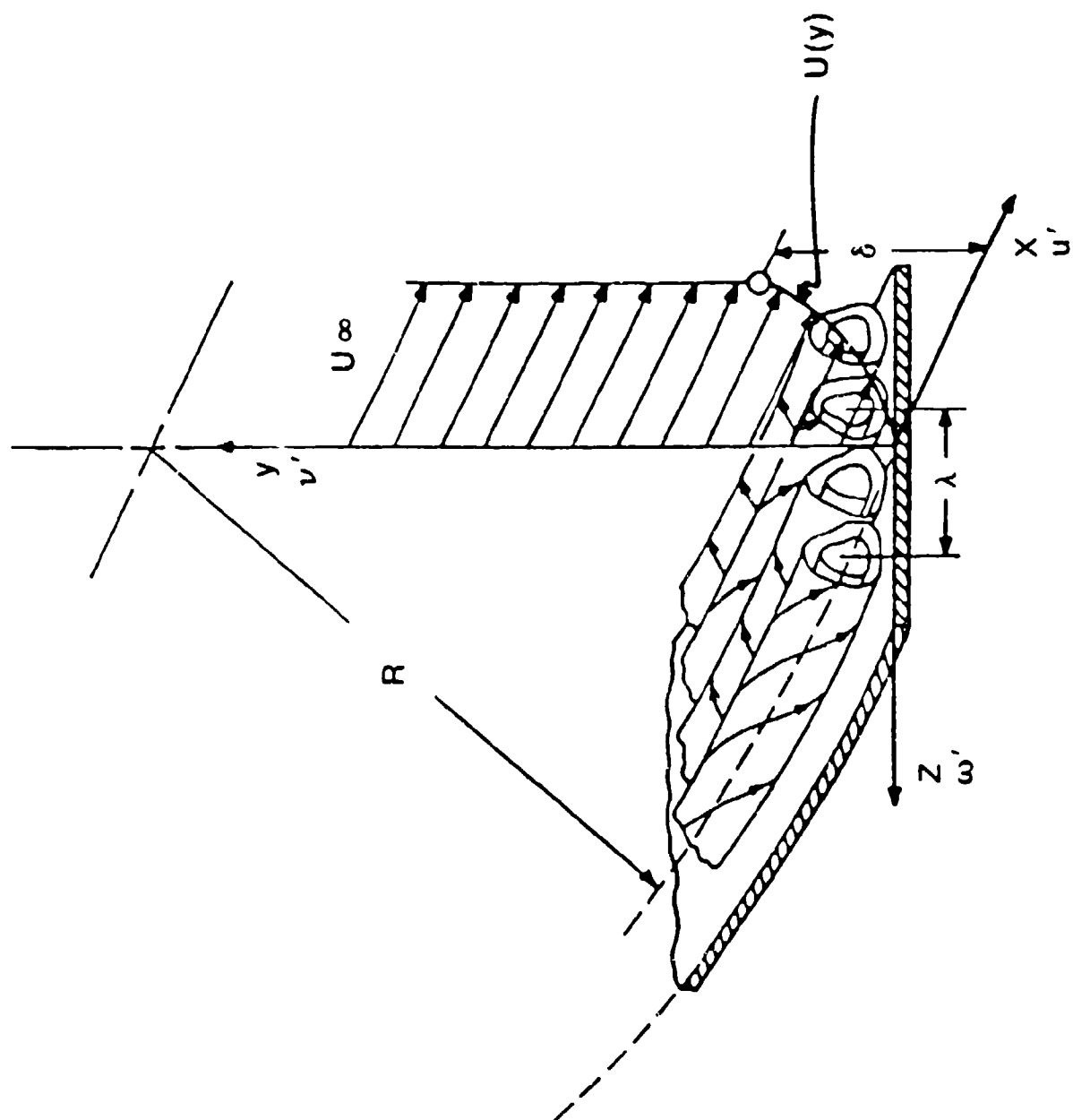


FIG. 92 A Schematic Illustration of Görtler Vortices

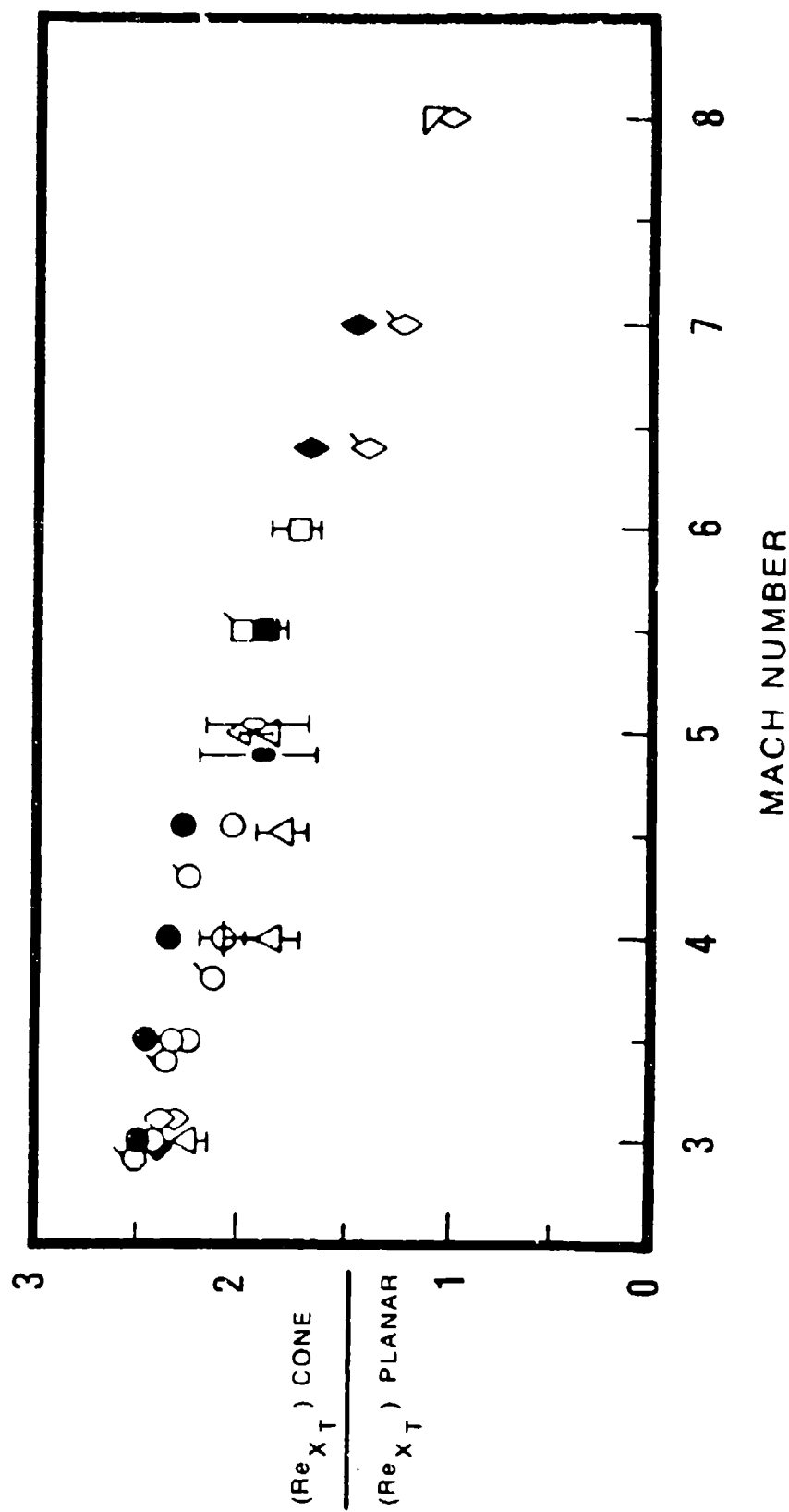


FIG. 33 Correlation of Axisymmetric and Planar Transition Reynolds Numbers

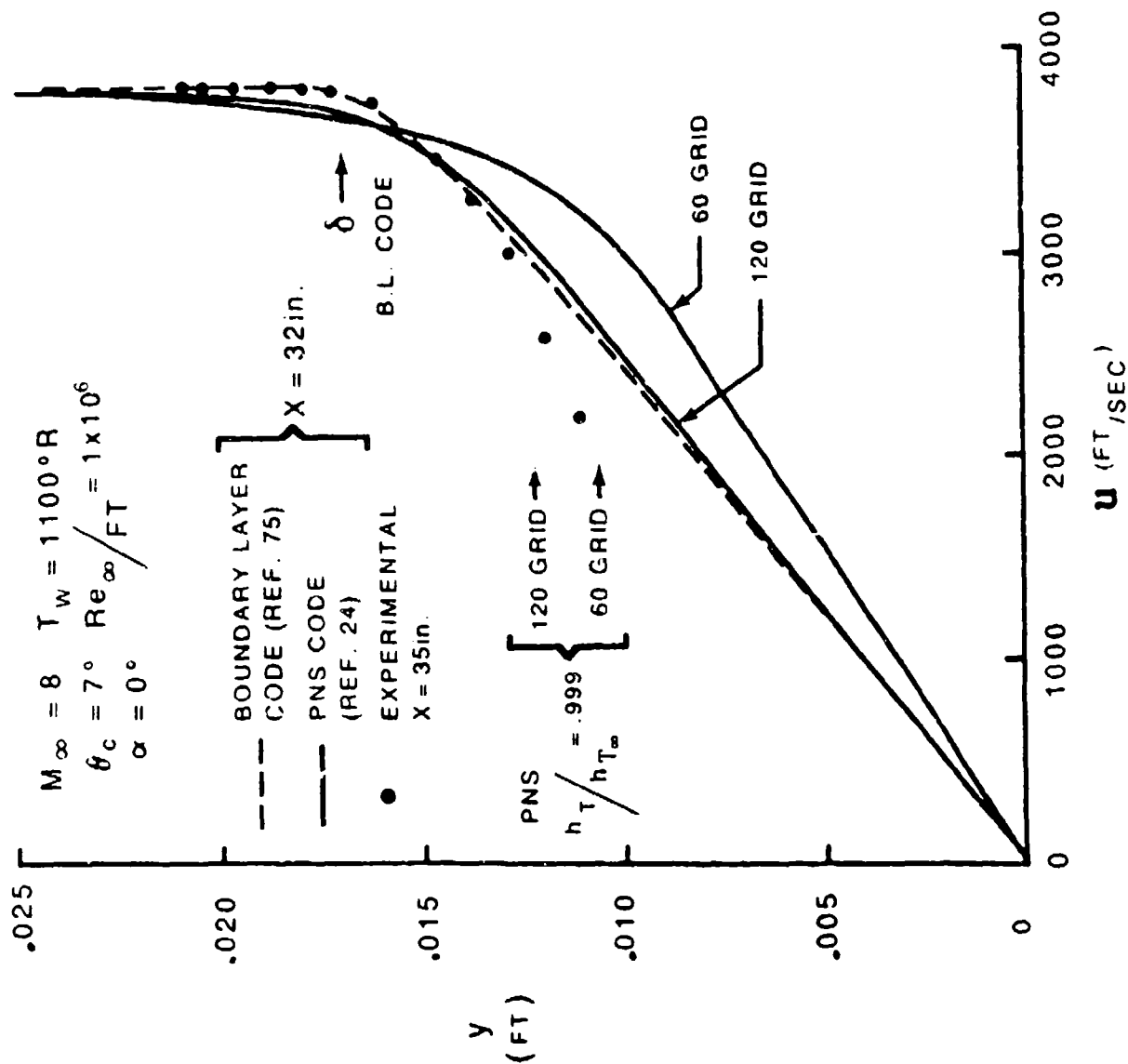


FIG. 34 Boundary-Layer Profiles

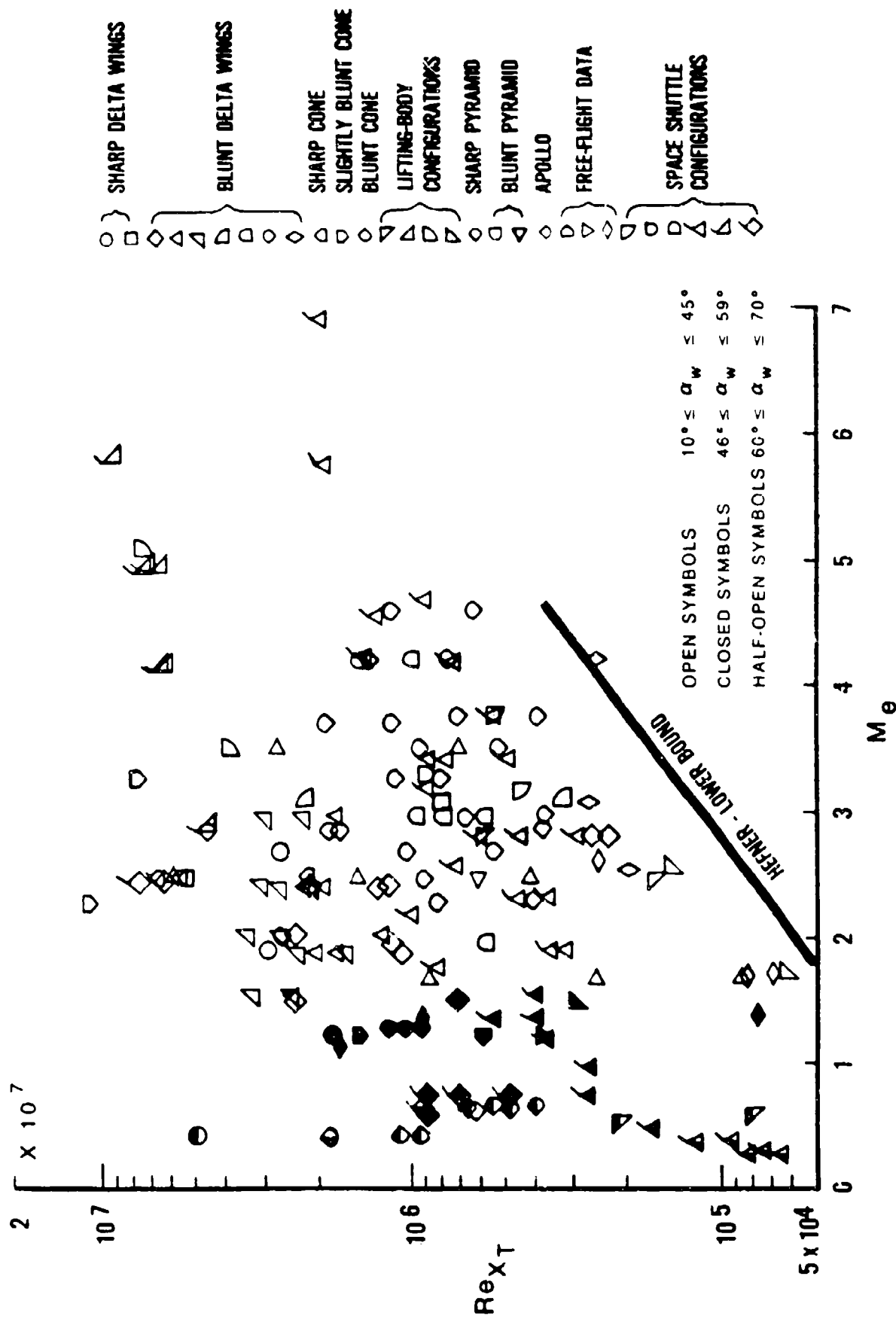


FIG. 35 Transition Reynolds Number as a Function of Local Mach Number

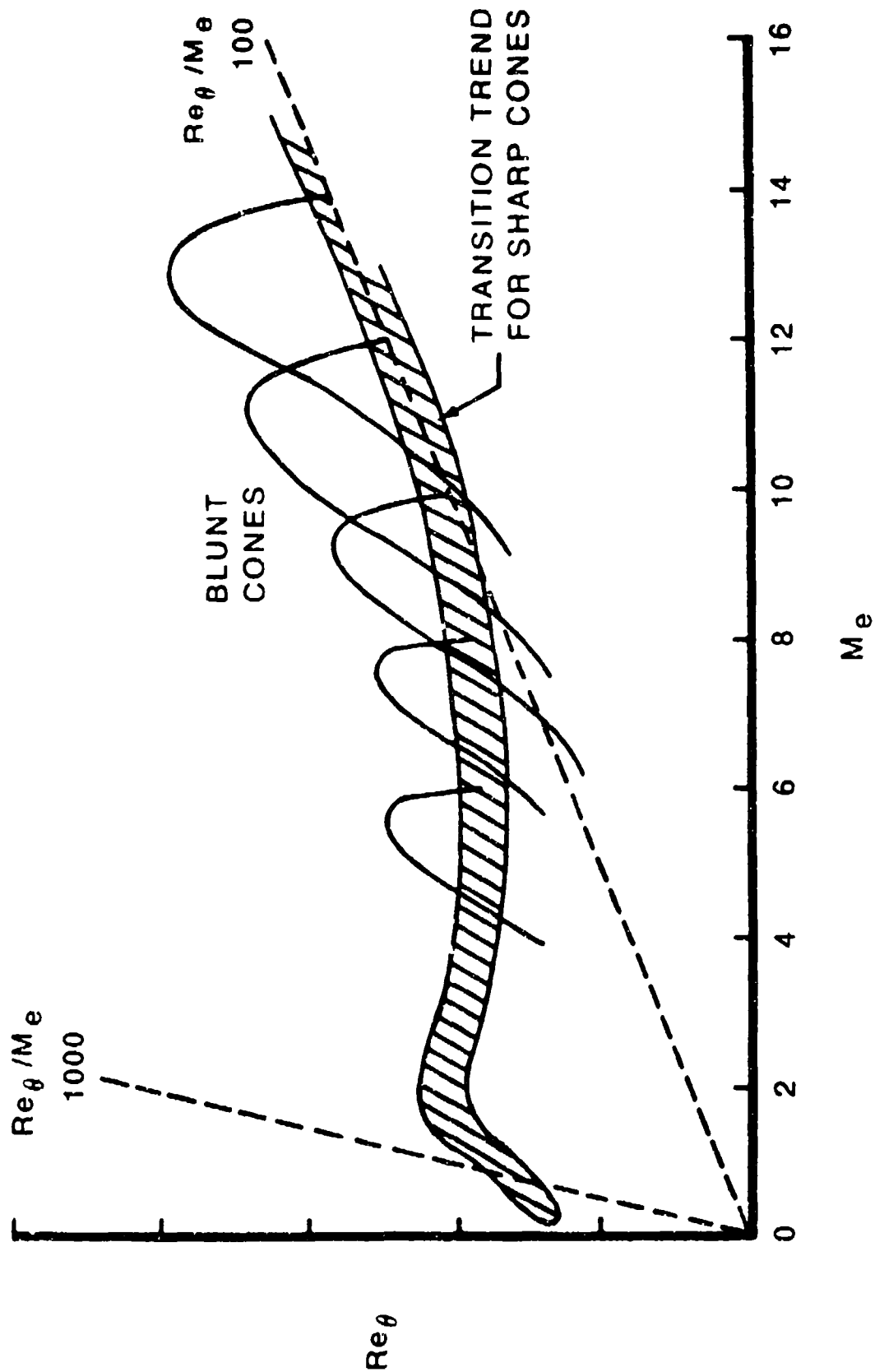


FIG. 36 An Illustration of Re_θ / M_e Variations

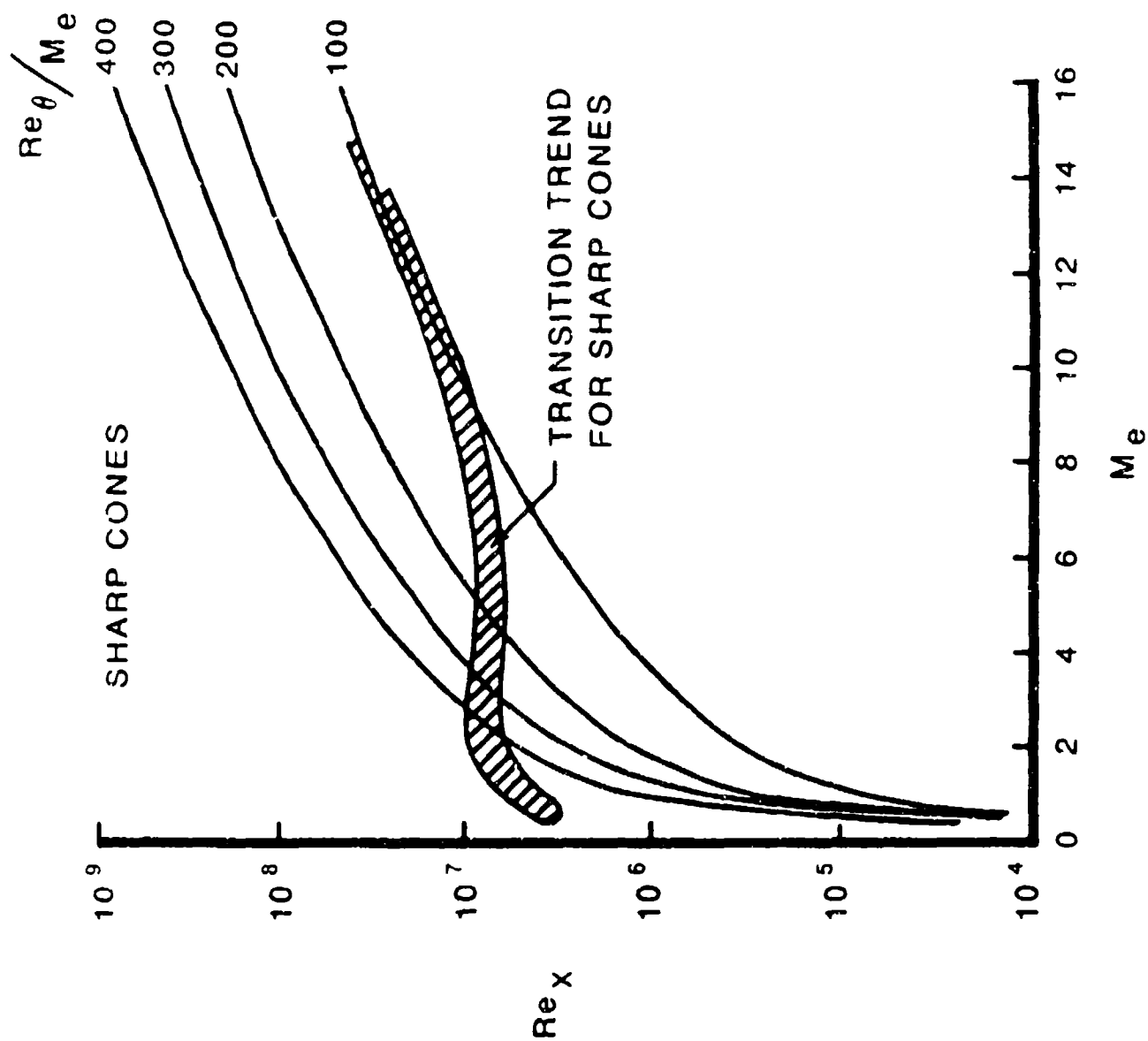
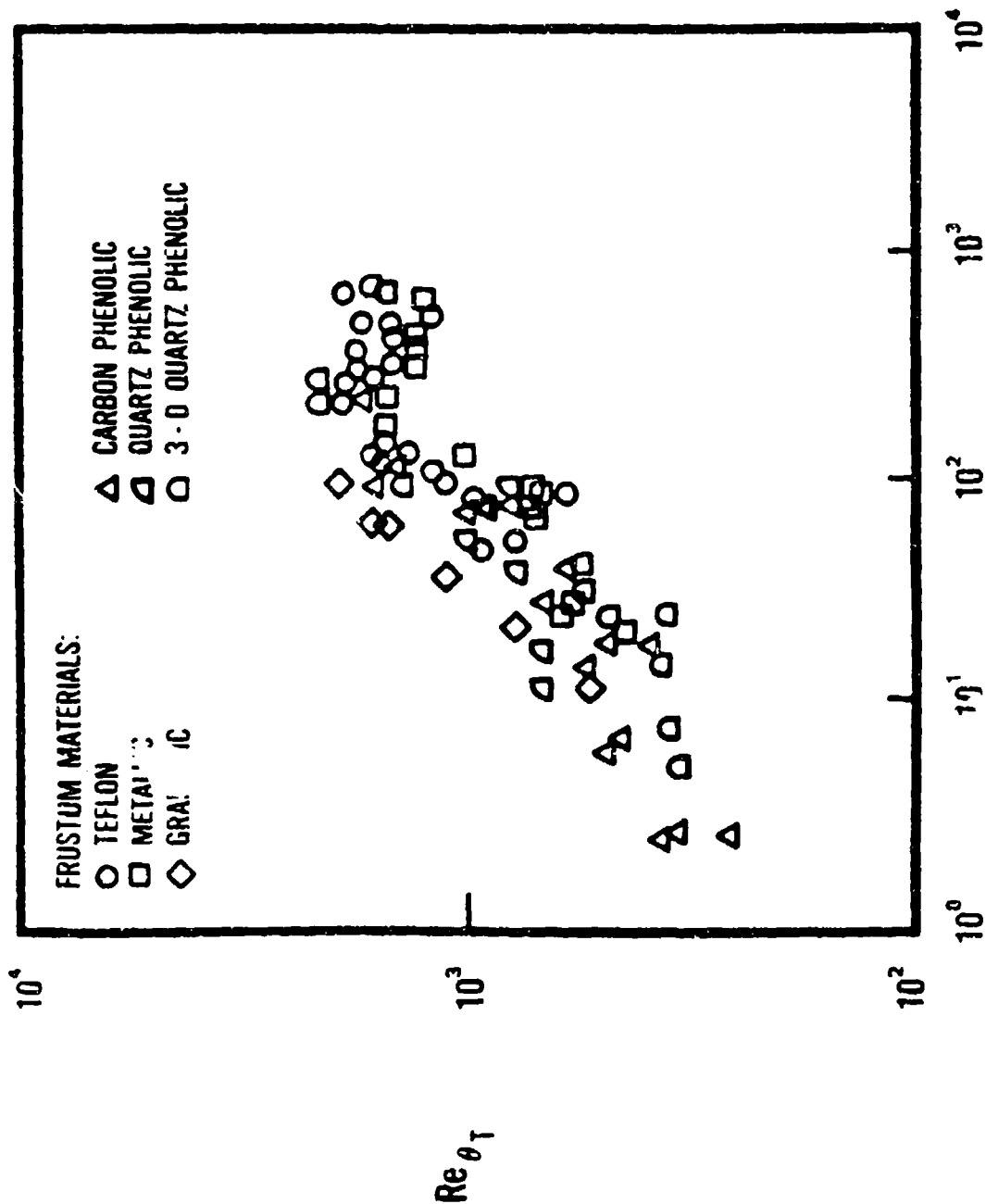


FIG. 37 Re_x Variations as a Function of $Re_\theta/M_e = \text{Constant}$



$$X_T/R_N$$

FIG. 38 Re_{θ_T} vs X_T/R_N Correlation for Mach 20 Reentry Vehicles

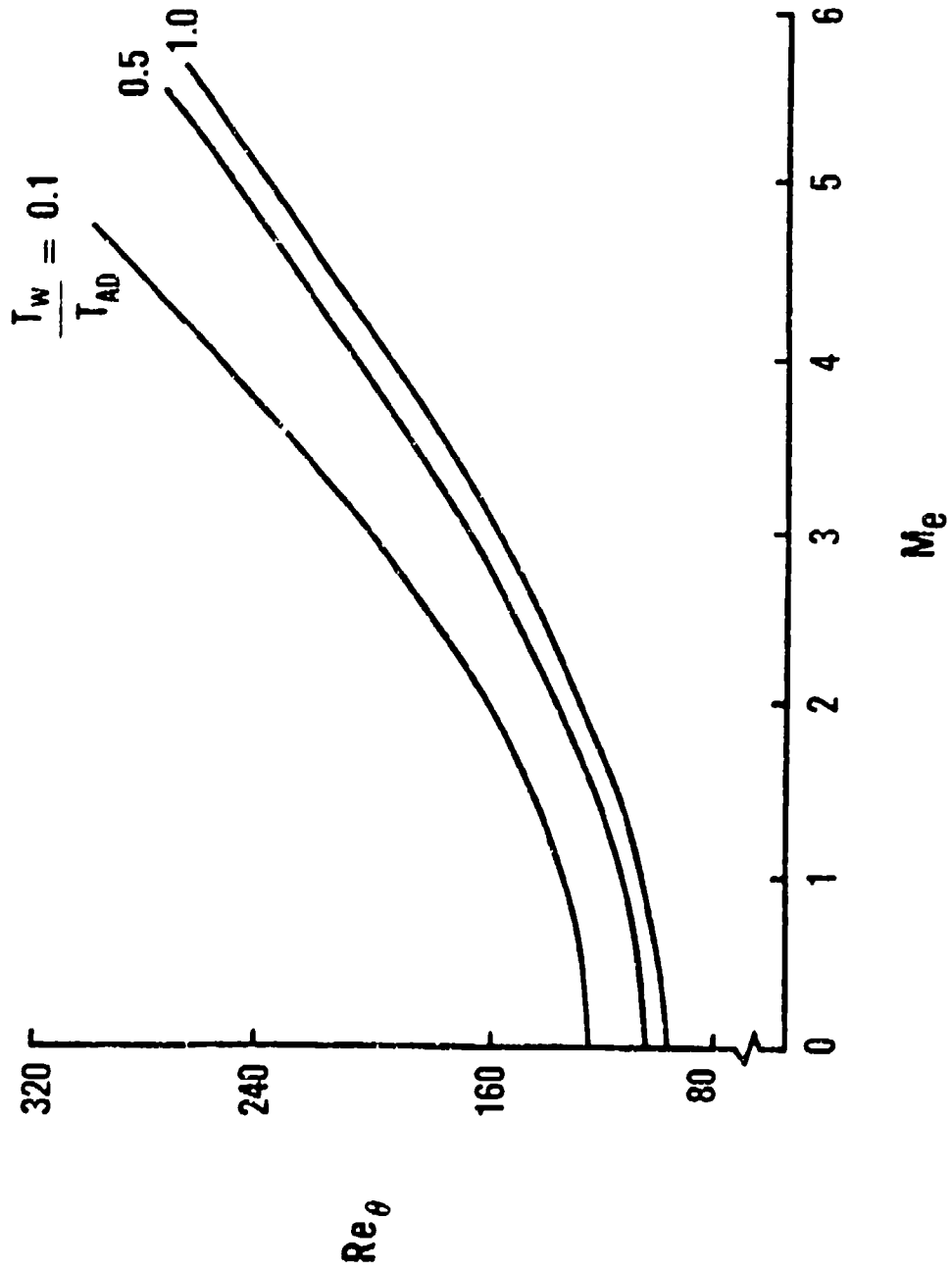


FIG. 39 Transition Onset at the Attachment Line of a Swept Cylinder

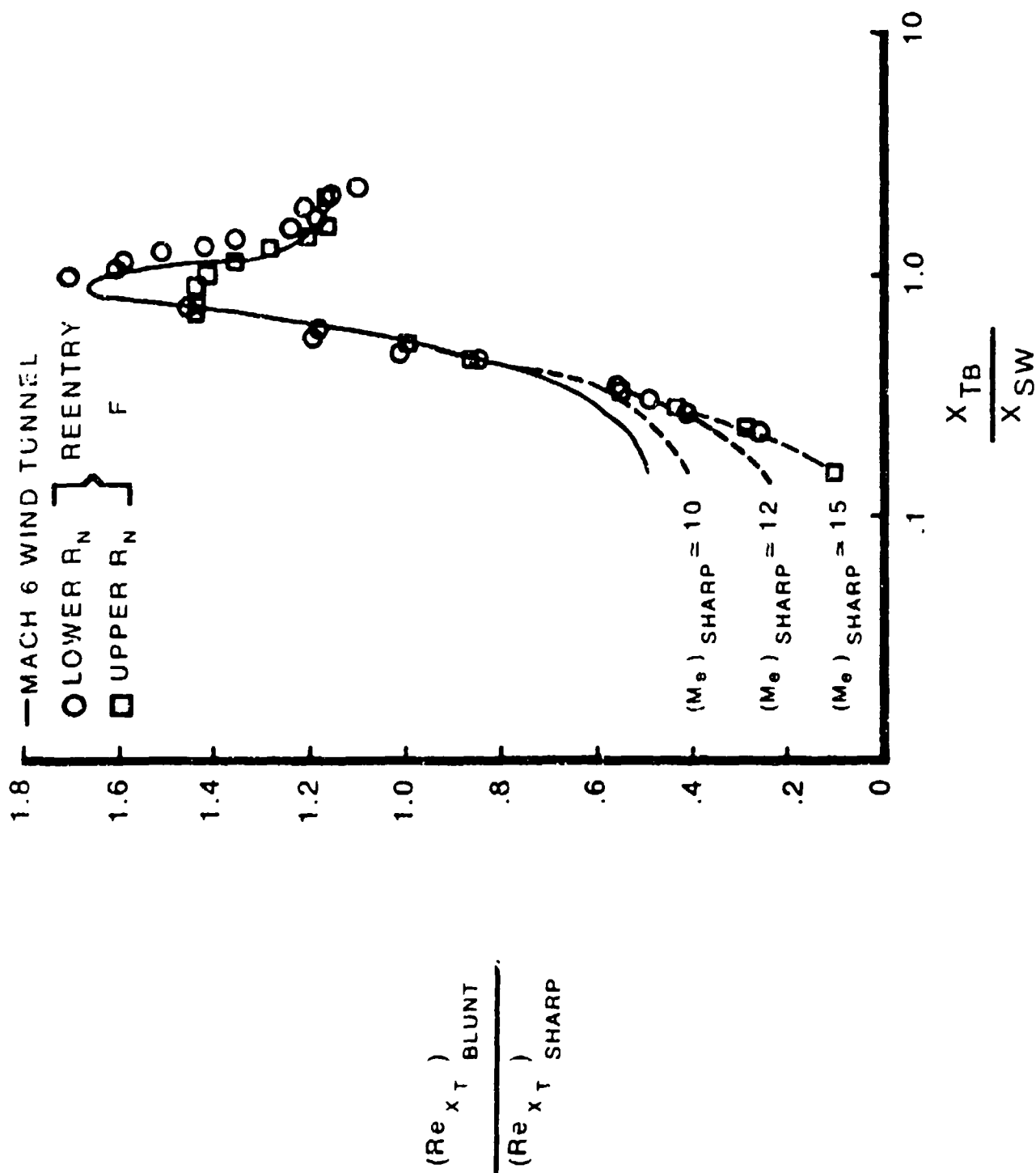


FIG. 40 Transition Reynolds Number Variations Within the Entropy Layer

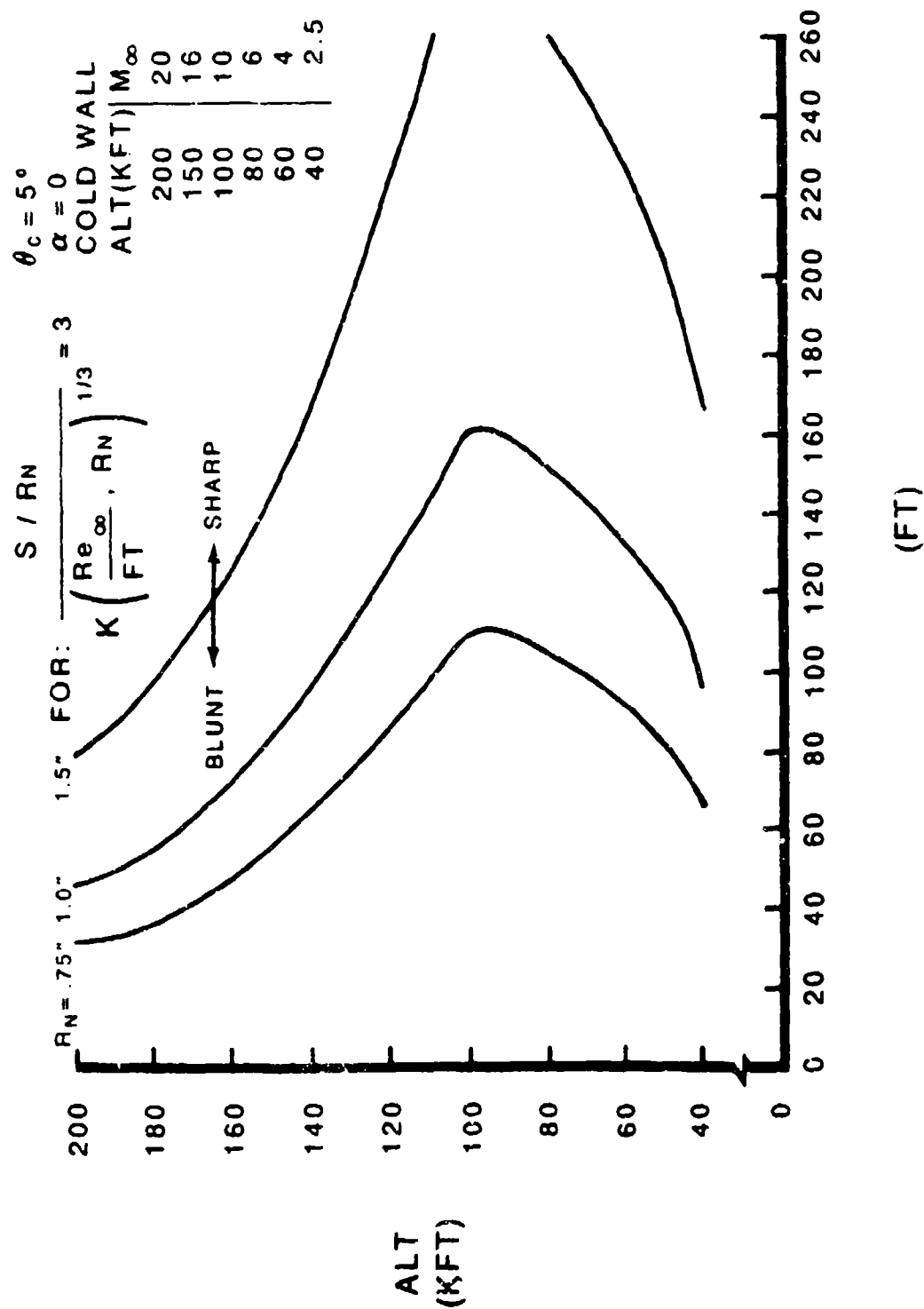


FIG. 41 Entropy Layer Effects on a Slender Cone